University : **İstanbul Technical University**
Institute : **Institute of Science and Technology**
Science Programme : **Chemistry**
Programme : **Chemistry**
Supervisor : **Prof. Dr. Tülay TULUN**
Degree Awarded and Date : **M.Sc.Thesis – May 2003**

ABSTRACT

CHEMOMETRIC ANALYSIS OF SEM-EDAX, POROSITY, AND SOLUBLE SALTS DATA FOR ARCHAEO-CERAMICS

Nejla ÇİNİ

The goal of this study is to apply chemometric techniques on a large number of Iznik ceramics obtained from the excavation of Iznik Kiln sites in order to provide information regarding the compositional, technological, provenance and age characteristics. This work has also had a mission to have an idea on chemometry, which comprises various techniques, and used to solve problems particularly, in chemistry and other scientific and industrial fields. In this study, the data for 107 body pastes, and 61 slips, and 75 glazes samples obtained by Scanning Electron Microscope (SEM) online X-Ray Energy (EDX) technique (Tulun's et al.) were analyzed by Principal Component (PCA) and Cluster Analysis (CA) methods. Besides, porosity data (apparent and density, total pore volume, and porosity %, for 40 samples) obtained from Tulun's et al. previous study and soluble salts data (in this work, 23 samples) were analyzed with the same chemometric techniques regarding deterioration characteristics. In experimental part, the contents of soluble salts were determined in variations of temperatures (0ºC to 35ºC) and durations (5 to 25 days) considering the average climate conditions. Prior to quantitative determination of anions (chloride, phosphate, nitrate, and sulphate) and cations (sodium, potassium, calcium, and magnesium) were examined by wet chemistry (spot tests) and then quantitative determinations were carried out. In addition, Saturation Coefficient, which is a pore characteristics and durability criteria for ceramics, and weights loss due to acid and base exposure (enviromental conditions) for a given sample were determined.

Keywords: Archaeo-Ceramics, Chemometry, Principle Component Analysis (PCA), Cluster Analysis (CA), Soluble Salts.

Science Code: 405

ACKNOWLEDGEMENT

I sincerely appreciated Prof. Dr. Tülay Tulun for giving opportunity to work with her, and for her deep interests, productive comments and helps on this research work.

I would like thank Prof. Dr. Ara Altun and Associate Prof. Belgin Arlı for providing me the ceramic samples.

I also thank my friends Ferah Çalışır and Nilgün Tokman for their kind helps during my work.

I very much indepted to my family for their giving me moral and substantial support during all my life and education.

It is acknowledged to Institute of Science and Technology of Istanbul Technical University for the financial support in this study carried out in the Analytical Chemistry Department of Science and Letters Faculty.

May 2003 Nejla ÇİNİ

CONTENTS

ABBREVIATIONS **v**
LIST OF FIGURES **vi**
LIST OF TABLES **x**
SUMMARY **xii**
ÖZET **xvi**

1. INTRODUCTION **1**
2. THEORETICAL PART I **3**
2.1. Chemometry **3**
2.2. Pattern Recognition Techniques **5**
2.3. Principal Component Analysis (PCA) **6**
2.3. Preprocessing **7**
2.3.1. Standardization and Normalization 7
2.3.2. Eigen Analysis 7
2.3.3. Determination of Significant Principal Components 8
2.3.3.1. Size of Eigenvaleus 8
2.3.3.2. Cross-Validation 9
2.3.4. Graphical Representation 9
2.4. Cluster Analysis (CA) **10**
2.4.1. Similarities and Distances 10
2.4.2. Linkage 13
3. THEORETICAL PART II **16**
3.1. Deterioration of Ceramics **16**
3.2. Effects of Composition and Production Technology on Deterioration **16**
3.2.1. Deterioration Types of Body 17
3.2.2. Deterioration Types of Glaze 17
3.3. Effects of Soluble Salts of Deterioration **19**
3.3.1. Salt Crystallization 20
3.3.2. Freezing and Thawing 20
3.4. Other Factors of Deterioration **21**
4. EXPERİMENTAL PART **22**
4.1. Chemicals and Solutions **22**
4.2. Standarts **23**
4.3. Instruments **24**
4.4. Experiments **24**
4.4.1. Determination of Soluble Salts 24
4.4.1.1. Spot Tests 25
4.4.1.2. Quantitative Determination of CI- 25
4.4.1.3. Quantitative Determination of PO_4^{3-} 28
4.4.1.4. Quantitative Determination of NO_3^- 28
4.4.1.5. Quantitative Determination of SO_4^{2-} 29

4.4.1.6. Quantitative Determination of Cations (Na+, K^+, Ca^{2+}, and Mg^{2+}) 31
4.4.2. Determination of Saturation Coefficient 34
4.4.3. Weight Lost of Ceramic by Acid and Base Attack 34
5. CHEMOMERTIC ANALYSIS 36
5.1. Chemometric Analysis of Body Composition 36
5.1.1. Principle Component analysis (PCA) of Body Composition 36
5.1.2. Cluster Analysis (CA) of Body Composition 40
5.2. Chemometric Analysis of Slip Composition 44
5.2.1. Principle Component Analysis (PCA) of Slip Composition 44
5.2.2. Cluster Analysis (CA) of Slip Composition 48
5.3. Chemometric Analysis of Glaze Composition 52
5.3.1. Principle Component Analysis (PCA) of Glaze Composition 52
5.3.2.Cluster Analysis (CA) of Glaze Composition 56
5.4. Chemometry of Glaze Data from Tulun's, Amara's, and Tite's Studies 60
5.4.1. Principle Component Analysis (PCA) of Glaze Data From from Tulun's, Amara's, and Tite's Studies 60
5.4.2. Cluster Analysis (CA) of Glaze Data From from Tulun's, Amara's, and Tite's Studies 63
5.5. Chemometric Analysis of Porosity Characteristics 67
5.5.1. Principle Component Analysis (PCA) of Porosity Characteristics 67
5.5.2. Cluster Analysis (CA) of Porosity Characteristics 70
5.6. Chemometric Analysis of Soluble Salts 74
5.6.1. Principle Component Analysis (PCA) of Soluble Salts 74
5.6.2. Cluster Analysis (CA) of Soluble Salts 77
6. RESULTS and DISCUSSIONS 81
6.1. Results of Experimental Part 81
6.1.1. Soluble Salts 81
6.1.2. Saturation Coefficient 82
6.1.3. Weight Lost of Ceramic by Acid and Base Attack **82**
6.2. Results of Chemometry Analysis 82
6.2.1. Results for Body Composition 82
6.2.2. Results for Slip Composition 82
6.2.3. Results for Glaze Composition 84
6.2.4. Results for Glaze Composition From Tulun's, Amara's, and Tide's Studies 84
6.2.5 Results for Porosity Data 85
6.2.6 Results for Soluble Salts 85
7. CONCLUSION 87
REFERENCES 89
APPENDIX A 92
APPENDIX B 101
CURRICULUM VITAE 117

ABBREVIATIONS

SEM	:Scanning Electron Microscope
EDX	:X-Ray Energy Dispersive
ANOVA	:Analysis of variance
HPLC-DAD	: High Performance Liquid Chromatography- Diode Array Dedector
LC-MS	:Liquid Chromatography-Mass Spectrometry
LC-NMR	:Liquid Chromatography-Nuclear Magnetic Resonance
UV Spectrophotometry	:Ultraviolet Visible Spectrophotometry
NMR	:Nuclear Magnetic Resonance
EDA	:Explatory Data Analysis
UPR	:Unsupervised Pattern Recognition
SPR	:Supervised Pattern Recognition
MPR	:Multiway Pattern Recognition
PCA	:Principle Component Analysis
FA	:Factor Analysis
CA	:Cluster Analysis
LP	:Loadings Plot
SP	:Scores Plot
MD	:Mahalonobis Distance
ED	:Euclidean Distance

LIST OF FIGURES

Page No

Figure 2.1 : Geometric Represantaion of the ED in which there are two samples presented……………………………………………….……....11
Figure 2.2 : A Dendogram illustrating two groups………….. …………...…..15
Figure 4.1 : Conductmetric titration plot of sample 4 for immersion at 0^oC….. 27
Figure 4.2 : Conductmetric titration plot of sample 7 for immersion at 0^oC…...27
Figure 4.3 : Conductmetric titration plot of sample 9 for immersion at 0^oC.......28
Figure 4.4 : Comparison of weight loss of ceramic sample 3 by an acid and base attack…………….……………………………………....….35
Figure 5.1 : Scores plot showing the results of PCA of body composition data of 107 samples for PC1 and PC2…………….……………..…..…37
Figure 5.2 : Loadings plot showing the results of PCA of body composition data of 107 samples for PC1 and PC 2. ………………………….…..…37
Figure5.3 : Scoress plot showing the results of PCA of body composition data of 107 samples for PC1, PC2, and PC3. ………………..……38
Figure 5.4 : Loadings plot showing the results of PCA of body composition data of 107 samples for PC1, PC2, and PC3. …………….…..….39
Figure 5.5 : SiO_2 versus Fe_2O_3 percentage content (wt) for body composition of 107 samples. ……………………….……………….……….…..…40
Figure 5.6 : SiO_2 versus Al_2O_3 percentage content (wt). ………...……………40
Figure 5.7 : Dendogram showing the results of clustering body composition data of 107 samples based of Single Linkage. ……..………..……41
Figure 5.8: Dendogram showing the results of clustering body composition data of 107 samples based of Complete Linkage..………………...42
Figure 5.9: Dendogram showing the results of clustering variables for body composition of 107 ceramic samples Single Linkage. ……………43
Figure 5.10: Dendogram showing the results of clustering variables for body composition of 107 ceramic samples based of Complete Linkage..43
Figure 5.11: Scores plot showing the results of PCA of slip composition data of 61 samples for PC1 and PC2. ……………………………….....45
Figure 5.12: Loadings plot showing the results of PCA of slip composition data of 61 samples for PC1 and PC2. ………………………….………45
Figure 5.13: Scores plot showing the results of PCA of slip composition data of 61 samples for PC1, PC2, and PC3………………………..46
Figure 5.14: Loadings plot showing the results of PCA of slip composition data of 61 samples for PC1, PC2, and PC3. …………………......47
Figure 5.15: SiO_2 versus Fe_2O_3 percentage content (wt) for slip composition of 61 samples……………………….……………………..…….…...48
Figure 5.16: SiO_2 versus Al_2O_3 percentage content (wt) for slip composition of 61 samples. ……………….…….……………………………….…48

Figure 5.17: Dendogram showing the results of clustering slip composition data of 61 samples based of Single Linkage…………………......49
Figure 5.18: Dendogram showing the results of clustering slip composition data of 61 samples based of Complete Linkage. ……………..……...50
Figure 5.19: Dendogram showing the results of clustering variables for slip ccomposition of 61 ceramic samples based of Single Linkage..…51
Figure 5.20: Dendogram showing the results of clustering variables for slip ccomposition of 61 ceramic samples based of Complete Linkage..51
Figure 5.21: Scores plot showing the results of PCA of glaze composition data of 75 samples for PC1 and PC2. ………………………...….53
Figure 5.22: Loadings plot showing the results of PCA of glaze composition data of 75 samples for PC1 and PC2. …………………...….....53
Figure 5.23: Scores plot showing the results of PCA of glaze composition data of 75 samples for PC1, PC2, and PC3. ………..………...…55
Figure 5.24: Loadings plot showing the results of PCA of glaze composition data of 75 samples for PC1, PC2, and PC3. …….……………....56
Figure 5.25: Dendogram showing the results of clustering glaze composition data of 75 samples based of Single Linkage.. …………………...57
Figure 5.26: Dendogram showing the results of clustering glaze composition data of 75 samples based of Complete Linkage. ………..……....58
Figure 5.27: Dendogram showing the results of clustering variables for glaze composition of 75 ceramic samples based of Single Linkage……..59
Figure 5.28: Dendogram showing the results of clustering variables for glaze composition of 75 ceramic samples based of Complete Linkage….59
Figure 5.29: Scores plot showing the results of PCA of glaze data of Tulun, Amara, and Tite samples for PC1 and PC2………………..….......61
Figure 5.30: Loadings plot showing the results of PCA of glaze data of Tulun, Amara, and Tite samples for PC1 and PC………….……………...61
Figure 5.31: Scores plot showing the results of PCA of glaze data of Tulun, Amara, and Tite samples for PC1, PC2 and PC3……………….…62
Figure 5.32: Loadings plot showing the results of PCA of glaze data of Tulun, Amara, and Tite samples for PC1, PC2 and PC3…………………63
Figure 5.33: Dendogram showing the results of clustering glaze composition Data from Tulun's, Amara's, and Tite's studies based of Single Linkage...64
Figure 5.34: Dendogram showing the results of clustering glaze composition Data from Tulun's, Amara's, and Tite's studies on based of Complete Linkage…………………………………………………65
Figure 5.35: Dendogram showing the results of clustering variables glaze composition data from Tulun's, Amara's, and Tite's studies based of Single Linkage……………………………….………..66
Figure 5.36: Dendogram showing the results of clustering variables glaze composition data from Tulun's, Amara's, and Tite's studies based of Complete Linkage………………………….……..…...66
Figure 5.37: Scores plot showing the results of PCA of porosity data of 40 samples for PC1 and PC2. ……………….…………...……...68
Figure 5.38: Loadings plot showing the results of PCA of porosity data of 40 samples for PC1 and PC2. ……………….……....………....68
Figure 5.39: Scores plot showing the results of PCA of porosity data of 40 samples for PC1, PC2 and PC3. ………………………….......69

Figure 5.40: Loadings plot showing the results of PCA of porosity data of 40 samples for PC1, PC2 and PC3. ……………………….……......70
Figure 5.41: Dendogram showing the results of clustering porosity data of 40 samples based of Single Linkage. …………………….……..……..71
Figure 5.42: Dendogram showing the results of clustering porosity data of 40 samples based of Complete Linkage. ……………………….…………72
Figure 5.43: Dendogram showing the results of clustering variables for porosity data of 40 ceramic samples based of Single Linkage. …………….73
Figure 5.44: Dendogram showing the results of clustering variables for porosity data of 40 ceramic samples based of Complete Linkage. ………..73
Figure 5.45: Scores plot showing the results of PCA of soluble salts data of 23 samples for PC1 and PC2. ………………………….………….…………75
Figure 5.46: Loadings plot showing the results of PCA of soluble salts data of 23 samples for PC1 and PC2. …………………….…………….…75
Figure 5.47: Scores plot showing the results of PCA of soluble salts data of 23 samples for PC1, PC2 and PC3……………………………….....76
Figure 5.48: Scores plot showing the results of PCA of soluble salts data of 23 samples for PC1, PC2 and PC3. ………………...……….……77
Figure 5.49: Dendogram showing the results of clustering soluble salts data of 23 samples based of Single Linkage. ……………………...…..78
Figure 5.50: Dendogram showing the results of clustering soluble salts data of 23 samples based of Complete Linkage. ……………….………79
Figure 5.51: Dendogram showing the results of clustering variables for soluble Salts data of 23 ceramic samples based of Single Linkage………..80
Figure 5.52: Dendogram showing the results of clustering variables for soluble salts data of 23 ceramic samples based of Complete Linkage……80
Figure A.1 : Cl^- % =f (time) for 20^o C concerning to samples 2, 3, 5, 6, 8, and 10.. 92
Figure A.2 : Cl^- % =f (time) for 20^{o}C concerning to samples 4, 7, and 9 92
Figure A.3: Cl^- % = f (t ^{o}C) for 20 days soaking period concerning to samples 1 and 2..93
Figure A.4 : Cl^- % = f (t ^{o}C) for 20 days soaking period concerning to samples 5 and 6…………………...93
Figure A.5 : Cl^- % = f (t ^{o}C) for 20 days soaking period concerning to samples 3 and 8..94
Figure A.6 : Cl^- % = f (t ^{o} C) for 20 days soaking period concerning to samples 4, 7, and 9...………………94
Figure A.7 : Calibration curve of Cl^- analysis for 0^{o}C…....………………….....95
Figure A.8 : Calibration curve of Cl^- analysis for 10^{o}C...…………………...…95
Figure A.9 : Calibration curve of Cl^- analysis for 20^{o}C...……………………..…96
Figure A.10: Calibration curve of Cl^- analysis for 25^{o}C…...…………………….96
Figure A.11: Calibration curve of Cl^- analysis for 30^{o}C and 35^{o}C……………..97
Figure A.12: Calibration curve of PO_4^{3-} analysis. ◆——: 10, 15, 20 days for 10^{o}C; ●– – –: 25 days for 10^{o}C, 10 and 15 days for 20^{o}C;○— - — -: 20 and 25 days for 20^{o}C, 10, 15, 20, and 25 days for 25^{o}C; ⋇——: 10 and 15 days for 30^{o}C □——: 20 and 25 days for 30^{o}C, 10 and 15 days for 35^{o}C; ▲- - - -: 20 and 25 days for 35^{o}C ……..97
Figure A.13: Calibration curves of SO_4^{2-} analysis by flame spectroscopy……...98
Figure A.14: Calibration curves of SO_4^{2-} analysis by Turbidimetry…………......98

Figure A.15: Calibration curves of Na^+ and Ca^{2+} analysis for 10 and 15 days immersion at 30°C…………………………………………………...99
Figure A.16: Calibration curves of K^+ analysis for 10 and 15 days immersion at 30°C …………………………………………..........99
Figure A.17: Calibration curves of Na^+, K^+, and Ca^{2+} analysis in both 20 and 25 days immersion at 30°C, and 10 and 15 days immersion at 35°C…………………………………………………………..…100

LIST OF TABLES

		Page No
Table 3.1.	Coefficient of Expansion Values for Some Oxides (Rhodes, 1966)	18
Table 4.1.	Results of Cl^- by UV Spectrophotometry.......................................	26
Table 4.2.	Results of Cl^- by Conductometry ....… ..	26
Table 4.3.	Results of PO_4^{3-} Analysis..	29
Table 4.4.	Results of NO_3^- Analysis	29
Table 4.5.	Results of SO_4^{2-} Analysis by Spectrophotometry...........................	30
Table 4.6.	Results of SO_4^{2-} Analysis by Turbidimetry....................................	31
Table 4.7.	Results of Soluble Salt Content for 23 Samples…………..……	32
Table 4.8.	Results of Cation Analysis..	33
Table 4.9.	Results for Sample Soaked for 24 hours...	34
Table 4.10.	Results for Sample Boiled for 5 hours..	34
Table 4.11.	Results of Weight Loss...	35
Table 5.1.	Correlation Matrix for Body Composition Data of 107 Samples...	36
Table 5.2.	The eigen values, the percentages of variances, and cumulative percentages corresponding to the each principal components for Body Composition Data of 107 Samples…………………………	36
Table 5.3.	Values of Principal Component Loadings for Body Composition Data of 107 Samples………………………………..	38
Table 5.4.	Correlation Matrix for Slip Composition Data of 61 Samples…...	44
Table 5.5.	The eigen values, the percentages of variances, and cumulative percentages corresponding to the each principal components for Slip Composition Data of 61 Samples……………………………	44
Table 5.6.	Values of Principal Component Loadings for Slip Composition Data of 61 Samples………………………………...	46
Table 5.7.	Correlation Matrix for Glaze Composition Data of 75 Samples	52
Table 5.8.	The eigen values, the percentages of variances, and cumulative percentages corresponding to the each principal components for Glaze Composition Data of 75 Samples…………………………..	52
Table 5.9.	Values of Principal Component Loadings for Glaze Composition Data of 75 Samples…………………………………	54
Table 5.10.	Correlation Matrix for Glaze Data of Tulun's, Amara's, and Tite's samples...	60
Table 5.11.	The eigen values, the percentages of variances, and cumulative percentages corresponding to the each principal components for Glaze Data of Tulun's, Amara's, and Tite's samples…………….	60
Table 5.12.	Values of Principal Component Loadings for Glaze Data of Tulun's, Amara's, and Tite's samples…………………………...	62
Table 5.13.	Correlation Matrix for Porosity Data of 40 Samples....................	67

Table 5.14. The eigen values, the percentages of variances, and cumulative percentages corresponding to the each principal components for Porosity Data of 40 Samples.. 67
Table 5.15. Values of Principal Component Loadings for Porosity Data of 40 Samples.. 69
Table 5.16. Correlation Matrix for Soluble Salts Data of 23 Samples……… 74
Table 5.17. The eigen values, the percentages of variances, and cumulative percentages corresponding to the each principal components for Soluble Salts Data of 23 Samples.. 74
Table 5.18. Values of Principal Component Loadings for Soluble Salts Data of 23 Samples.. 76
Table B.1. Descriptions of Ceramics... 101
Table B.2. Body Composition (for 107 samples)... 105
Table B.3. Slip Composition (for 61 samples)... 109
Table B.4. Glaze Composition (for 76 Samples of Tulun).............................. 111
Table B.5. Glaze Composition of Amara's Samples.. 114
Table B.6. Glaze Composition of Tite's Samples... 114
Table B.7. Porosity Data (for 40 samples)... 115

CHEMOMETRIC ANALYSIS OF SEM-EDAX, POROSITY, AND SOLUBLE SALTS DATA FOR ARCHAEO-CERAMICS

SUMMARY

Studies on archaeo-ceramics provide significant information for cultural heritages of different civilizations. Besides, investigation of chemical and minerological, physical and technological characteristics of archaeo-ceramics contribute a great deal to reveal the mixture of different cultures, world chronology, ancient trade routs, and production technologies. However, it is not easy to make research on these subjects because of the necessity for quite a large number of samples. In addition, numerous variables must be considered in this kind of studies. Therefore, mathematical and statistical methods have to be applied necessarily.

In the recent years, chemometric analysis has been used by many scientists in the archaeometry and there are numbers of papers in this subject. The result of a vast search for litrature on chemometry of archaeo-ceramics showed that there is no study on this subject in our country.

The goal of this study is to apply chemometric techniques on a large number of Iznik ceramics obtained from the excavation of Iznik Kiln sites in order to provide information regarding the compositional, technological, provenance and age characteristics. This work has also had a mission to have an idea on chemometry, which comprises various techniques, and used to solve problems particularly, in chemistry and other scientific and industrial fields.

In this study, the data for 107 body pastes, and 61 slips, and 75 glazes samples obtained by Scanning Electron Microscope (SEM) online X-Ray Energy (EDX) technique (Tulun's et al.) were analyzed by chemometry.

Pattern Recognition that is one of the main five techniques of chemometrics, and within of which Principal Component and Cluster Analysis, given under Explatory Data Analysis and Unsupervised Pattern Recognation methods, respectively were

applied for the classification of ceramics in respect of body, slip, and glaze composition. Besides, porosity data (apparent and density, total pore volume, and porosity %, for 40 samples) obtained from Tulun's et al. previous study and soluble salts data (this work, 23 samples) were analyzed with the same chemometric techniques regarding deterioration characteristics.

In experimental part, the contents of soluble salts were determined in variations of temperatures (0ºC to 35ºC) and durations (5 to 25 days) considering the average climate conditions. Prior to quantitative determination of anions (chloride, phosphate, nitrate, and sulphate) and cations (sodium, potassium, calcium, and magnesium) were examined by wet chemistry (spot tests) and then quantitative determinations were carried out by the techniques given below.

Chloride: UV Spectrophotometry and Conductometry

Phosphate: UV Spectrophotometry

Nitrate: Quantitative Test Sticks

Sulphate: Turbidimetry and Flame Photometry

Sodium, Potasium, and Calcium: Flame Photometry

Magnesium: Atomic Absorption Spectrophotometry

In addition, Saturation Coefficient, which is a pore characteristics and durability criteria for ceramics, and weights loss due to acid and base exposure (enviromental conditions) for a given sample were determined.

Result and Discussion

The concentration of chloride varied with in a large range at 20ºC for almost all soaking time except the samples of 1, 7, and 8. Unlinear relation between concentration and time, and temperature revealed the inhomogeneity in composition of some samples. Besides, the soluble amount of chloride was found to be higher than the solubility of rest of the anions.

Quantitative phosphate analysis showed that almost all samples contained phosphate after the temperature of 25ºC for all period of time. Besides, the concentration of phosphate was lower than chloride but higher than nitrate and suphate.

The extracted amount of nitrate was found to be lower than chloride and phosphate.

Sulphate was detected after the experiment carried out at 35ºC within 10 and 15 days duration. The soluble amount of sulphate became constant at 35ºC in the samples of 3, 8, and 9.

The results of cation analysis showed that concentrations of sodium, potassium, calcium, and magnesium slightly increased at 30ºC and 35ºC for every soaking period of time.

Saturation coefficient for sample 6 was found to 0.9423 and 1.2510 for 110 ºC and 220 ºC respectively.

It was seen that the weight lost as a function of time was slightly dependent on pH of the solution. In addition, the increase in the weight lost was in the similar ratio in water and acid solution.

Chemometric Analysis of body composition resulted in three major groups of samples. The first group of samples mainly comprised of Blue and White, Monochrome glazed, Golden Horn, and Damascus types of tile samples belonging to different centuries whereas the second group consisted of Sgrafitto and Miletus types. The last third group was both Sgrafitto and Monochrome glazed type of samples. Na_2O, MgO, and SiO_2 were the main oxides contributing the separation of samples regarding their body composition. However, the variables of MgO, Al_2O_3, K_2O and Fe_2O_3 were the main oxides for the separation of groups according to slip composition.

Grouping of ceramics depending on their glaze composition was concluded that there is no distinctive separation between them. The three coordinate diagrams for loadings and scores plot, and also dendograms in Cluster Analysis (CA) confirmed this result by showing the uniform distribution of each samples and variables. As a result of chemometric analysis of glaze data from Tulun's, Amara's and Tite's studies, it was found that although both Amara's and Tite's samples were clustered together with Tulun's samples, their samples did not show any significant similarities in common with each other. Apparent density and total pore volume were found to be the main variables responsible in classification of the samples regarding their porosity characteristics. Chemometric Analysis of soluble salts for 23 samples showed that high amount of chloride and nitrate ions in all the given temperatures were the responsible variables in classification. Cluster Analysis (CA) dendograms as well as three-dimensional diagrams in Principal Component Analysis (PCA) also confirmed all these results given above.

ARKEO-SERAMİKLERİN SEM-EDAX, POROZİTE VE ÇÖZÜNEN TUZLARA AİT VERİLERİNİN KEMOMETRİK ANALİZİ

ÖZET

Arkeo–seramikler üzerine yapılan çalışmalar, farklı medeniyetlerin kültürel mirasları hakkında önemli bilgiler sağlar. Ayrıca, arkeolojik seramiklerin kimyasal, mineralojik, fizikzel ve teknolojik karakteristikleri, farklı kültürlerin karışımını, dünya kronolojisini, eski ticaret yollarını ve üretim teknolojilerini ortaya çıkarmak yönünden geniş ölçüde katkılar sağlar. Bununla beraber, bu konularda araştırma yapmak, çok sayıda örnek gerektirdiğinden kolay değildir. Bundan başka, bu tür çalışmalarda çok sayıda değişkeni dikkate almak gerekir. Bu nedenle, matematik ve istatistiksel yöntemlerin uygulanması zorunludur.

Son yıllarda, arkeometri dalında bir çok bilim adamı kemometri analizini kullanmaktadır ve bu konuda çok sayıda makaleler mevcuttur. Arkeolojik seramiklerin kemometrisi hakkında yapılan geniş literatür incelemesi ülkemizde bu konuda çalışma olmadığını gösterdi.

Bu çalışmanın amacı, İznik fırınları kazılarından çıkan çok sayıdaki İznik seramiğinin, bileşim, teknoloji, kaynak, yüzyıl karakteristikleri hakkında bilgi sağlamak için kemometrik teknikleri uygulamaktır. Bu çalışma, aynı zamanda, kimyada ve diğer bilimsel ve endüstriyel alanlardaki problemleri çözmek için kullanılan ve bir çok teknikleri kapsayan kemometri hakkında fikir almak için bir misyon üstlenmektedir. Bu çalışmada, Tulun ve arkadaşları tarafından daha önce Taramalı Elektron Mikroskop (SEM) insitu Enerji Dağılımlı Spektrometrik yöntemlerle incelenen 107 hamur, 61 astar ve 75 sır örneğine ait verilerin kemometrik analizleri yapıldı. Seramiklerin hamur, astar, ve sır bileşimlerinin sınıflandırılması için kemometrinin başlıca 5 tekniğinden biri olan "Düzen Tanıma" tekniklerinden, sırasıyla "Veri İnceleme Analizi" ve "Yönetilemeyen Düzeni Tanıma" metotları içinde verilen "Temel Komponent" ve "Kümeleme" teknikleri uygulandı. Ayrıca, Tulun ve arkadaşlarının önceki çalışmasından elde dilen porozite

(40 örnek için, görünür ve bulk dansite, total por hacmi ve % porozite) ve çözünen tuzlara (bu çalışmada, 23 örnek) ait veriler, bozunma karakteristikleri yönünden aynı kemometrik tekniklerle analiz edildi.

Deneysel bölümde, çözünen tuz içerikleri çeşitli sıcaklıklar (0-35^oC) ve sürelerde (5-25 gün) iklim koşulları düşünülerek tayin edildi. Kantitatif analizlerden önce, anyonlar (klorür, fosfat, nitrat ve sülfat) ve katyonlar (sodyum, potasyum, kalsiyum ve magnezyum) yaş kimya (spot testler) ile belirlendi ve sonra aşağıda verilen yöntemler uygulanarak kantitatif tayinleri yapıldı.

-Klorür: UV Spektrofotometri ve Kondüktometri

-Fosfat: UV Spektrofotometri

-Nitrat: Kantitative Test Çubukları

-Sülfat: Turbidimetri ve Alev Spektrofotometri

-Sodyum, Potasyum ve Kalsiyum: Alev Spektrofotometri

-Magnezyum: Atomik Absorpsiyon Spektrofotometri

Ayrıca, belirli bir örnekte, seramikler için bir por karakteristiği ve dayanma kriteri olan Doygunluk Katsayısı ve asit baza maruz kalmasıyla oluşan (çevre faktörü) kütle kaybı tayin edildi.

Sonuçlar ve Tartışma

Çözünen klor miktarları 1, 7 ve 8 no' lu örnekler dışında suda kalma periyotları için 20^oC de geniş bir aralıkta değişti. Konsantrasyon ve zaman, ve sıcaklık arasındaki doğrusal olmayan ilişki bazı örneklerin bileşiminin homojen olmadığını ortaya çıkardı. Bunun yanında, çözünen klor miktarlarının diğer anyonlara göre daha yüksek olduğu bulundu.

Fosfatın kantitatif analizi 25^oC' den sonra tüm bekleme zamanları için tüm numunelerin fosfat içerdiğini gösterdi. Ayrıca çözünen fosfat konsantrasyonunun klordan düşük fakat nitrat ve sülfattan yüksek olduğu görüldü.

Çıkan nitrat miktarının klor ve fosfattan düşük olduğu bulundu.

Deneyin 35^oC de 10 ve 15 günlük süreler içinde uygulanmasından sonra sülfat tayin edildi. 3, 8 ve 9 nolu örnekler için 35^oC den sonra çözünen sülfat miktarı sabit kaldı.

Katyon analizi sonuçları, sodyum, potasyum, kalsiyum ve magnezyum derişimlerinin 30^oC ve 35^oC den sonra her bekleme periyodu için çok az arttığını gösterdi.

6 nolu örneğin doygunluk katsayısının 110^{o}C için ortamala 0,9423, 220^{o}C için 1,2510 bulundu.

Zamanın bir fonksiyonu olarak kütle kaybının çözeltinin pH'ı na çok az bağlı olduğu görüldü. Ayrıca, su ve asit çözeltilerinde kütle kaybı benzer oranda arttı.

Hamur bileşiminin kemometrik analizi örnekleri 3 temel gruba ayırdı. 1 inci grup temel olarak farklı yüzyıllara ait olan Mavi ve Beyaz, tek renk sırlı, Haliç ve Şam seramiklerini kapsarken 2 inci grup Sgrafito ve Milet tipi seramikler içerdi. Son grup ise Sgrafito ve Milet seramiklerinin her ikisinden oluştu. Na_2O, MgO ve SiO_2 örneklerin hamur bileşimlerine göre sınıflandırılmalarından sorumlu temel oksitlerdir. Örneklerin astar bileşimlerine göre sınıflandırılmasında ise MgO, Al_2O_3, K_2O ve Fe_2O_3 temel oksitlerdir.

Seramiklerin sır bileşimlerine gruplaştırılması örneklerin arasında belirgin bir ayırım olmaması ile sonuçlandı. Temel Komponent (PCA) analizi 3 lü koordinat diyagramları ve kümeleme analizi (CA) dendogramları her bir örneğin ve değişkenin üniform dağılımlarını göstererek bu sonuçları doğruladı. Tulun, Amara ve Tite' ın çalışmalarından gelen sır verilerinin kemometrik analizi sonucunda, Amara ve Tite' ın örneklerini Tulun'un örnekleri ile beraber gruplandırmasına rağmen bu örneklerin birbirleriyle önemli benzerlikler göstermediği bulundu.

Görünür dansite ve toplam por hacminin, örneklerin por karakteristiklerine göre sınıflandırılmasından sorumlu değişkenler olduğu bulundu.

23 örneğin çözünen tuzlarının kemometrik analizi, yüksek sıcaklıklarda klor ve nitrat iyonlarının sınıflandırmada etkili değişkenler olduğunu gösterdi. 3 boyutlu temel komponent analiz diyagramları kadar kümeleme analizi dendogramları da yukarıda verilen tüm sonuçları doğruladı.

1. INTRODUCTION

The ceramic samples were obtained from the excavation of different kiln sites in Iznik which is a small town on the north-west region of anatolia (Altun et al., 1997). The brilliant period of Iznik ceramics was between 15th and 17th century. Basically, they are categorized into two groups as red (also called Earthen wares) and white depending on the color of body. Thousands of ceramic finds contributed a great deal to the scientific studies, investigations of kiln types, as well as archaeological art historical investigations.

The red bodied ceramics comprise three different techniques and style. These are sigrafitto, slip, and miletus wares. The Sgrafitto technique was used in anatolia througout the middle ages by both Seljuk and Byzantine potters. This type of ceramic is well distinguished from others by its colorful glazes. In the slip decoration, a transparent glaze is applied after a white slip paste is painted on the red body. This technique leads to a lively tone obtained by Monochrome Glaze. In the Miletus ware type of ceramic, transparent glaze (sometimes colored) is applied over a white slip painted by blue color on red body.

White bodied ceramics are characterized by hard white body with and without slip, and thin transparent glaze over blue and white colored paint. They were started to produced in the 15th century. Blue and white ceramics are classified according to decoration style as Golden Horn, Damascus, and Rhodes. The traditional charecteristic of Golden Horn is spiral decoration which earlier appears on Seljuk ceramics and has no connection with Istanbul, Golden Horn potteries. Damascus type of ceramic is known by its colorful paints (like misty purple and green) on slip layer. Decoration style and colors for Iznik ceramic began to change from the second half of 16th. They were produced in coral red color with some other colors like black, green, turquoise over white body under transparent glaze begining from the second half of 16th. This kind of production is referred as Rhodes types of which are characteristic production for the second half of 16th century.

Investigation on archeo-ceramics regarding the chemical, minerological, physical, and technological characteristics comprises numerous variables and needs large number of samples. Therefore, mathematical and statistical methods have to be applied to the data obtained from such studies.

In the recent years, chemometric analysis has been used by many scientists (Mirti et al., 1994; Yap and Hua, 1994; Hall, 2001; Attanasio et al., 2001; Heimann et al., 2001). However, there is no study on the chemometric and the field of archaeo-ceramics in our country.

The goal of this study is to apply chemometric techniques on a large number of Iznik ceramics obtained from the excavation of Iznik Kiln sites in order to provide information regarding the compositional, technological, provenance and age characteristics. This work has also had a mission to have an idea on chemometry, which comprises various techniques, and used to solve problems particularly, in chemistry and other scientific and industrial fields.

Besides, it is aimed to investigate the effect of soluble salts of ceramics regarding the deterioration characteristics. Results of deterioration studies might contribute to solve the problems encountered. In the restoration and conservation of ancient ceramics. In addition a full database for ceramics can also be useful in supporting the hypothesis of archeologogists related to the age, provenance, and production technology.

The data of SEM-EDX and porosity used chemometrical analysis was taken from Tulun’s et al studies. A part of the data related to the body, slip, and glaze compositions were published in Archaeolingua, (Tulun et al., 2002). A part of porosity data was presented in the first Black Sea Basin Conference (Tulun et al., 2001). In addition, a part of results related to soluble salts were presented in 3rd Aegean Analytical Chemistry Days (Cini and Tulun, 2002).

2. THEORETICAL PART I

2. 1 Chemometry

The methods to determine the composition of compounds have been greatly improved and the number of methods has been greatly enlarged for last 20 years. These new techniques yield large amounts of data that is difficult and very complicated to evaluate, which leads problems in choosing the most suited method and strategy to obtain results as most efficiently as possible. Therefore, the necessity of mathematical and statistical techniques is inevitable. Chemometry is the dicipline within chemistry that develops methods to obtain maximum information from a data set by optimizing experimental design, data processing, calibration, quality control, and organization of the analytical process.

Chemometry have been applied a wide variety of research problems for example in the field of environmental engineering, biochemistry and medicine. In addition, it has been routinely applied in archaeometry, particularly, after improvements in computer programs related to classification techniques (Mirti et al., 1994; Mirti et al., 1990; Yap and Hua, 1994; Mirti and David, 2001; Baxter, 2001; Papageorgiou et al., 2001).

There are several chemometric techniques comprising application of various mathematical, statistical, and graphical methods. These techniques are given five groups that are Experimental Design, Signal Processing, Pattern Recognation, Calibration, and Evolunationary Signal. Each techniques has it various data analysis methods.

Experimental Design **:**The quality of the data is improved by experimental design which enables the experiment proceed optimally (Morgan, 1997). The criteria of an experimental design, first, begin with the definitions of variables that certainly affect the outcome of the experiments. Then, the environment and factors that are controlled by experiment are stated. Finally, the variables are classified according to being of little of large significance in the outcome of experiment in order to find optimum experimental conditions under which the experiment runs. Analysis of variance (ANOVA) is most often used for the assumption of significance of variables. It examines the variances in a set of data and thus determines whether a significant difference in means exists. On the basis of the variance in the data, ANOVA is assessed in two ways which are one-factor ANOVA and two-factor ANOVA. One- factor ANOVA deals with the variances between the treatments whereas two-factor ANOVA concerns the variances within the treatments. In other words, one-factor ANOVA compares multiple means of one variable but two-factor ANOVA determines the effect of one variable on another or interaction between them.

Signal Processing and Signal Improvement: The quality of the data gathered is improved by signal processing and signal improvement techniques. In other words, these techniques are performed to improve the sensitivity and precision of chemical analyses. Difficult measurements became easier by the way of these methods since they lead to extraction of more useful information from the available data. These methods, generally, are applied to distinguish between signal and noise in the system. Decomposition of complex signals into their component parts and improvement of the resolution for overlapping peaks in chromatography can be given as an example for the application of signal processing and signal techniques.

Calibration: Multivariate calibration has historically been a measure technique of chemometrics. Calibration involves connecting one (or more) sets of variables together. Usually, one set (often called a 'block') is a series of physical measurements, such as some spectra and the other contains one or more parameter such as concentrations of a number of compounds. Can we predict the concentration of a compound in a mixture spectrum or the properties of material from its known structural parameters? Calibration provides the answer. In its simplest form, calibration is simply a form of regression. The methods of calibration are Univariate Calibration (Classical and Inverse Calibration, and Intercept and Centering), Multiple Linear Regression, Principle Component Regression, Partial Least Squares, and Model Validation (Autoprediction, Cross-Validation, Independent Test Sets).

Evolutionary Signals: Some of the classical applications of chemometrics are to evolutionary data. Such a type of information is increasingly common, and normally involves simultaneously recording spectra whilst a physical parameter such as time or pH is changed and signals evolve during the change of this parameter. In the modern laboratory, one of the most widespread applications is in the area of coupled chromatography, such as HPLC-DAD (High Performance Liquid Chromatography-Diode Array Dedector), LC-MS (Liquid Chromatography-Mass Spectrometry), and LC-NMR (Liquid Chromatography-Nuclear Magnetic Resonance). A chromatogram is recorded whilst a UV/Vis, Mass or NMR spectrum is recorded. The information can be presented in matrix form, with time along the rows and wavelength, mass number or frequency along the columns. Multivariate approaches can be employed to analyze these data, and it is possible to obtain huge quantities of information with modern laboratory computers very rapidly. All the above given approaches are considered under evolutionary signals technique of chemometrics.

2.2 Pattern Recognition Techniques

One of the first and most successful technique in chemometrics is Pattern Recognition. For example, is it possible to use measurements of heavy metals to discover the source of pollution in a river, can a chromatogram be used to decide on the origin of wine, if so what main features in the chromatogram distinguish the different wines? and is it possible to determine the time of year the wine grown? Can IR spectra be used to classify compounds in to ketones and esters?

The group of measurements that describe each sample in the data is called a pattern. and therefore, the term pattern recognition means determination of the property of interest by assigning a sample to its respective category. Pattern recognition techniques detect the hidden structure and similarities in the data set.

There are several groups of methods for chemical pattern recognition. These methods are Explatory Data Analysis (EDA), Unsupervised Pattern Recognition (UPR), Supervised Pattern Recognition (SPR), Multiway Pattern Recognition (MPR).

- EDA consist mainly of the techniques of Principle Component Analysis (PCA) and Factor Analysis (FA). The statistical origins are in biology and psychology.
- UPR is a more formal method of treating samples, normally consisting of Cluster Analysis (CA).

- SPR has a large number of methods, mostly aimed at classification multivariate statisticians have developed many discriminant function, some of relevance to chemist.

- MPR is the method which has interest over the past decade. MPR is concerned with three-way chemical data whereas most traditional chemometrics is concerned with two-way data, often represented by matrices. In MPR, instead of organizing the information as a two-dimensional array, a three-dimensional “tensor” or box is used. MPR method is mostly used for an environmental chemical experiment.

In this thesis, Principle Component (Explatory Data Analysis method of Pattern Recognation, EDA), and Clustering (Unsupervised Pattern Recognition, UPR), which are the most particular techniques for the data analysis of archaeometric studies, were used.

2.3 Principal Component Analysis (PCA)

History: There are numerous claims to the first use of PCA in the literature (Brereton, 2003). Probably the most early paper was by Pearson in 1901. The fundamental ideas based on approaches well known to physicists and mathematicians for much longer, namely those of Eigen Analysis. In fact some school mathematics syllabuses teach ideas about matrices which are relevant modern chemistry. An early description of the method in physics was by Cauchy in 1829. It has been claimed that the earliest non-specific reference to PCA in the chemical literature was in 1878, although the author of paper almost certainly did not realize the potential, and was dealing mainly with a simple problem of linear calibration.

PCA, which is the most widespread multivariate statistical technique, enables methodologists both to discover or to reduce the dimensionality of the data set of interest and to identify new meaningful underlying variables that have special properties in terms of variances (Anderson, 1984; Brereton, 1992).

This technique involves a mathematical procedure in which a number of possibly correlated variables are transformed into a smaller number of uncorrelated variables that are called principal components. Algebraically, principal components are particular linear combination of original measurement variables. The first principal component accounts for as much of the variability in the data as possible, and each succeeding component accounts for as much of the remaining variability as possible. For the explanation of information present in the data, only two or three principal components are necessary.

2.3.1 Preprocessing

PCA is applied directly on the raw data very rarely because of the possibility of some properties for principal components such as orthogonality (the correlation coefficient between two components being equal to 0) are no longer valid for raw data. Therefore, data preprocessing, or preparing information prior to application of statistical evaluation is sometimes necessary. This process can be defined as preparation of data prior to chemometric analysis. It is often called scaling and generally performed before PCA. The most appropriate way of scaling depends on the aim of the analysis.

2.3.1.1 Standardization and Normalization

Standardization and normalization are the main methods of data preprocessing. Standardization is a common method for data scaling and occurs after mean centering in which each variable is divided by its standard deviation after subtracting the mean from each variable. Standardization organizes each variable in a way that they all approximately have same scale. It is also useful in cases where one or more variables are measured on very different scales, such as bond lengths and dipoles. Normalization is, simply, scaling the variables to a constant total, usually 1 or 100. In some cases, both combination of two methods, standardization and normalization, is possible to apply. For example, first to normalize and then standardize a data set. Logarithmic scaling can be also used if there are large variations in the raw data set. Normalization of over a selective part of the variables is sometimes used. This method could be useful when there were several types of measurement.

2.3.2 Eigen Analysis

The mathematical technique used in PCA is called Eigen Analysis. The first step in PCA is the calculation of covariance (or correlation) matrix for the variables and then performing an Eigen Analysis on this matrix. If a few variables have very large values that are one or two orders of magnitude greater than the others, the analysis will be dominated by these few large variables. In these situations, the correlation matrix[•] is used instead of covariance matrix (Baxter, 1995). This procedure is known as normalization of the data prior to PCA.

The eigenvalues of the square correlation (or covariance matrix) may be found by finding the roots to the determinant equation:

$$|C - \lambda I| = 0 \tag{2.1}$$

where λ are the eigenvalues of the matrix and I is the identity matrix in which all diagonal elements are 1 and all off-diagonal elements are zero. The roots of the determinant equation are eigenvalues that are a measure giving information about the size of each component. From each of the roots, an eigenvector may be calculated (Hecht, 1990). The eigenvector associated with the largest eigen value has the same direction as the first principal component. The eigenvector associated with the second largest eigenvalue determines the direction of the second principal component and so on. Therefore, the principal components are said to be characteristic vectors of correrlation (or covariance) matrix. The sum of the eigenvalues equals the trace of the square matrix and the maximum number of eigenvectors equals the number of rows (or columns) of this matrix. If the eigenvalues and associated eigenvectors are sorted in decreasing sequence of eigenvalues, the principal components are sorted in order of importance. Thus, the first principal component represents the component that has the greatest variance.

2.3.3 Determination of Significant Principal Components

2.3.3.1 Size of Eigenvalues

The second step in PCA is the determination of the number of the most significant principal components. Determination of how much of the variance in the principal components represents variance in the data is necessary for determination what numbers of principal components are significant. Since the eigenvalue of the eigenvector is the variance of the principal component the total variance of all of the principal components is

$$\text{variance}_{\text{total}}: \sum_{i=1}^{p} \lambda_i \tag{2.2}$$

[•] The covariance matrix from standardized data equals the correlation matrix.

where the p and λ are the numbers of components and eigenvalues respectively. Then the percentage of the variance represented by any eigenvector is

$$f_j = \lambda_j / \sum_{i=1}^{p} \lambda_i \tag{2.3}$$

and the sum of all f_j s (cumulative percentage) is equal to 1.

When the cumulative percentage is less then for a certain percentage of the data or it exceeds the predetermined limit, the numbers of principal components are found.

2.3.3.2 Cross-Validation

Cross-validation is another method for determining the number of significant components in PCA. In this method, the significance of the each principle component is tested out by determining how well an "unknown" sample is predicted. The steps of cross-validation starts with removing each sample once from the data set and then continue to the prediction of the remaining. This cycle is repetead until all samples have been removed once. However, removing a block of objects instead of removing one object and then doing prediction of remaining could can be applied to speed up the cross validation algorithm.

2.3.4 Graphical Representation

Graphically, the principal components are arranged in a coordinate system that has statistical properties. The axis with the greatest variance represents the first principal component axis since the eigenvector associated with the largest eigenvalue has the same direction as the first principal component. Therefore, it can be said that first few principal component axises represent the greatest amount of variation in the data set. There are many ways of visualizing principal components such as loadings and scores plots.

Loadings Plot (LP): Each variable in the original data matrix has a component loading associated with it in the eigen vector. These loadings are a measure of the relative importance of each variable in the extracted principal component axis. Thus, LP shows impact of variables on each samples. In other words, it provides a detailed information about which variable are most associated with which sample.

Scores Plot (SP): Multiplication of the component loadings by the original data gives a set of scores for each principal component axis. Plotting of the score of one principal component to another gives SP in which the individual points indicate the samples. The relation of samples can be easily interpreted by this plot.

All scores and loadings vectors have the property of orthogonality which means the correlation coefficients between any two scores or two loadings vectors are equal to 1 and the angle between any two scores or two loadings vectors equal 90^o.

2.4 Cluster Analysis (CA)

CA is among the most versatile of all multivariate statistical methods. The samples of no known information about the number and location of groups are clustered to where the sample belongs. It is defined as the process yield a data description in which samples can be classified into groups where elements of the groups share properties in common.

Chemistry have classification schemes to identify compounds, for instance, grouping a set of chemical compounds according to its molecular weight, solubility in solvents, whether it contains a specific element or not. The classification can also be accomplished based on composition of samples. A large number of chemical compounds are divided into smaller sections considering such classifying factors with the help of CA.

2.4.1 Similarities and Distances

A common approach to apply cluster analysis is to do, first, compute a table or relative similarities (or dissimilarities) between all samples, and second, to use this information to combine the samples into groups. The idea of the distance between two or more samples can be used as a measure of the similarity (or dissimilarity) between two samples (Graham, 1993; Duda et al., 2001). The distance between samples in the same clusters is less than the distance between samples in different clusters, which means the samples in one cluster are more like one another than like samples in other clusters. The table of relative similarities is called a proximity matrix. It is a suitable measure and gives matrix of distances between all pairs of samples.

There are different kinds of distance techniques that can be based on a single dimension or multiple dimensions. The two most popular measures of similarity are Euclidian Distance and Mahalonobis Distance.

Euclidean Distance (ED): ED, which is defined as the geometric distance in the multidimensional space, is the most commonly chosen type of measure of similarity. It is simply computed as

$$\text{distance}(x,y) = \sqrt{\{\sum_i (x_i - y_i)^2\}} \quad (2.4)$$

where x and y are the samples.

If we consider the situation in which two samples may each be described by a set of two variables that are binormally distributed, then the distance between two samples may be described by the ED (Figure 2.1)

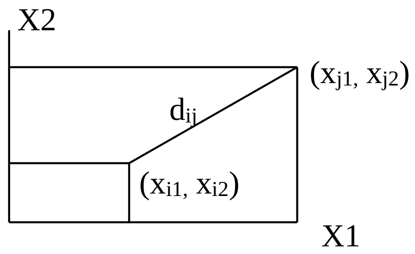

Figure 2.1: Geometric representation of the ED in which there are two samples represented.

The distance between the two samples is then

$$d_{12} = \left[\left\{\sum_{n=1}^{2} (x_{1n} - x_{2n})^2\right\}\right]^{½} \quad (2.5)$$

Calculation of the ED may be extended to any number of potential data with any number of data variables (N) describing each sample. The expression where gives the distance between samples i and j is simply expressed as

$$d_{ij} = \left[\left\{\sum_{n=1}^{N} (x_{in} - x_{jn})^2\right\}\right]^{½} \quad (2.6)$$

where there are N measurements, and x_{mn} is the n^{th} measurement on sample m.

Samples in the same sub-set, representing a cluster, have smaller distance value that means that they are more similar to each other. In other words, the smaller this value, the more similar the samples, so this distance measure works in an opposite manner to the correlation coefficient. Although correlation coefficients vary between –1 and +1, ED has no limit. The equation is also represented in matrix format as follows;

$$d_{ij} = (x_i – x_j).(x_i – x_j)' \qquad (2.7)$$

where i and j are the samples and they are row vectors.

ED method has certain advantages for example the distance between any two samples is not affected by the addition of new samples to the analysis. However, the distance can be greatly affected by differences in scale among the dimensions from which the distances are computed. Another problem with this particular type of description of a data system is the probability of collinear relation of two or more of the variables. Besides, if one or more variables are more variable then the other variables, then it will clearly dominate the distance. Consequently, the results of CA may be very different.

In this work, Cluster Analysis was applied on the basis of Euclidean Distance using Single and Complete Linkage Methods.

Mahalonobis Distance (MD): This method is popular with many chemometricians and it is more satisfying measure of the distance between two samples. It simply defined as the distance of a sample to the center of a group in an multi-dimensional space (Maesschalck et al., 2000). MD is very useful for determining whether a given data record is out of agreement with the rest of the data records for a given sample. Similarly, it is also useful to determine how far a single sample is from the center of set of samples that has been determined to be close together.

This particular measure is scalar and is expressed as the product of

$$d_{ij} = \left[\sum_{r=1}^{p} \sum_{s=1}^{p} (\upsilon_{ri} – \upsilon_{rj}) c_{rs} (\upsilon_{si} – \upsilon_{sj})\right]^{½} \qquad (2.8)$$

where the υ_{ri} is the mean of the r^{th} variable in the i^{th} sample. The rest of the means are similarly described, except being described for the j^{th} variable of the s^{th} sample. c_{rs} is the element of the r^{th} row and the s^{th} column of the inverse of the covariance matrix of the p variables.

MD between two samples i and j can be also defined in matrix format as follows;

$$d_{ij} = (x_i - x_j). C^{-1}. (x_i - x_j)' \quad (2.9)$$

where C is the variance – covariance matrix of the variables which is symmetric about diagonal of dimensions NxN whose elements represented the covariance between any two variables. As it is seen from the equation, the MD is very similar to ED except that the inverse of the C, C^{-1}, which is inserted as a scaling factor.

MD method takes into account that some variables may be correlated and so measure more or less the same properties. In other words, it takes into consideration the possible correlation between two or more of the variables in the samples, since it is calculated using the inverse of the variance – covariance matrix of the data set. However, this method cannot easily be applied where the number of the variables exceeds the number of the samples because the variance – covariance matrix would not have an inverse and computation of it can cause problems. Therefore, the number of samples in a data set has to be larger than the number of variables in order to apply MD method otherwise there are insufficient degrees of freedom for measurement of this parameter. When the investigated data are measured over a large number of variables, they can contain much correlated information. This situation is so-called multicollinearity in the data set and leads to a variance-covariance matrix that cannot be inverted.

2.4.2 Linkage

The second step in cluster analysis is to combine the samples into groups based on the distances between those samples defined by the chosen distance measure.

There are various possibilities to link samples together but the most common linkage technique is "Agglomerative Hierarchical Clustering" analysis where single samples are gradually connected to each other in groups. In the agglomerative methods, every sample being in its own subset makes clusters, and then these clusters link with the closest clusters. These methods can be regarded as a useful descriptive method for an initial investigation of the data. Some of the principle ways of agglomerative clustering methods are Average Linkage, Ward's method, Single Linkage (Nearest Neighbor), and Complete Linkage (Farthest Neighbor) methods.

Average Linkage: In this method, the distance between two clusters is calculated as the average distance between all pairs of samples in the two different clusters. In other words, groups are fused according to their average distance between pairs of samples in the respective sets. There are, in fact, two different ways of doing this. The both methods are equivalent in the event of size of each groups are equal. These two different ways of average linkage is unweighted pair – group average and weighted pair – group average.

The equations expressing the unweighted pair – group average and weighted pair – group are given in below, respectively.

$s_{AB} = (n_A\, s_A + n_B\, s_B) / (n_A + n_B)$ (unweighted pair – group average) (2.10)

$s_{AB} = (s_A + s_B) / 2$ (weighted pair – group average) (2.11)

where group A consists of n_A samples and group B of n_B samples.

Ward's Method: This method is distinct from all other methods because it uses an analysis o variance (ANOVA) approach to evaluate the distances between clusters. It attempts to minimize the sum of squares of any two clusters that can be formed at each step.

Single Linkage (Nearest Neighbor): In this method, the distance between two clusters is determined by the distance of the two closest samples in the different clusters. In other words, it computes the distance between two subgroups as the minimum distance between two members of the opposite groups. The similarity of the new group from all other groups is then given by the highest similarity of either of the original samples to each other sample.

Complete Linkage (Farthest Neighbor): In this method, the distances between two clusters are determined by the maximum distance between any two samples in the different clusters. It is the opposite of single linkage and the lowest similarity is used to link the subgroups. Complete linkage method usually performs quite well in cases when the two samples actually form naturally distinct groups.

The presentation of the results of linkages in the form of tree diagram is the final step of clustering analysis. A tree diagram that depicts the results of clustering is called a dendogram, which organizes the samples according to their similarities in a row and shows how the samples are grouped. The branches of the tree are drawn with lengths that are proportional to the distance between the clusters. If two samples are very similar, they are next to each other, and apart as they become more divergent. A simple example of dendogram is given in Figure 2.2.

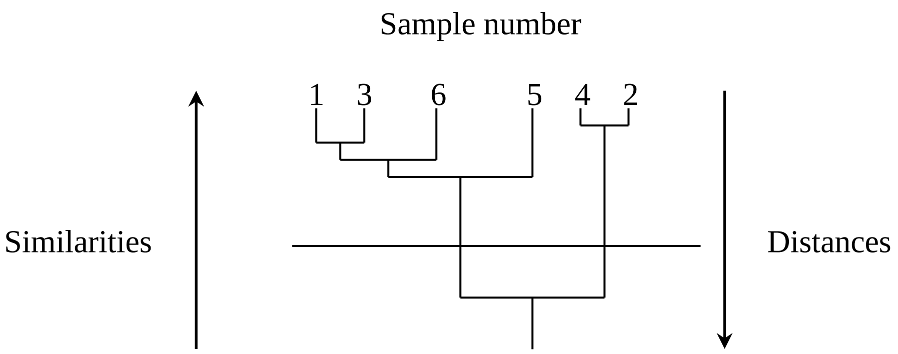

Figure 2.2: A dendogram illustrating two clear groups

However, it is possible to obtain different dendogram result upon using different linkage methods. A good approach is to perform several different methods of cluster analysis and compare the results. If similar groups remain, no matter which method is employed, we can rely on the results.

3. THEORETICAL PART II

3.1 Deterioration of Ceramics

Materials made of ceramic are all hard, brittle, and fragile materials that have been used since ancient times as decorative or adornment on the walls of various buildings. Although these materials have excellent durability, they are subject to deterioration to an extent. Restoration and conservation of monuments, buildings, mosques that are adorned by Iznik tiles, and wares materials in museum are inevitable in order to maintain the cultural heritages of our country. Deterioration of ceramic materials results from several mechanisms that are the function of composition, soluble salts, pore structure, and production technology.

3.2 Effects of Composition and Production Technology on Deterioration

Ceramic materials are made up of a mixture containing Na_2O, MgO, Al_2O_3, SiO_2, K_2O, CaO, Fe_2O_3 as main components. After combination of these basic materials and variety of processes to shape, ceramic is fired in a kiln and then allowed to air-dry slowly. The pattern of properties at different firing temperatures and extent of firing is distinctive for each raw material used in production so that firing temperature varies regarding to chemical composition. Firing is a key step in production since the physical and chemical structure of ceramic changes and thus extent of firing determine the major characteristics of ceramic. Ceramic takes on solid, hard, and brittle characteristics during firing processes. Different firing temperatures results in production of ceramics with different range of hardness and porosity that is a factor for determinining the susceptibility of ceramic materials to which of deterioration mechanism. Pore structure and variation in pore sizes and types (closed or sealed pores, channel pores, blindalley pores, loop pores, pocket pores with narrow neck, micro pores) have also an influence on deterioration since all the pores are subject to gases attack, such as air, water vapor, sulphur dioxide or trioxide, carbon monoxide or dioxide, oxygen, hydrocarbons.

Deterioration types of body related to composition and production technology are called as cracking, warping, spalling or delamination, sagging, and bloating. Besides, deterioration types of glaze regarding as composition and production technology can be also explained by crazing, shivering, crawling, pitting, blistering, and devitrification. These most common deterioration types are summarized as follows.

3.2.1 Deterioration Types of Body

Body parts of the ceramic materials can undergo cracking, warping, spalling or delamination, sagging, and bloating during firing-cooling cycle in the production process. It is possible to occur shrinkage cracks in the ceramic body unless the air-drying process is done carefully. Cracking is caused by cooling the object too quickly. Warping occurs due to uneven heating or cooling of the object. If the firing temperature is not high enough, spalling or delamination occurs. Similarly, firing at a temperature that is too high for the clay body results in sagging. Bloating may occur upon heating rapidly in which the gases formed during firing do not have enough time to be released and are trapped in the body.

Potters, very often, apply slip which is a thin layer of colored or white clay to the surface of the ceramic body during firing process or after firing has finished. This addition make ceramic not only be less porous but also decorative.

3.2.2 Deterioration Types of Glaze

Glaze, varying widely in appearance, is vitrified surface coatings over slip or body. It also has an influence on color and quality of ceramic. It can be colored with any of the coloring oxides used in slips. Crazing, shivering, crawling, pitting, blistering, and devitrification are common deterioration kinds in glazes.

Glaze is subject to crazing which is the development of a fine network of cracks on the finished glaze surface immediately or much later (days or months) after firing. Over firing and rapid cooling, are the main reasons for crazing. Glazes are molten and spread over body in the kiln during firing but while the object cools a tension develops in the glaze, which results crazing. The mechanism of crazing depends on coefficient of expansion that is the value expressing the relative tendency of solids to expand and contract upon heating and cooling. In the case of crazing, the glaze contracts more than the body on cooling. In other words, crazing occurs if the coefficient of expansion is high for the glaze relative to body.

Table 3.1. Coefficient of Expansion Values for Some Oxides (Rhodes, 1966)

SiO_2	0.05 x 10^{-7}, per °C, linear
Al_2O_3	0.17
B_2O_3	0.66 (for small amounts)
Na_2O	4.32
K_2O	3.90
PbO	1.06
ZnO	0.07
CaO	1.63
MgO	0.45
BaO	1.73

Crazing can be prevented by either thinner application of the slip or change in glaze formulation (Storch, 1986). Therefore, increasing the amount of oxides with low coefficient of expansion such as SiO_2, Al_2O_3, and B_2O_3 or decreasing the amount of oxides with high coefficient of expansion such as Na_2O and K_2O can be accomplished by reduction of thermal expansion of the glaze hence it prevents crazing (Larsen et al., 1999). Table 2.1 gives the coefficient of expansion for the oxides most widely used in ceramic glazes.

Shivering is known as opposite of crazing. Unlike crazing, the glaze may peel or flake off the surface in the case of shivering. Increasing the high expansion oxides in the glaze make it contract more than body during cooling, which minimize shivering.

Crawling, especially, occurs when glaze is applied over a dirty or greasy clay surface since the raw glaze will be in poor contact with the body. The area in which glaze is not in good contact will loosen, crack, and fold back thus it leaves a bare spot during the early stages of heating in the kiln. In such a case, glaze does not adhere properly to the surface of body. Too viscous glaze, high clay content, and lack or too much of adhesiveness are some other possible causes for crawling. Reducing feldspar to decrease viscosity, addition or reduction of gum to glaze formula as an adhesive can minimize the effect of crawling providing to hold the glaze in closer contact with the body in the early stages of firing.

Pitting can vary in size from pinholes to larger spots. All glazes contain some volatile compounds that are released during firing. If firing temperature is raised and lowered, too quickly these volatile materials are not completely released before the glaze solidifies. In this case, air pockets are formed in the surface of body and they pop through the molten glaze leaving a small break in the glaze part. Pitting can be minimized by carefully adjusting the firing cycle, for example, lengthen the firing duration, application of thinner glaze, adding more flux to reduce viscosity of glaze, and decreasing the ZnO content which causes excessive gassing.

Blistering takes place in the case of trapping air between the glaze and the body. It generally occurs due to application of thick glaze. Prevention of blistering is simply application of thinner glaze. In addition, decreasing the amounts of compounds such as borax, potassium carbonate, magnesium sulfate, and fluorine that produce excessive gassing in the stage of firing can also minimize blistering of glaze.

Formation of small areas of crystal growth in the amorphous structure is known as devitrification. These crystals can be either produced due to slow cooling or containing high amounts of crystal forming compounds in the glaze formula, for example, high silica, alumina, calcium, titanium, and zinc. Therefore, it is possible to prevent devitrification by accelerating the cooling or reducing the amount of compounds that contribute to crystallization.

3.3 Effects of Soluble Salts on Deterioration

The most common causes for the deterioration and damage of historic ceramics or tiles are water-related problems. Salt crystallization and freezing-thawing are the important physico-chemical reactions which exert additional influence on deterioration. Archaeo-Ceramics have absorbed soluble salts (chloride, phosphate, nitrate, and sulfate) from the burial. Ground water, seawater can carry these salts into pores of ceramics during burial over years, and accumulate in pores when water evaporates. However, there is no agreed standard for what level of salt removal is valid for the determination of soluble salts since the amount of salt that cause damage can vary from sample to sample. Recent studies suggested that safe level could be considered the lowest level. This level depends on many factors, such as; chemical an mineralogical composition of ceramics, types and amount of soluble salts, porosity of the object, environmental conditions and so on.

3.3.1 Salt Crystallization

Salt crystallization occurs with mainly two mechanisms. In the first mechanism, the salt crystallize within the pores of the material and repeated temperature cycling due to environmental conditions such as seasonal effects cause an expansive force. As a result, the crystal break occurs because of the significant local pressure within the pores and the surface spalls off and flakes. This pressure together with the capillary action also causes migration and transportation of salts towards the surface through the pores or channels. The relative amount and character of the salt crystals varies related to the nature and source of the soluble salts such as chloride, sulfate, sodium, calcium, and magnesium. When the humidity is low, the salt-bearing water evaporates before reaching the surface of the ceramic leaving behind salt deposits. If deposition of salt takes place on the surface of material, a white powder forms on the surface. This phenomenon is called as efflorescence. The relative humidity and rate of evaporation are the main physical factors which cause the formation of salt crystals.

The second deterioration mechanism depends on the reaction of acids, produced by pollutant gases coming from both the burial wood and wood products and from atmosphere, and salts within the pores. This result in crystal forming in the pores so the crystal growth proceeds and eventually breaks down the internal structure of the ceramic.

3.3.2 Freezing and Thawing

Freezing and thawing follows a mechanism of physico-chemical reaction depending on environmental conditions (climate, temperature, humidity), chemical attack of water and water absorption of ceramic material (Rivera and Karbhari, 2002). For instance, materials that are not as hard-fired are mostly suspectible to deteriorate if subjected to constant moisture. A failure similar to salt crystallization takes place as a consequence of volume expansion of water, and hydraulic pressure occurs within the pores by freezing.

Porosity, determined by weight percentage of water absorption, and pore structure are the certain keys to these type of damage. The greater the water absorption, the higher porosity thus the greater the possibility of freezing and thawing mechanism (Butterworth, 1964; Robinson et al., 1977).

Saturation coefficient is a criteria, which gives an idea about the durability of ceramic tiles. It is a measure of the proportions of large pores and small pores. Although saturation coefficient below 0.75 gives good assurance of durability, there are old ceramic examples with excellent durability having values above 0.75. for such an ancient ceramic, other factors of deterioration are possibly predominant rather than pore structure.

3.4 Other Factors of Deterioration

Mismatch in dimensional characteristics of ceramic samples and structure of wall component can be a deterioration reason, too. The wrong mortar type can damage the ceramic material and ultimately makes it to become loose. The result of weakened or deteriorated grout or mortar, which allows the tiles to become loose.

In addition to the factors discussed above, the following kinds of damage take place in deterioration of ceramic materials.

- Crizzling: It occurs mainly because of lime content (CaO). Humidity reacts with the glaze containing insufficient amount of lime leading to weakening of structure and serious cracks on the surface.
- Weeping: It results from hydrolysis of sodium or potassium in glaze structure. As a result of this hydrolysis, sodium or potassium hydroxide accumulate on the surface and give a greasy feeling. These compounds can also react with CO_2 in the air to produce carbonates leading to absorption more water and deterioration (Odigure, 2002).
- Iridescence: It is a rainbow like effect due to air filled layers of glaze in case of diffraction of light.

4. EXPERIMENTAL PART

4.1 Chemicals and Solutions

i-Hydrochloric Acid

HCl (Carlo Erba) was used in necessary treatments.

ii-Nitric Acid

HNO_3 (Merck) was used in necessary spot tests.

iii-Silver Nitrate

$AgNO_3$ (Merck) was used to prepare 100 ppm Ag^+ solution

vii-Amonium Moliybdate

8.75 g of $(NH_4)_6Mo_7O_{24}.4\ H_2O$ (Merck) was dissolved in distilled water and diluted to 250 ml after addition of 50 ml of NH_4OH (Fluka).

iv-Stannous chloride

It was prepared freshly before each treatment. 2.8075g of $SnCl_2.6H_2O$ (Merck) were dissolved in a small amount of distilled water with the addition of a piece of solid Sn (Merck). This solution was allowed to stand for 1 day and then diluted to 100ml with distilled water.

v-Barium Chloride

1N barium chloride solution was prepared from $BaCl_2.2H_2O$ (Fluka).

vi-Miller's Reagent

Approximately 1.85 g of $AgNO_3$ (Merck) and 25 g of KNO_3 (Merck) were dissolved in distilled water. Then, 17 ml of NH_4OH (Fluka) was added. This final solution was diluted to 1 lt with distilled water.

vii-Dextrin Solution

It was prepared freshly before each treatment. Analytical grade solid dextrin was used for preparation of 1% dextrin solution.

viii-Amonium Ethylenediaminetetra-Acetate Solution

5g of analytical grade ethylenediaminetetra-acetic acid (EDTA) was dissolved in 100 ml of distelled water, and 50 ml of NH_4OH (Fluka) was added and diluted to 500 ml with distilled water.

ix-NaCl-HCl Solution

60 g of NaCl (Merck) was dissiolved in 200 ml of distilled water, and 5 ml of concentrated HCl (Merck) and diluted to 250 ml with distilled water.

x-Glycerol-Alcohol Solution

1 volume of glycerol (Technique) was mixed in 2 volumes of absolute ethanol (Merck).

4.2 Standards

i-Sodium Chloride

A stock solution of Cl^- (100 ppm) was prepared from NaCl (Merck) and it was diluted to desired concentration for preparation of standard solutions in a range of 5-30 ppm.

ii-Potassium Dihydrogen Phosphate

A stock solution of PO_4^{3-} (30 ppm) was prepared from KH_2PO_4 (Merck) and it was diluted to desired concentration of standard solutions in a range of 0.6-3.0 ppm.

iii-Sodium Sulphate

1000 ppm stock solution of SO_4^{2-} was prepared from $Na_2SO_4.10H_2O$ (Carlo Erba). Standard solutions in a range of 5.0-30.0 ppm were prepared from this solution upon dilution with distilled water.

iv-Sodium Nitrate

100 ppm stock solution of Na^+ (100 ppm) was prepared from $NaNO_3$ (Carlo Erba). Standard solutions in a range of 1.0-5.0 ppm were prepared from this solution upon

dilution with distilled water.

v-Potassium Nitrate

A stock solution of K^+ (100 ppm) was prepared from KNO_3 (Fluka) and it was diluted to desired concentration of standard solutions in a range of 1.0-5.0 ppm.

vi-Calcium Nitrate

100 ppm stock solution of Ca^{2+} (100 ppm) was prepared from $Ca(NO_3)_2.4H_2O$ (Merck). Standard solutions in a range of 1.0-5.0 ppm were prepared from this solution upon dilution with distilled water.

vii-Magnesium Nitrate

A stock solution of Mg^{2+} (100 ppm) was prepared from $Mg(NO_3)_2.6H_2O$ (Merck) and it was diluted to desired concentration of standard solutions in a range of 1.0-5.0 ppm.

4.3 Instruments

The following instruments were used in measurements.

Circulation Ultrathermostat, J. P Selecta, Digit-Cool 3001373

Quantitative test sticks, Quantofix.

UV-Visible Spectrophotometer, Jenway 6105.

Conductometer, InoLab WTW, Level 2.

Flame Spectrophotometer, Analytic Jena Vario 6 Type

Atomic Absorption Spectrophotometer,Unicam, 929.

Turbidimetry, InoLab WTW, 555.

4.4 Experiments

4.4.1 Determination of Soluble Salts

A group of 10 ceramic samples (from 1to 10 in Table B.1) was immersed in a known volume of distilled water and left to soak. The duration of soaking were taken as 10, 15, 20, 25 days for each temperature studied. There is no agreed standard for what level of salt removal is valid for the determination of soluble salts since the salt amount that cause damage can vary from sample to sample. However, recent studies suggested that safe level could be considered the lowest level, which depends on many factors, such as; types and amount of soluble salts, porosity of the object, environmental conditions and so on. Therefore, variations of temperature were chosen between 0-35^{o}C assuming different climate condition in this experiment. At the end of each soaking period, ceramic pieces were removed from the solution and then it was immersed in clean water for the next soaking. Determinations of concentration of soluble anions (chloride, phosphate, nitrate, and sulphate) and in some case cations (sodium, potassium, calcium, and magnesium) were carried out for all solutions. Spectrophotometric and conductometric methods were used for quantitative determination after qualitative spot tests.

4.4.1.1 Spot Tests

Chloride, phosphate, and sulphate were determined preliminarily for quantitative analysis of each soaking solution.

Chloride ion was determined with the presence of its white precipitate, AgCl, formed by mixing 2 drops of soaking water solution, 4 drops of 3M HNO_3, and 1 drops of Miller's Reagent.

Similarly, phosphate ion was determined with the presence of its blue molybdenum complex formed by addition of 5 drops of ammonium molybdate and 1 drops of stannous chloride to 5 drops of soaking water solution.

Qualitative determination of sulfate was carried out with the presence of its white precipitate, $BaSO_4$, formed by addition of 3 drops of barium chloride and 1 drops of 6M HCl to 5 drops of soaking water solution.

4.4.1.2 Quantitative Determination of Cl^-

Determination of chloride ion, Cl^-, was performed by UV spectrophotometry. The absorbance of colloidal AgCl solution that maintained by the addition of dextrin solution (1%). All standards and analytes were measured at 625 nm. Calibration curves and results are shown in figures from A.7 to A.11 and table 4.1 respectively. Determination of Cl^- content was also performed by conductometric titration of soaking solutions for samples 4, 7, and 9 after 10, 25, 20 days immersions at 0^0C.

Titration curves and the results are given in figures 4.1-4.3 and Table 4.2 respectively.

Table 4.1. Results of Cl^- by UV Spectrophotometry

Sample No		1	2	3	4	5	6	7	8	9	10
Temp.	Days	Concentration of Cl^- as ppm									
0ºC	10	nd	nd	23.10	230.20	1.80	9.60	149.10	15.90	191.00	19.20
	15	nd	nd	32.82	232.31	2.05	17.95	163.10	22.65	247.65	24.10
	20	nd	nd	34.48	232.79	7.47	18.97	164.37	27.59	342.24	24.14
	25	12.50	19.38	55.73	240.88	10.60	28.97	178.72	34.46	361.62	34.14
10ºC	10	12.60	19.51	56.02	247.39	13.57	30.76	179.00	38.97	361.75	34.30
	15	12.60	19.51	56.02	247.40	13.60	31.80	179.00	38.97	361.80	34.30
	20	12.60	23.79	56.02	252.31	13.60	31.80	179.00	38.97	364.25	34.30
	25	17.73	24.63	56.02	273.04	13.60	31.80	179.00	45.38	364.36	35.58
20ºC	10	22.86	38.73	63.69	276.89	13.60	44.62	186.69	60.76	378.47	35.58
	15	22.86	46.42	66.25	287.15	21.29	47.61	188.44	60.76	380.95	35.58
	20	22.86	47.33	67.99	287.64	21.66	48.92	188.44	60.76	380.95	36.12
	25	22.86	51.63	68.53	296.25	21.67	58.60	188.44	61.84	385.79	36.66
25ºC	10	22.86	53.06	68.51	298.06	21.67	58.82	188.44	62.32	386.16	38.20
	15	22.86	54.62	69.03	303.27	21.67	59.86	188.44	63.89	386.68	38.20
	20	22.86	54.62	69.03	303.27	22.71	59.86	189.36	63.89	386.68	38.20
	25	22.86	54.62	69.03	303.27	22.71	60.90	189.36	63.89	386.68	38.20
30ºC	10	30.97	62.73	69.03	303.27	22.71	77.12	189.36	63.89	398.39	51.26
	15	30.97	62.73	82.54	303.27	22.71	77.12	189.36	66.14	398.39	51.26
	20	30.97	62.73	82.54	303.27	22.71	77.12	189.36	66.14	398.39	51.26
	25	30.97	62.73	82.54	303.27	22.71	77.12	189.36	66.14	398.39	51.26
35ºC	10	30.97	62.73	82.54	303.27	22.71	86.96	189.36	66.14	398.39	51.26
	15	30.97	62.73	82.54	317.04	22.71	86.96	189.36	66.14	405.28	56.18
	20	30.97	62.73	82.54	317.04	22.71	86.96	189.36	66.14	405.28	56.18
	25	30.97	62.73	82.54	317.04	22.71	86.96	189.36	66.14	405.28	56.18

Table 4.2. Results of Cl^- by Conductometry

Sample No		4	7	9
Temp.	Days	Concentration of Cl^- as ppm		
0ºC	10	230.51	148.18	148.18
	15	230.51	164.64	246.97
	20	246.97	164.64	355.64

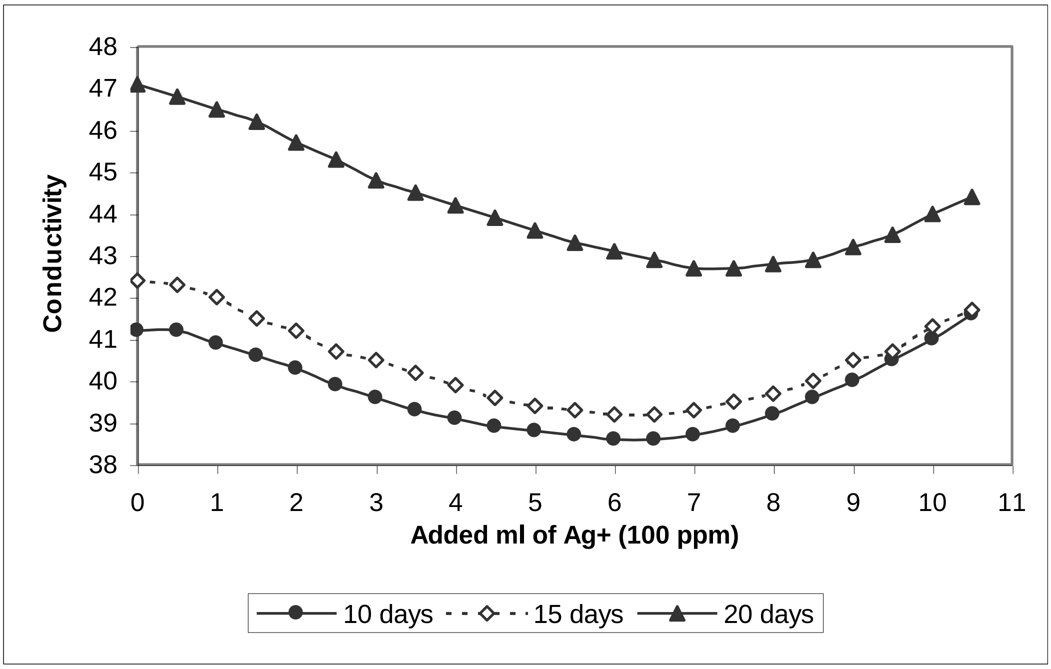

Figure 4.1: Conductmetric titration plot of sample 4 for immersion at 0^oC

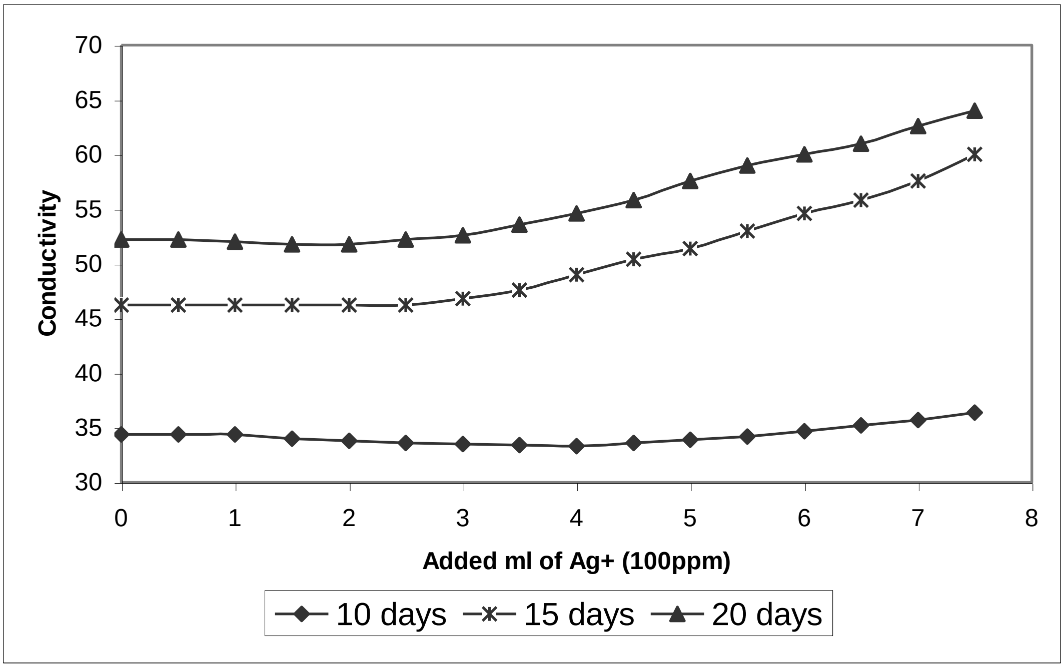

Figure 4.2: Conductmetric titration plot of sample 7 for immersion at 0^oC

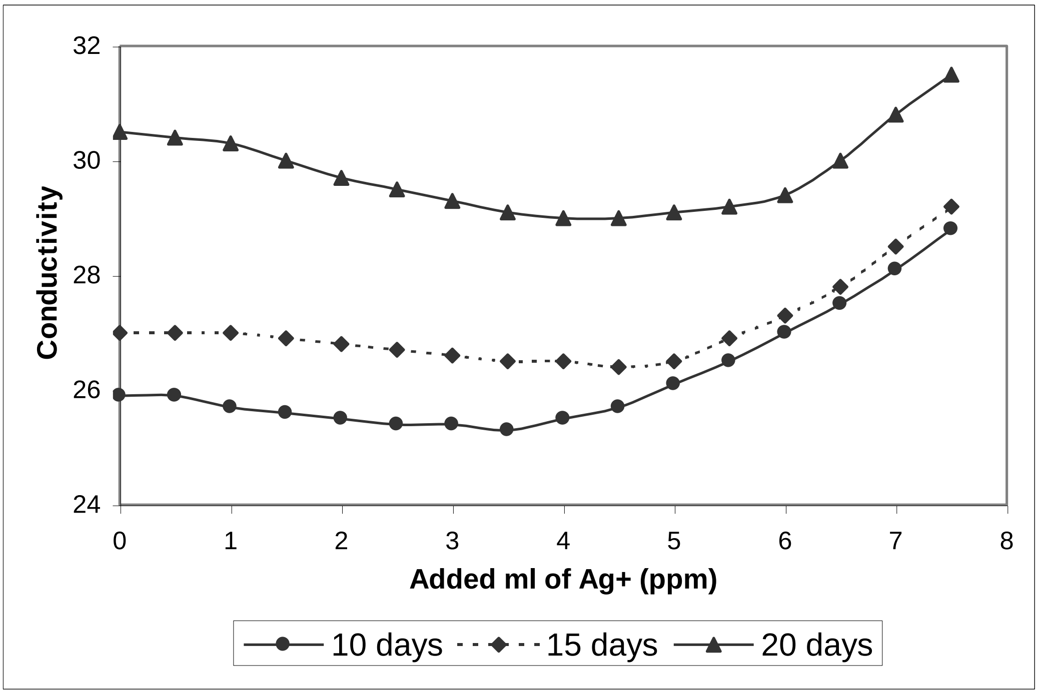

Figure 4.3: Conductmetric titration plot of sample 9 for immersion at 0^{o}C

The curves of time (days) versus percentage of chloride for samples 2, 3, 4, 5, 6, 7, 8, 9, and 10 concerning to 20^{o}C experimental conditions and the curves of temperature versus percentage of chloride for samples 1, 2, 3, 4, 5, 6, 7, 8, and 9 were drawn. All results are given in figures A.1-A.6 in respectively.

4.4.1.3 Quantitative Determination of PO_4^{3-}

Determination of phosphate ion, PO_4^{3-}, was also performed by UV spectrophotometry. The absorbance of blue molybdenum complex formed by addition of ammonium molybdate and stannous chloride to both standards and analyte measured at 690nm. All measurements were made after allowing each solution to sit for 10 minutes in order to provide development of colour. Calibration curves and the results are given in figure A.13 and Table 4.3 respectively.

4.4.1.4 Quantitative Determination of NO_3^-

Quantitative test sticks were used to determine the NO_3^- content extracted from ceramic pieces (Table 4.4).

Table 4.3. Results of PO_4^{3-} Analysis

Sample No		1	2	3	4	5	6	7	8	9	10
Temp.	Days	Concentration of PO_4^{3-} as ppm									
0ºC	10	nd	nd	nd	nd	nd	nd	nd	nd	nd	nd
	15	nd	nd	nd	nd	nd	nd	nd	nd	nd	nd
	20	nd	nd	nd	nd	nd	nd	nd	nd	nd	nd
	25	nd	nd	nd	nd	nd	nd	nd	nd	nd	nd
10ºC	10	nd	nd	nd	nd	nd	nd	nd	nd	78.13	nd
	15	nd	nd	nd	nd	nd	nd	nd	nd	140.82	nd
	20	nd	nd	nd	nd	nd	nd	nd	nd	153.98	nd
	25	nd	nd	nd	nd	nd	nd	nd	nd	211.10	nd
20ºC	10	nd	nd	nd	nd	nd	nd	nd	nd	220.84	nd
	15	nd	nd	nd	nd	2.78	nd	nd	4.18	273.03	11.83
	20	nd	nd	nd	nd	2.78	nd	nd	4.18	283.68	11.83
	25	nd	nd	nd	nd	2.78	nd	nd	4.18	284.03	11.83
25ºC	10	nd	2.86	53.55	55.34	2.78	nd	nd	4.18	348.65	11.83
	15	nd	4.47	53.73	57.12	32.77	39.63	nd	18.99	378.29	11.83
	20	nd	4.47	61.23	57.66	32.77	39.63	nd	18.99	420.95	11.83
	25	nd	10.19	124.24	57.66	32.77	39.63	nd	18.99	421.66	15.04
30ºC	10	57.45	12.13	134.53	57.74	72.75	62.72	32.33	56.58	508.85	86.02
	15	73.04	49.08	174.37	79.97	103.06	62.73	84.01	104.79	645.68	99.02
	20	73.04	49.08	174.37	79.97	103.06	62.73	84.01	104.79	645.68	113.52
	25	73.47	55.90	175.22	80.18	118.41	62.73	84.01	107.35	684.70	119.70
35ºC	10	78.58	71.89	187.80	80.18	138.45	62.73	84.01	119.29	764.66	137.40
	15	78.58	78.50	187.80	86.15	138.45	62.73	84.01	127.82	779.37	141.88
	20	78.58	78.50	213.14	86.15	138.45	62.73	84.01	127.82	907.19	141.88
	25	78.58	78.50	218.93	86.15	138.45	62.73	84.01	127.82	935.29	141.88

Table 4.4. Results of NO_3^- Analysis

Sample No		1	2	3	4	5	6	7	8	9	10
Temp.	Days	Concentration of NO_3^- as mg/l									
0ºC	10	nd	nd	nd	10	nd	nd	nd	nd	nd	nd
	15	nd	nd	nd	50	nd	nd	10	nd	<10	nd
	20	nd	nd	nd	100	nd	nd	25	nd	10	nd
	25	10	10	10	110	nd	nd	25	10	20	10
10ºC	10	10	10	10	110	nd	nd	25	10	20	10
	15	10	10	10	110	nd	nd	25	10	20	10
	20	20	10	10	110	nd	nd	25	10	20	10
	25	20	10	10	110	nd	nd	45	10	20	10
20ºC	10	20	10	10	110	nd	10	35	30	30	20
	15	20	10	10	110	nd	10	35	30	30	20
	20	20	10	10	110	nd	10	35	30	30	20
	25	20	10	10	110	nd	10	35	30	30	20
25ºC	10	20	10	10	110	nd	10	35	30	30	20
	15	20	10	10	110	nd	20	45	30	30	20
	20	20	10	10	110	nd	20	45	30	30	20
	25	20	10	10	110	nd	20	45	30	30	20
30ºC	10	20	10	10	110	nd	20	45	30	30	20
	15	20	10	10	110	nd	20	45	30	30	20
	20	20	10	10	120	nd	20	45	30	30	20
	25	20	10	10	120	nd	20	45	30	30	20
35ºC	10	20	10	10	120	nd	20	45	30	30	20
	15	20	10	10	120	nd	20	45	30	30	30
	20	20	10	10	120	nd	20	45	30	30	30
	25	20	10	10	120	nd	20	45	30	30	30

4.4.1.5 Quantitative Determination of SO_4^{2-}

Sulphate ion was determined depending upon the solubilization of barium sulphate in ethylenediamine tetra acetic acid ammonium salt. For this purposes, sulphate ion in the samples was precipitated as $BaSO_4$ and centrifuged for three minutes at 4000 rpm. The supernatant liquid was discarded. Ammonium ethylenediamine tetra-acetate solution was added to the precipitate and stirred until it completely dissolves. Then, it was diluted to 10 ml by the ammonium ethylenediaminetetra-acetate solution. Identical procedure was applied to standard SO_4^{2-} solutions. Then, the concentrations of Ba^{2+} ion were measured by atomic absorption spectrophotometry. Ba^{2+}, hence SO_4^{2-} concentration in both standards and analytes was determined from the calibration plot (Figure A.13). Results are shown in Table 4.5

Table 4.5. Results of SO_4^{2-} Analysis by Spectrophotometry

Sample No		1	2	3	4	5	6	7	8	9	10
Temp.	Days	Concentration of SO_4^{2-} as ppm									
0ºC	10	nd	nd	nd	nd	nd	nd	nd	nd	nd	nd
	15	nd	nd	nd	nd	nd	nd	nd	nd	nd	nd
	20	nd	nd	nd	nd	nd	nd	nd	nd	nd	nd
	25	nd	nd	nd	nd	nd	nd	nd	nd	nd	nd
10ºC	10	nd	nd	nd	nd	nd	nd	nd	nd	nd	nd
	15	nd	nd	nd	nd	nd	nd	nd	nd	nd	nd
	20	nd	nd	nd	nd	nd	nd	nd	nd	nd	nd
	25	nd	nd	nd	nd	nd	nd	nd	nd	nd	nd
20ºC	10	nd	nd	nd	nd	nd	nd	nd	nd	nd	nd
	15	nd	nd	nd	nd	nd	nd	nd	nd	nd	nd
	20	nd	nd	nd	nd	nd	nd	nd	nd	nd	nd
	25	nd	nd	nd	nd	nd	nd	nd	nd	nd	nd
25ºC	10	nd	nd	nd	nd	nd	nd	nd	nd	nd	nd
	15	nd	nd	nd	nd	nd	nd	nd	nd	nd	nd
	20	nd	nd	nd	nd	nd	nd	nd	nd	nd	nd
	25	nd	nd	nd	nd	nd	nd	nd	nd	nd	nd
30ºC	10	nd	nd	nd	nd	nd	nd	nd	nd	nd	nd
	15	nd	nd	nd	nd	nd	nd	nd	nd	nd	nd
	20	nd	nd	nd	nd	nd	nd	nd	nd	nd	nd
	25	nd	nd	nd	nd	nd	nd	nd	nd	nd	nd
35ºC	10	nd	nd	nd	nd	8.82	nd	nd	nd	nd	nd
	15	nd	nd	nd	nd	26.47	nd	8.82	8.82	5.88	8.82
	20	nd	11.76	2.94	8.82	32.35	nd	14.71	8.82	5.88	14.71
	25	nd	14.71	2.94	14.71	32.35	nd	14.71	8.82	5.88	14.71

Determination of sulphate ion was also carried out by turbidimetry. 10 ml of NaCl-HCl solution and 20 ml of glycerol-alcohol were added to each standard SO_4^{2-}

solution, and then diluted to 100 ml with distilled water. Approximately 0.3 g of barium chloride in grain size were added to each one and shaken about 1 minute to obtain uniform particle size. Then it was allowed to stand for 3 minutes before measurement. All vessels were shaken at the same rate and numbers of time. Unknown solutions were treated exactly like the standards. SO_4^{2-} concentration in analytes was determined from the calibration plot (Figure A.14). All results are given in table 4.6

Table 4.6. Results of SO_4^{2-} Analysis by Turbidimetry

Sample No		1	2	3	4	5	6	7	8	9	10
Temp.	Days	Concentration of SO_4^{2-} as ppm									
0ºC	10	nd	nd	nd	nd	nd	nd	nd	nd	nd	nd
	15	nd	nd	nd	nd	nd	nd	nd	nd	nd	nd
	20	nd	nd	nd	nd	nd	nd	nd	nd	nd	nd
	25	nd	nd	nd	nd	nd	nd	nd	nd	nd	nd
10ºC	10	nd	nd	nd	nd	nd	nd	nd	nd	nd	nd
	15	nd	nd	nd	nd	nd	nd	nd	nd	nd	nd
	20	nd	nd	nd	nd	nd	nd	nd	nd	nd	nd
	25	nd	nd	nd	nd	nd	nd	nd	nd	nd	nd
20ºC	10	nd	nd	nd	nd	nd	nd	nd	nd	nd	nd
	15	nd	nd	nd	nd	nd	nd	nd	nd	nd	nd
	20	nd	nd	nd	nd	nd	nd	nd	nd	nd	nd
	25	nd	nd	nd	nd	nd	nd	nd	nd	nd	nd
25ºC	10	nd	nd	nd	nd	nd	nd	nd	nd	nd	nd
	15	nd	nd	nd	nd	nd	nd	nd	nd	nd	nd
	20	nd	nd	nd	nd	nd	nd	nd	nd	nd	nd
	25	nd	nd	nd	nd	nd	nd	nd	nd	nd	nd
30ºC	10	nd	nd	nd	nd	nd	nd	nd	nd	nd	nd
	15	nd	nd	nd	nd	nd	nd	nd	nd	nd	nd
	20	nd	nd	nd	nd	nd	nd	nd	nd	nd	nd
	25	nd	nd	nd	nd	nd	nd	nd	nd	nd	nd
35ºC	10	nd	nd	nd	nd	9.23	nd	nd	nd	nd	nd
	15	nd	nd	nd	nd	24.69	nd	8.66	8.68	5.89	8.70
	20	nd	11.51	2.61	8.84	31.50	nd	14.07	8.68	5.89	14.80
	25	nd	14.73	2.61	14.80	31.50	nd	14.07	8.68	5.89	14.80

Another group of 23 ceramic samples (from 11 to 33 in Table A.1) were also analysed with respect to soluble salt content for 5 days duration at 20, 25 and 30ºC (Table 4.7).

Extracted amount of chloride, phosphate and nitrate of soaking water solutions were determined by the same methods described previously.

4.4.1.6 Quantitative Determination of Cations (Na+, K^+, Ca^{2+}, and Mg^{2+})

Quantitative determination of Na+, K^+, Ca^{2+}, and Mg^{2+} at 30 and 35ºC for 10, 15, 20, 25 days duration were also carried out. Na+, K^+, and Ca^{2+} were determined by Flame Spectrophotometry. Amount of extracted Mg^{2+} was determined by atomic absorption spectroscopy. All calibration curves and results are given in figures A.15-A.17 and Table 4.8.

Table 4.7. Results of Soluble Salt Content for 23 Samples

No of Samples	Cl^{-} conc. (ppm)				PO_4^{3-} conc. (ppm)				NO_3^{-} conc. (ppm)			SO_4^{2-} conc. (ppm)			
	Total Amou. of Cl by (w/v)%	For 5 Days at 20° C	For 5 Days at 25° C	For 5 Days at 30° C	Total Amou. of P_2O_5 by (w/v)%	For 5 Days at 20° C	For 5 Days at 25° C	For 5 Days at 30° C	For 5 Days at 20° C	For 5 Days at 25° C	For 5 Days at 30° C	Total Amou. of SO_4^{2-} by (w/v)%	For 5 Days at 20° C	For 5 days at 25° C	For 5 days at 30° C
11	nd	nd	nd	3.40	nd	nd	3.70	16.30	nd	nd	nd	0.45	nd	nd	3783
12	nd	nd	nd	nd	nd	nd	5.63	5.63	nd	nd	nd	0.32	nd	nd	4044
13	nd	nd	nd	4.37	nd	nd	0.30	20.30	nd	10	25	0.67	nd	nd	4696
14	nd	nd	1.94	2.43	nd	nd	23.85	42.22	nd	nd	nd	nd	nd	nd	4239
15	nd	nd	nd	5.34	0.34	nd	8.89	15.41	nd	nd	nd	nd	nd	3978	4631
16	nd	nd	nd	nd	nd	nd	3.41	3.47	nd	nd	nd	0.71	nd	nd	3978
17	0.64	nd	nd	nd	1.87	nd	11.41	11.41	nd	nd	nd	1.29	nd	nd	4434
18	0.50	nd	nd	3.40	2.08	nd	nd	8.44	nd	nd	nd	0.95	nd	3522	4435
19	0.75	nd	nd	nd	nd	nd	nd	nd	nd	nd	nd	nd	nd	nd	3978
20	nd	nd	nd	nd	nd	nd	nd	nd	nd	nd	nd	0.42	nd	2869	4696
21	nd	nd	0.97	10.19	1.43	nd	12.74	13.18	nd	25	50	0.66	nd	nd	2348
22	nd	nd	nd	12.62	0.52	nd	nd	50.67	nd	nd	nd	nd	nd	nd	2087
23	nd	nd	16.02	35.44	0.32	nd	15.41	61.63	nd	nd	nd	nd	nd	nd	2609
24	nd	41.75	64.56	85.92	0.41	nd	6.96	20.74	nd	nd	25	nd	nd	nd	3196
25	nd	106.77	150.48	150.48	0.63	nd	0.44	37.18	<10	10	25	nd	nd	3326	5544
26	nd	158.25	224.76	230.58	0.17	nd	3.85	20.90	50	50-100	100	nd	nd	2022	3718
27	nd	nd	nd	nd	0.52	nd	nd	nd	nd	nd	nd	1.86	nd	nd	2804
28	0.15	nd	7.77	7.79	0.30	nd	nd	17.18	nd	nd	nd	0.89	nd	nd	2152
29	nd	nd	nd	nd	0.85	nd	13.18	22.52	nd	nd	nd	2.24	nd	nd	3457
.30	0.17	nd	10.68	10.68	nd	nd	8.75	36.74	nd	nd	nd	1.28	nd	nd	3392
31	0.19	nd	nd	nd	0.65	nd	3.85	20.74	nd	nd	nd	0.55	nd	nd	3261
32	0.12	nd	nd	nd	1.31	nd	nd	nd	nd	nd	nd	1.35	nd	nd	2674
33	nd	5.34	11.16	16.02	0.56	nd	4.44	24.00	nd	nd	nd	0.35	nd	nd	2022

Table 4.8. Results of Cation Analysis

		Na^{+} (ppm)				K^{+} (ppm)				Ca^{2+} (ppm)				Mg^{2+} (ppm)			
Sample No	Temp .	10 days	15 days	20 days	25 days	10 days	15 days	20 days	25 days	10 days	15 days	20 days	25 days	10 days	15 days	20 days	25 days
1	30°C	1.96	1.96	2.45	2.45	3.06	3.06	4.19	5.10	5.96	6.95	8.32	9.01	1.75	1.90	2.41	2.68
	35°C	6.86	6.86	7.35	7.35	6.68	7.36	7.88	8.04	11.06	11.06	11.75	11.75	2.97	2.98	2.98	2.98
2	30°C	1.96	2.94	3.92	4.41	0.00	0.00	0.68	2.49	15.56	20.52	25.32	28.06	0.35	0.39	0.54	1.34
	35°C	6.86	6.86	6.86	6,86	2.94	3.17	4.89	5.41	33.54	34.91	35.98	35.60	1.99	2.22	2.22	2.22
3	30°C	18.63	20.59	21.08	21.08	26.53	31.63	39.10	44.75	23.18	30.46	35.94	39.37	3.73	5.13	7.43	9.22
	35°C	24.02	25.00	25.49	25.98	53.58	56.07	60.02	62.26	53.07	57.18	57.86	57.86	10.09	10.89	11.57	12.13
4	30°C	12.74	20.59	23.53	25.49	11.22	20.41	30.14	38.06	9.27	15.89	16.58	17.26	6.09	8.24	11.12	13.62
	35°C	30.39	33.33	34.13	34.80	44.84	45.30	52.01	56.48	20.00	20.69	21.37	22.06	16.29	17.32	18.83	20.03
5	30°C	14.71	16.67	17.65	18.14	39.80	50.00	61.31	72.62	24.83	30.79	32.17	32.16	6.47	8.54	11.46	13.71
	35°C	22.06	23.04	24.02	24.51	87.33	88.46	95.69	101.37	35.59	36.96	36.96	36.96	18.22	20.58	22.75	23.98
6	30°C	4.90	4.90	6.37	7.84	4.08	4.08	6.34	7.48	12.91	15.23	20.03	22.08	1.70	1.83	2.60	3.05
	35°C	12.75	13.24	14.71	15.20	10.87	15.39	16.43	16.77	30.30	31.67	32.36	33.04	3.95	4.13	4.13	4.13
7	30°C	6.86	7.84	11.76	14.22	13.26	17.35	22.10	21.19	11.59	17.55	22.34	25.08	2.95	3.81	8.21	11.38
	35°C	17.65	18.14	19.11	19.12	28.66	32.73	35.66	37.72	33.30	35.36	36.04	36.73	14.74	15.06	15.30	15.44
8	30°C	11.76	14.71	15.69	16.18	14.29	19.39	26.18	29.57	13.91	22.18	26.98	29.04	3.50	4.61	6.05	7.25
	35°C	18.63	19.12	19.61	19.61	37.49	45.41	49.19	50.91	37.94	41.36	46.16	47.53	9.62	10.82	11.62	12.20
9	30°C	8.82	10.78	13.73	15.69	19.39	27.55	50.18	61.49	13.91	19.20	23.32	26.06	7.48	10.57	14.59	17.60
	35°C	19.61	20.59	21.08	21.57	31.83	32.96	49.36	46.39	28.79	30.16	30.16	30.16	21.16	22.42	23.21	23.42
10	30°C	3.92	5.88	9.80	12.75	2.04	3.06	6.91	8.94	13.58	22.52	32.79	38.96	2.02	2.89	5.38	6.97
	35°C	17.65	37.26	38.24	38.73	11.88	12.79	14.17	15.20	49.23	56.08	60.87	62.93	8.6	10.14	11.49	11.71

4.4.2 Determination of Saturation Coefficient

Four pieces of sample 6, each in about 1 cm^2 area, was weighed. One pairs of the sample was stabilized at 110°C and another pair of sample was stabilized at 220 °C in a an oven. The stabilized weights of each sample were recorded. One of those pairs stabilized at 110°C was immersed in distilled water and allow standing for 24 hours at room temperature. The other one was immersed distilled water and boiled for 5 hours. Saturation coefficient as the ratio of weight after 24 hours immersion to that of boiled for 5 hours was calculated. The same procedure was applied for the pair of sample stabilized at 220 °C. All results are given in Tables 4.9 and 4.10.

Table 4.9. Results for Sample Soaked for 24 hours

Sample 10	Initial weight (g)	Stabilized weight (g)	Weighed after immersion (g)
1	0.2091	0.2088 (at 110°C)	0.2513
2	0.2835	0.2835 (at 220°C)	0.3389

Table 4.10. Results for Sample Boiled for 5 hours

Sample 10	Initial weight	Stabilized weight	Weighed after immersion
1^1	0.2240	0.2236 (at 110°C)	0.2667
2^1	0.2255	0.2245 (at 220°C)	0.2709

Saturation Coefficient at 110 °C= 0.9423

Saturation Coefficient at 220 °C= 1.2510

4.4.3 Weight Lost of Ceramic by Acid and Base Attack

Four pieces of sample 3 in about 1 cm^2 were weighed at room temperature and then they were immersed in acids (HCl, H_2SO_4), base (NaOH) solutions. Weights of each sample were determined for every 2 hours period (Table 4.11). Time versus lost of masses were drawn (Figure 4.4).

Table 4.11. Results of Weight Loss

Immersion Solution	Initial weight (g)	Weight after (g) 2 h	Weight after (g) 4 h	Weight after (g) 6 h	Weight after (g) 8 h
HCl (pH=4)	0.3926	0.4477	0.4515	0.4530	0.4538
H_2SO_4 (pH=4)	0.4009	0.4590	0.4639	0.4654	0.4662
NaOH (pH=9)	0.4614	0.5243	0.5246	0.5253	0.5262
H_2O	0.3926	0.4477	0.4515	0.453	0.4538

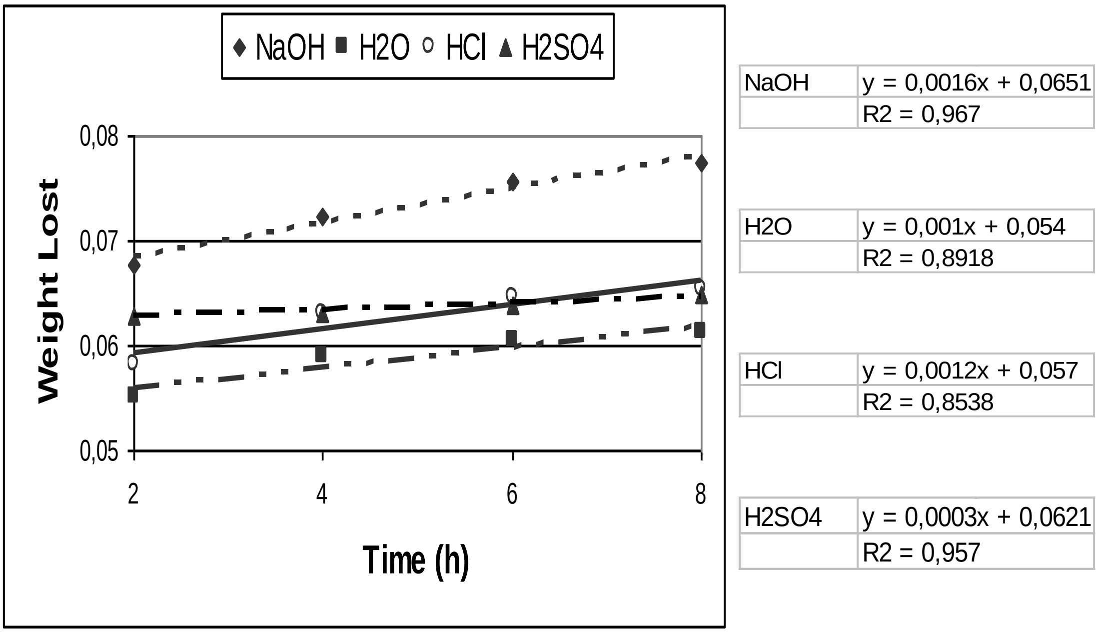

Figure 4.4: Comparison of weight loss of ceramic sample 3 by an acid and base attack

5. CHEMOMERTIC ANALYSIS

5.1 Chemometric Analysis of Body Composition

5.1.1 Principle Component analysis (PCA) of Body Composition

PCA was applied to the body composition of 107 ceramic samples whose value of oxide % are given in Table B.2. The correlation matrix and the eigen values, the percentages of variances, and cumulative percentages corresponding to the each principal components are shown in the following Table 5.1 and 5.2, respectively . A plot of principal component 1 and 2 showing the relationship between samples (SP) and impact of each variable (LP) are shown in figures 5.1 and 5.2.

Table 5.1. Correlation Matrix for Body Composition Data of 107 Samples

	CaO	**Fe_2O_3**	**K_2O**	**MgO**	**Na_2O**	**PbO**	**SiO_2**	**Al_2O_3**
CaO	1.00000	0 .41123	0.19695	0.15659	-0.26030	-0.26700	-0.75389	0.31693
Fe_2O_3		1.00000	0 .54656	0 .16060	-0.42654	-0.44287	-0.78466	0 .54729
K_2O			1.00000	0.16582	-0.29903	-0.32925	-0.56561	0.46603
MgO				1.00000	-0.10572	-0.19849	-0.44974	0.59689
Na_2O					1.00000	0.36193	0.37351	-0.39078
PbO						1.00000	0 .45515	-0.51534
SiO_2							1.00000	-0.78541
Al_2O_3								1.00000

Table 5.2. The eigen values, the percentages of variances, and cumulative percentages corresponding to the each principal components for Body Composition Data of 107 Samples

Variable	Communality	PC	Eigenvalue	% of Variance	Cumulative Pct.
CaO	1.00000	1	3.98989	49.9	49.9
Fe_2O_3	1.00000	2	1.07312	13.4	63.3
K_2O	1.00000	3	0.91439	11.4	74.7
MgO	1.00000	4	0.75685	9.5	84.2
Na_2O	1.00000	5	0.62284	7.8	92.0
PbO	1.00000	6	0.39386	4.9	96.9
SiO_2	1.00000	7	0.24905	3.1	100.0
Al_2O_3	1.00000	8	0.00000	0.0	100.0

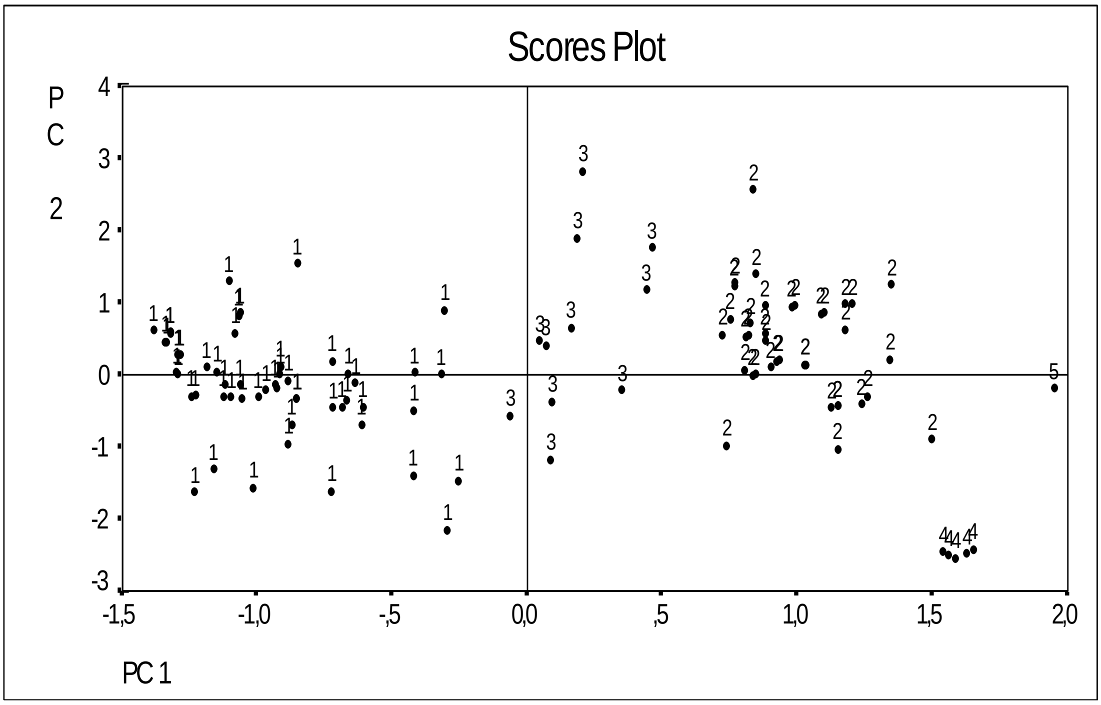

Figure 5.1: Scores plot showing the results of PCA of body composition data of 107 samples for PC1 and PC2.

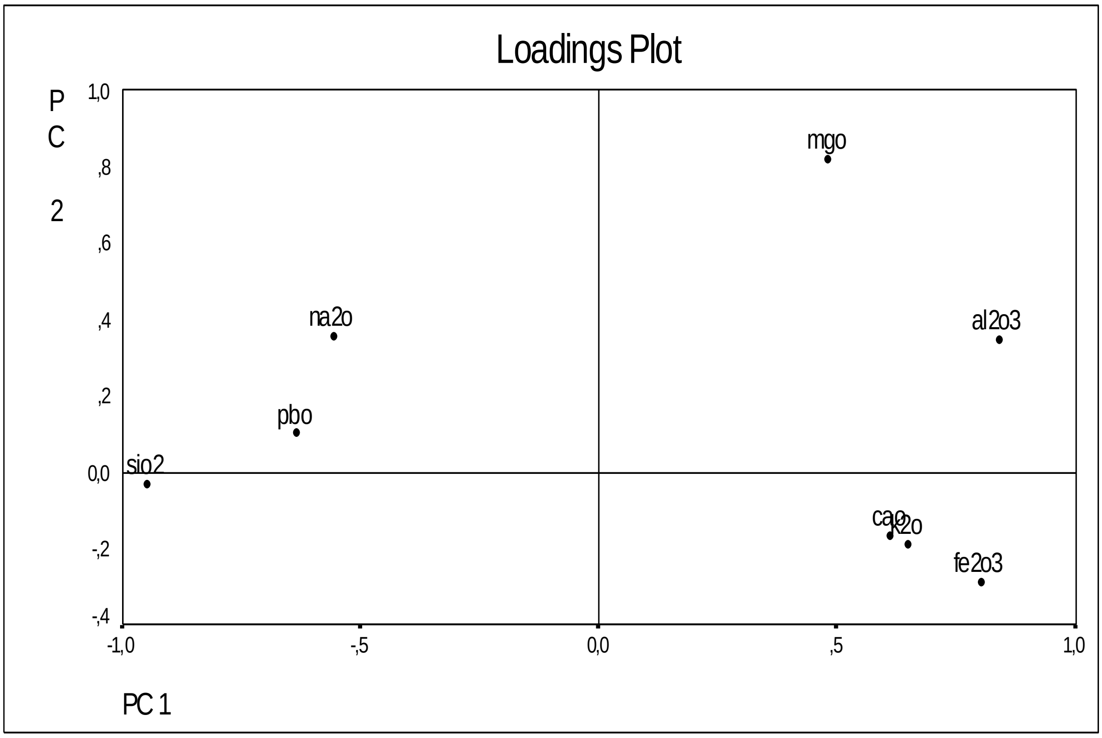

Figure 5.2: Loadings plot showing the results of PCA of body composition data of 107 samples for PC1 and PC 2.

A graphical visualizing in three coordinate system, PC1, PC2, and PC3, was also performed for these ceramics. Scores and loadings plots for three component system are given in the following figures 5.3 and 5.4. PC Loadings for each of principal components are seen in Table 5.3.

Table 5.3. Values of Principal Component Loadings for Body Composition Data of 107 Samples

	PC 1	**PC 2**	**PC 3**
PbO	-0.63363	0.09975	0.32384
SiO_2	-0.94743	-0.03245	-0.29109
Fe_2O3	0.80433	-0.28871	-0.00304
K_2O	0.64962	-0.18974	-0.28274
MgO	0.48324	0.81879	-0.03588
Na_2O	-0.55495	0.35288	0.31153
Al_2O_3	0.84041	0.34593	-0.16122
CaO	0.61160	-0.16780	0.72146

In all figures 5.1, 5.3, 5.5, and 5.6, the numbers 1, 2, 3, 4, and 5 represents the samples as follows;

1: 1, 3, 6, 16-19, 27-33, 36-39, 48-50, 52-59, 69-74, 76, 92-94, 113-117

2: 5, 7, 8, 11-15, 20, 24-26, 35, 41, 45-47, 59-62, 64-68, 83-91, 110, 111

3: 9, 22, 23, 34, 40, 42, 43, 51, 63, 75, 112 4 : 104-109 5: 44

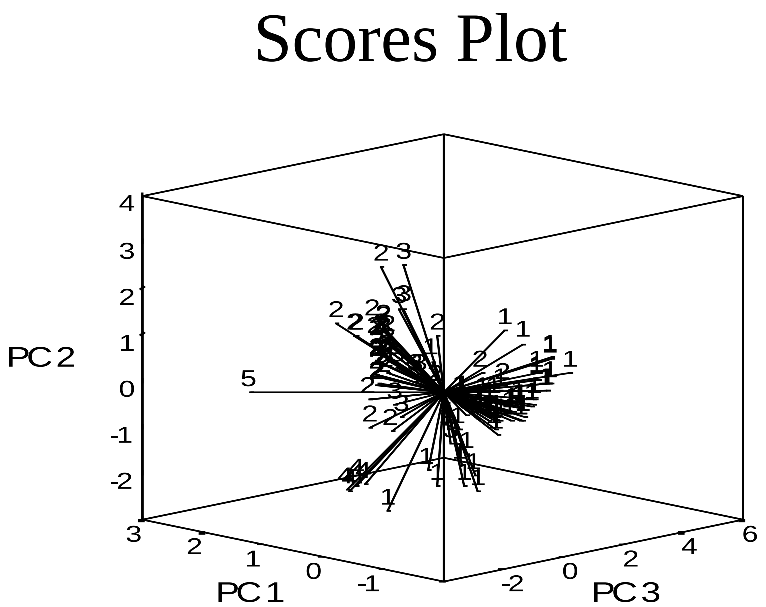

Figure 5.3: Scoress plot showing the results of PCA of body composition data of 107 samples for PC1, PC2, and PC3.

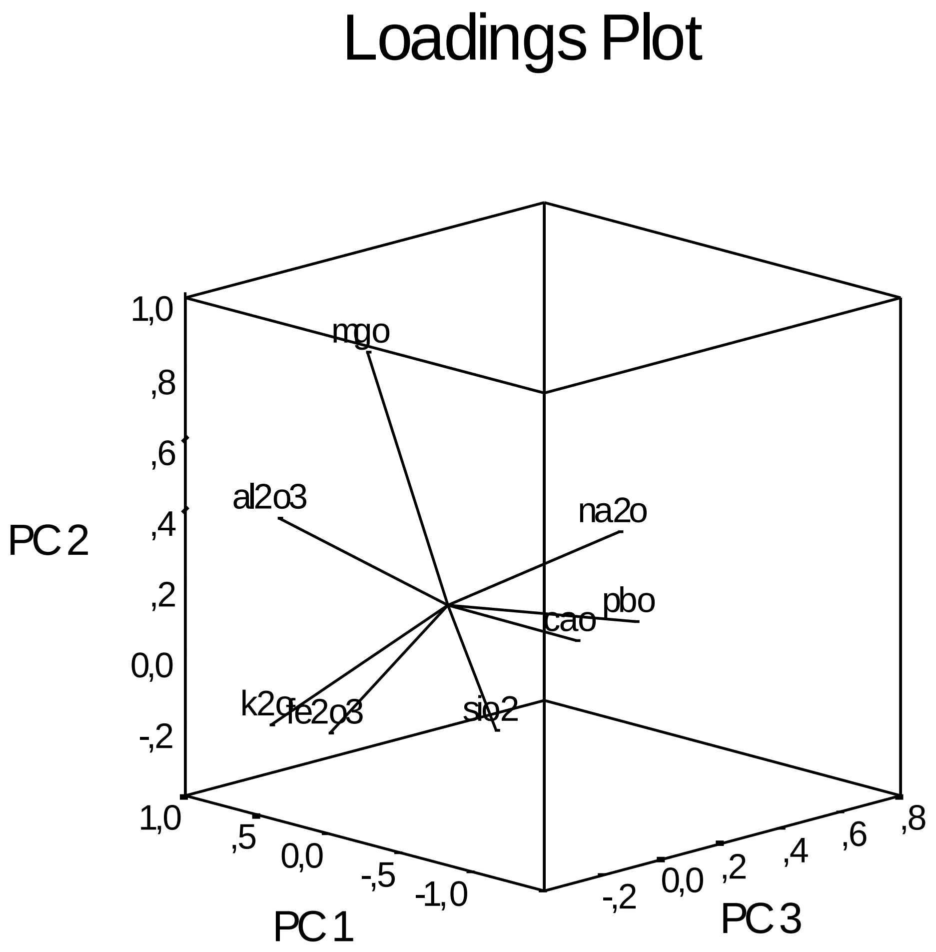

Figure 5.4: Loadings plot showing the results of PCA of body composition data of 107 samples for PC1, PC2, and PC3.

SiO_2 versus Fe_2O_3 and SiO_2 versus Al_2O_3 percentage content (wt) were also drawn in order to verify the effects of three oxides in grouping. The results are given figures 5.5 and 5.6

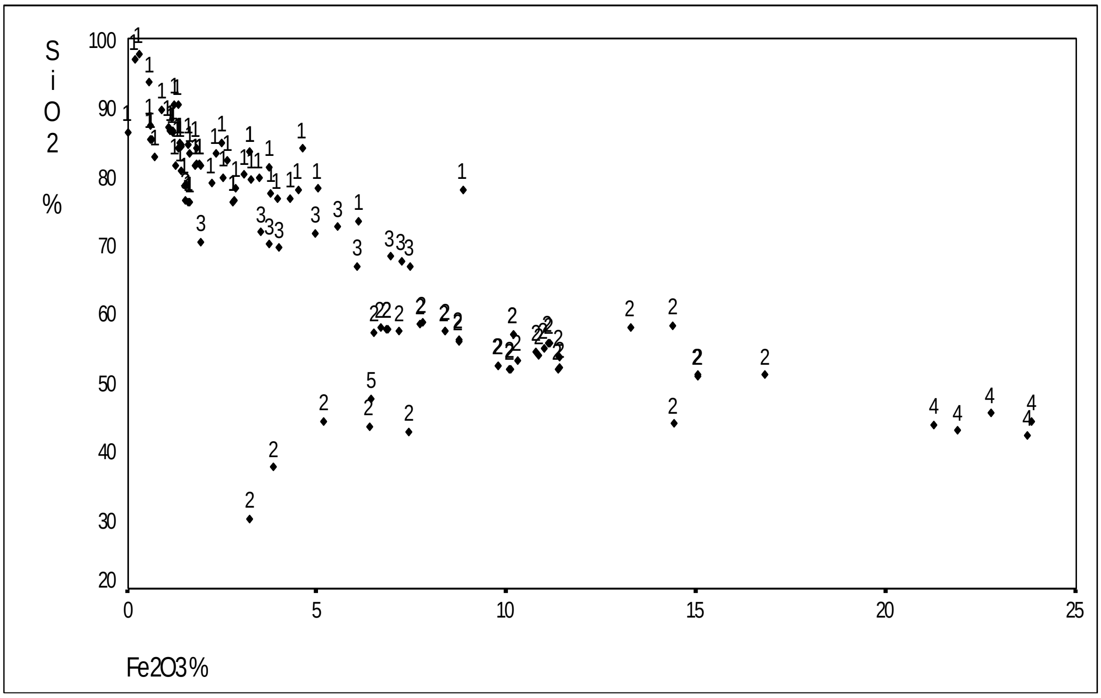

Figure 5.5: SiO_2 versus Fe_2O_3 percentage content (wt) for body composition of 107 samples.

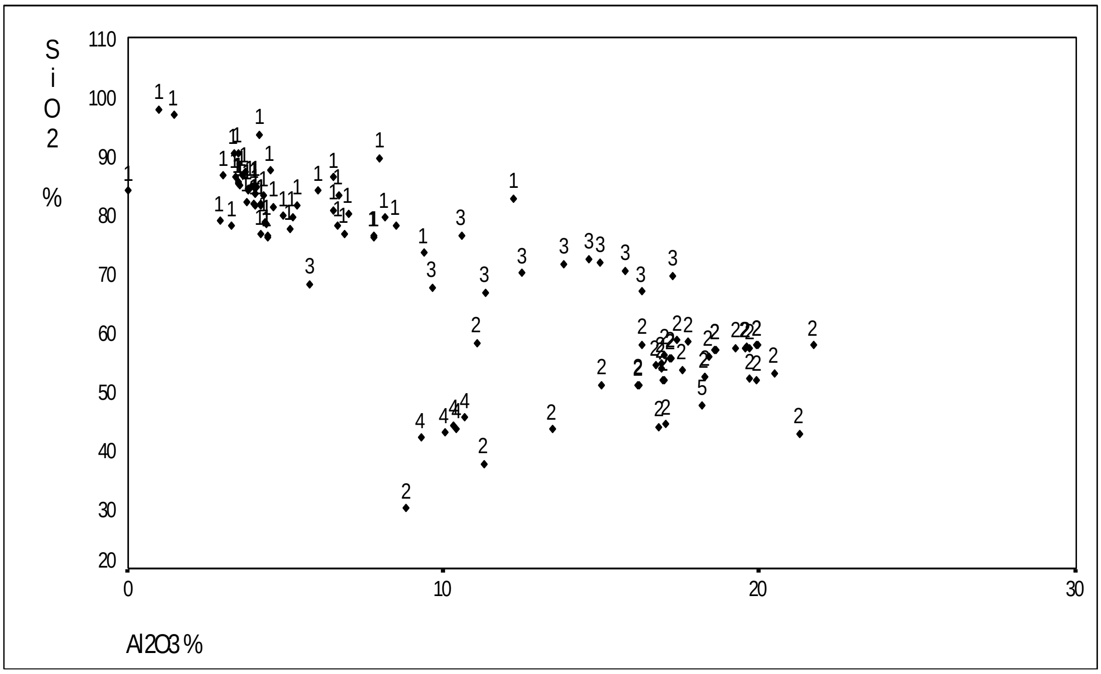

Figure 5.6: SiO_2 versus Al_2O_3 percentage content (wt).

5.1.2 Cluster Analysis (CA) of Body Composition

CA was applied to the body composition of 107 ceramic samples on the basis of Euclidean distance. The same chemical constituents were used as in the case of PCA in order to group the samples. Dendograms obtained by the clustering for the Single and Complete Linkage Methods are given the figures 5.7 and 5.8.

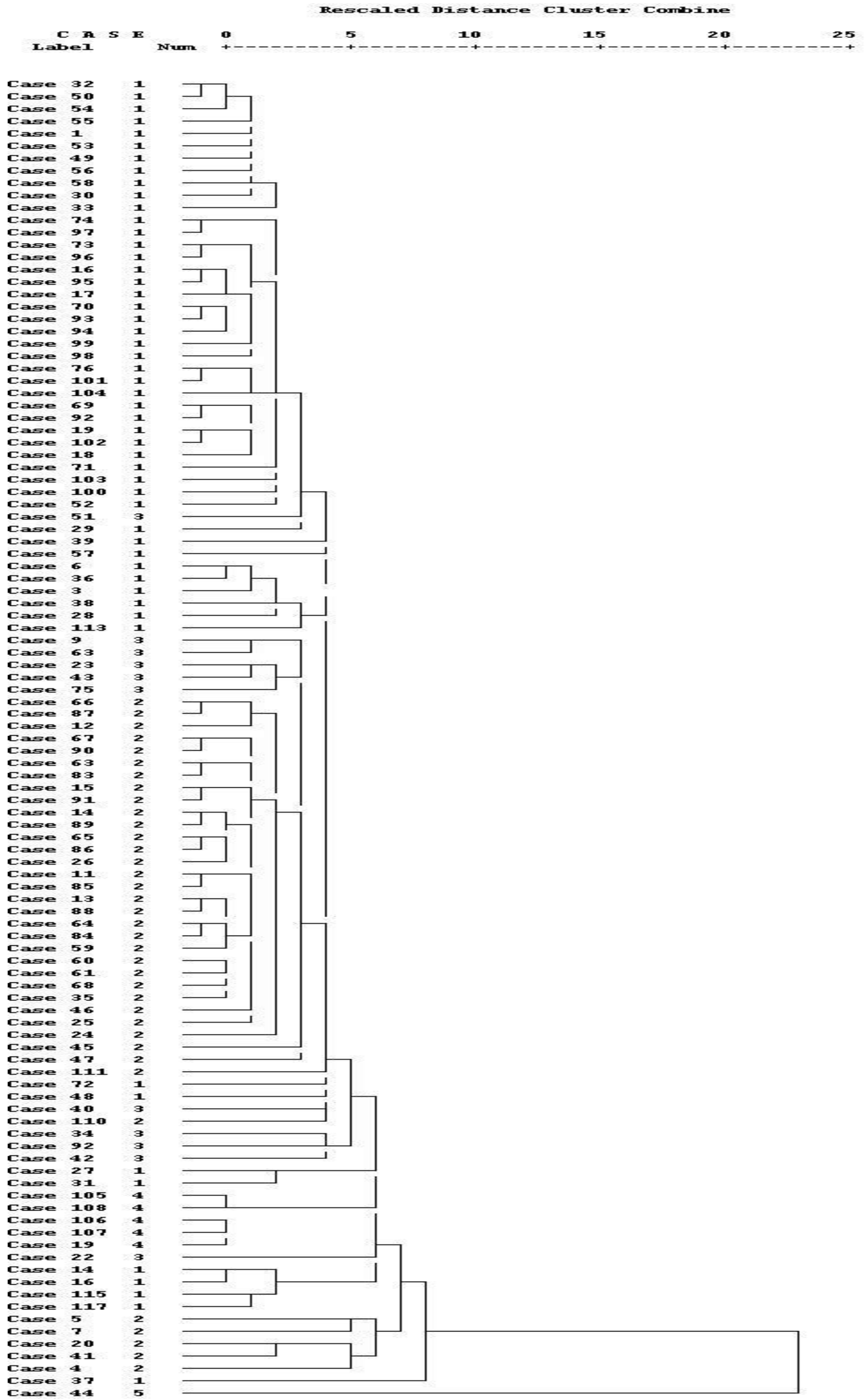

Figure 5.7: Dendogram showing the results of clustering body composition data of 107 samples based of Single Linkage.

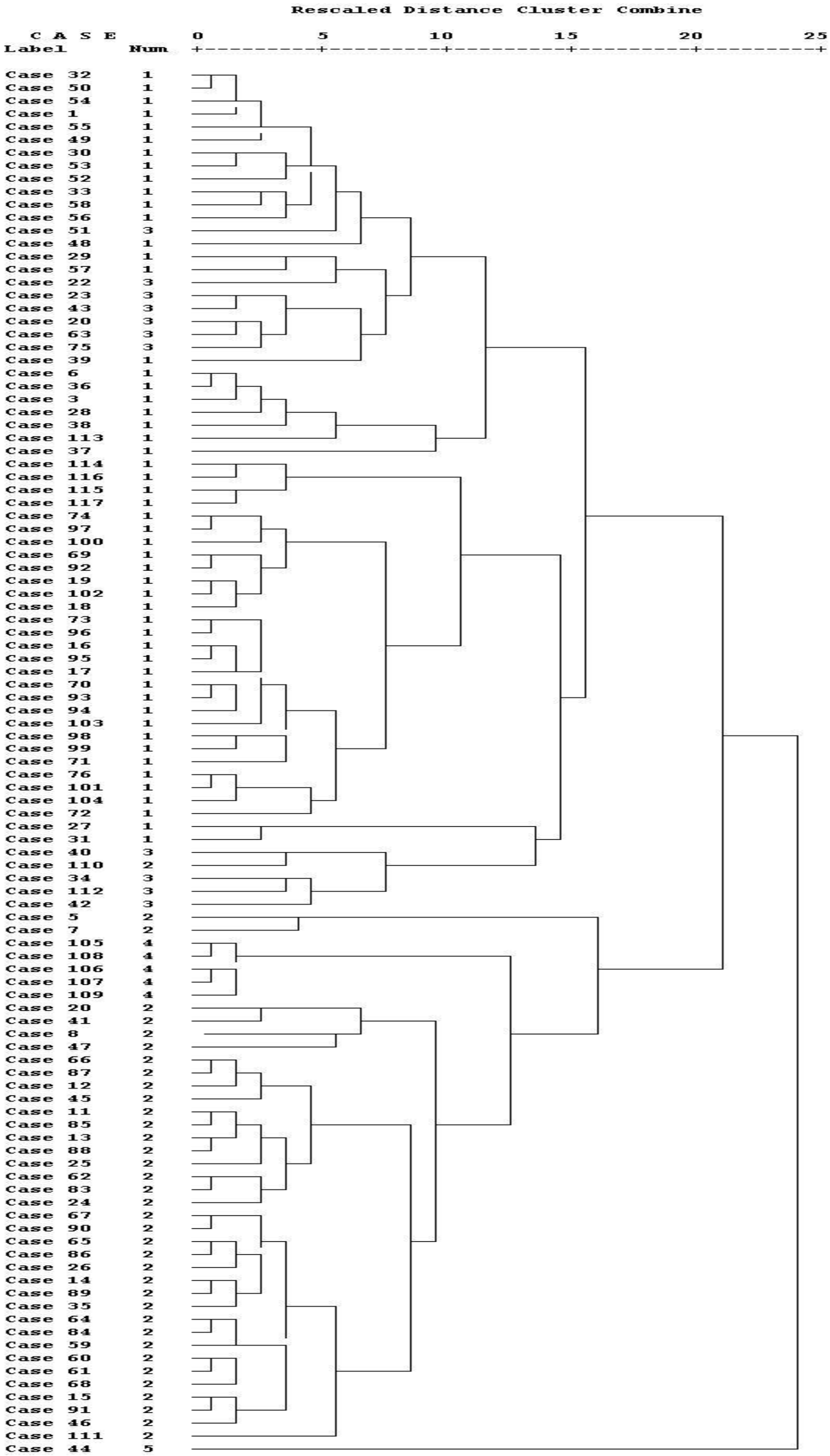

Figure 5.8: Dendogram showing the results of clustering body composition data of 107 samples based of Complete Linkage.

Dendogram showing the results of clustering variables for body composition of 107 ceramic samples are also given in the figures 5.9 and 5.10.

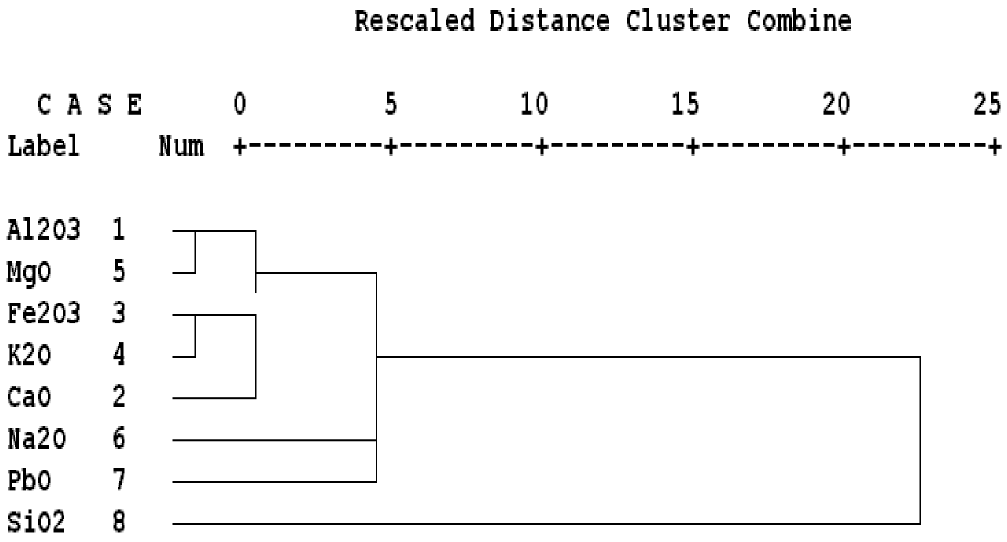

Figure 5.9: Dendogram showing the results of clustering variables for body composition of 107 ceramic samples Single Linkage.

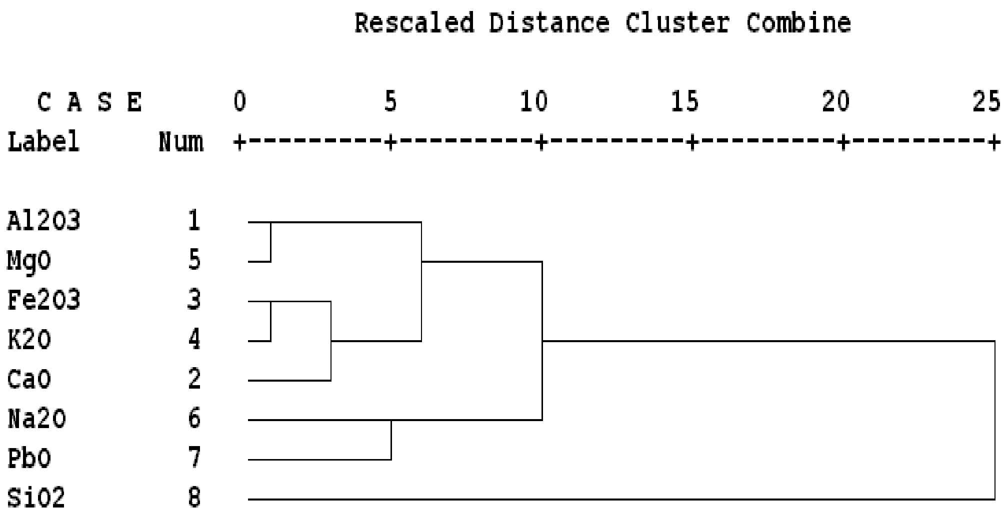

Figure 5.10: Dendogram showing the results of clustering variables for body composition of 107 ceramic samples based of Complete Linkage.

5.2 Chemometric Analysis of Slip Composition

5.2.1 Principle Component Analysis (PCA) of Slip Composition

PCA was applied to the slip composition of 61 ceramic samples whose value of oxide % are given in Table B.3. The correlation matrix and the eigen values, the percentages of variances, and cumulative percentages corresponding to the each principal components are shown in the following Table 5.4 and 5.5, respectively. A plot of principal component 1 and 2 showing the relationship between samples (SP) and impact of each variable (LP) are shown in figures 5.11 and 5.12.

Table 5.4. Correlation Matrix for Slip Composition Data of 61 Samples

	Al_2O_3	CaO	Fe_2O3	K_2O	MgO	Na_2O	PbO	SiO_2
Al_2O_3	1.00000	0.44178	0.39029	0.56982	0.26922	-0.58135	-0.60019	-0.63270
CaO		1.00000	0.28301	0.30818	0.44858	-0.46601	-0.50225	-0.55261
Fe_2O_3			1.00000	0.62695	0.18943	-0.51136	-0.38157	-0.49533
K_2O				1.00000	0.16716	-0.48865	-0.46487	-0.48911
MgO					1.00000	-0.30134	-0.35874	-0.27089
Na_2O						1.00000	0.69147	0.18275
PbO							1.00000	0.01024
SiO_2								1.00000

Table 5.5. The eigen values, the percentages of variances, and cumulative percentages corresponding to the each principal components for Slip Composition Data of 61 Samples

Variable	Communality	PC	Eigenvalue	% of Variance	Cumulative Pct.
Al_2O_3	1.00000	1	3.97434	49.7	49.7
CaO	1.00000	2	1.18648	14.8	64.5
Fe_2O_3	1.00000	3	1.06170	13.3	77.8
K_2O	1.00000	4	0.65116	8.1	85.9
MgO	1.00000	5	0.49674	6.2	92.1
Na_2O	1.00000	6	0.36544	4.6	96.7
PbO	1.00000	7	0.26414	3.3	100.0
SiO_2	1.00000	8	0.00000	0.0	100.0

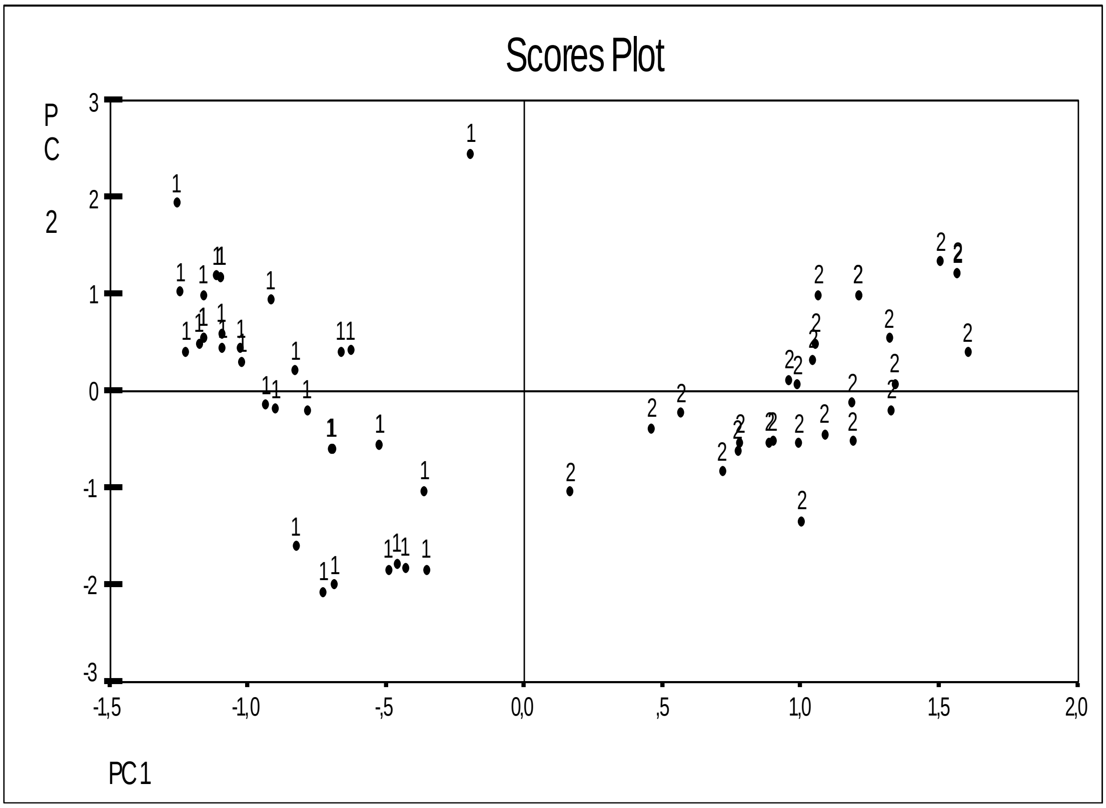

Figure 5.11: Scores plot showing the results of PCA of slip composition data of 61 samples for PC1 and PC2

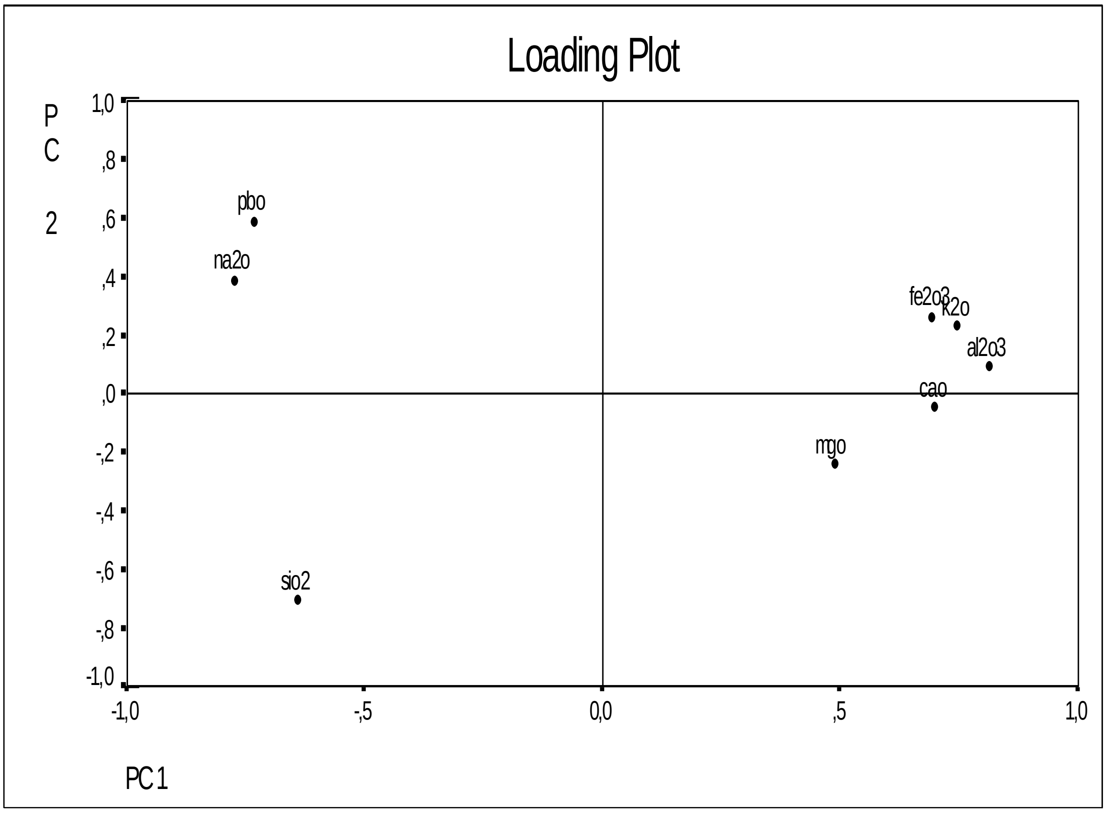

Figure 5.12: Loadings plot showing the results of PCA of slip composition data of 61 samples for PC1 and PC2.

A graphical visualizing in three coordinate system, PC1, PC2, and PC3, was also performed for these ceramics. PC Loadings for each of principal components are seen in Table 5.6. Scores and loadings plots for three component system are given in the following figures 5.13 and 5.14.

Table 5.6. Values of Principal Component Loadings for Slip Composition Data of 61 Samples

	PC 1	**PC 2**	**PC 3**
Al_2O_3	0.81653	0.09040	-0.03890
CaO	0.70123	-0.04640	0.49384
Fe_2O_3	0.69507	0.26110	-0.35546
K_2O	0.74856	0.23143	-0.37998
MgO	0.49011	-0.24077	0.63504
Na_2O	-0.77040	0.38857	0.21913
PbO	-0.72975	0.58805	0.13757
SiO_2	-0.63731	-0.70687	-0.27451

In all figures 5.11, 5.13, 5.15, and 5.16, the numbers 1 and 2 represents the samples as follows.;

1: 1, 18, 31-33, 45, 50, 51, 53, 54, 56, 57, 58, 64, 72, 74, 76, 77, 89, 91-104

2: 3, 5, 6, 8, 9, 13, 20, 22-26, 34, 37-42, 44, 46, 65-67, 87, 88, 90

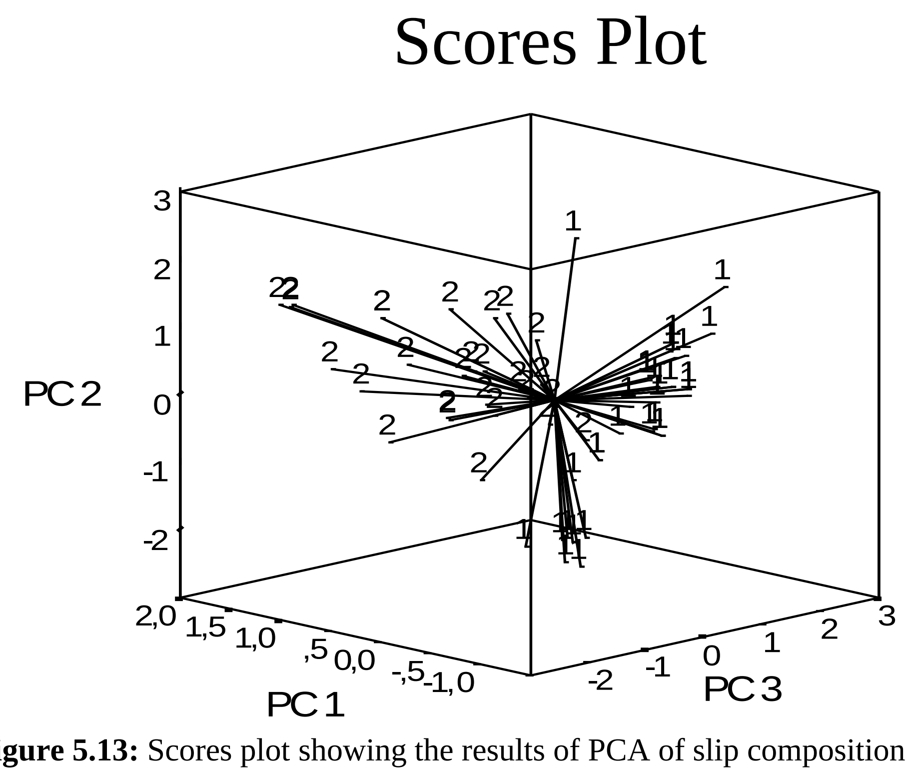

Figure 5.13: Scores plot showing the results of PCA of slip composition data of 61 samples for PC1, PC2, and PC3.

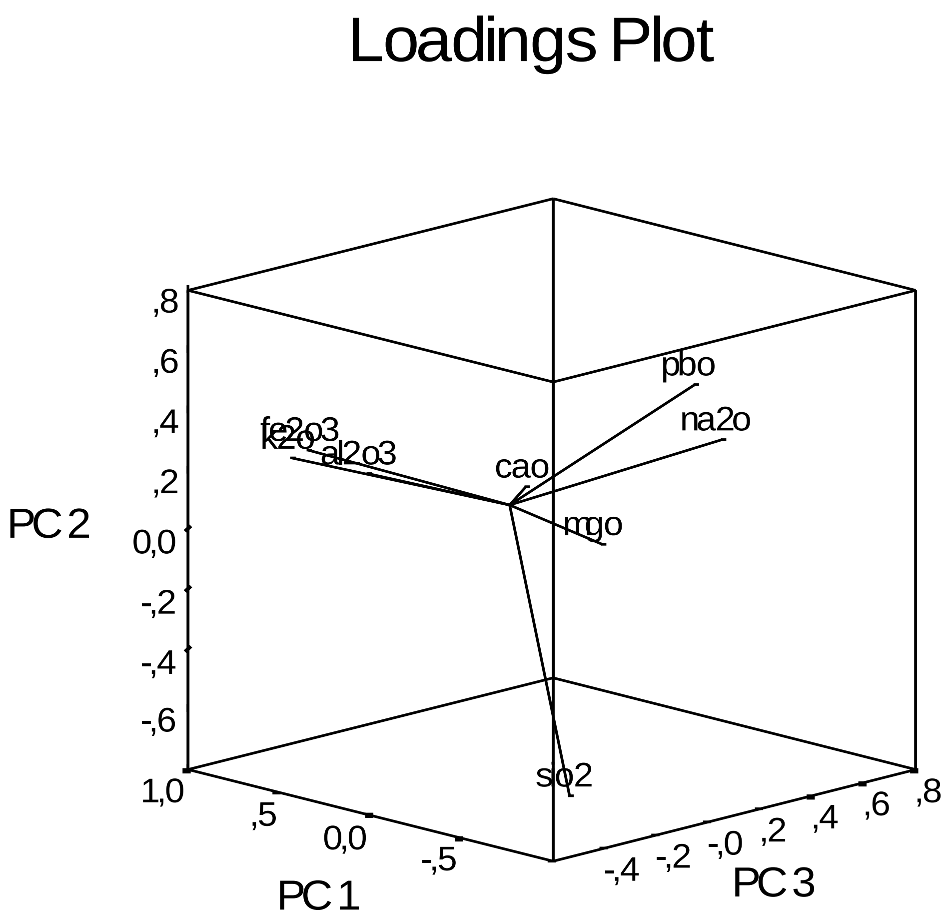

Figure 5.14: Loadings plot showing the results of PCA of slip composition data of 61 samples for PC1, PC2, and PC3.

SiO_2 versus Fe_2O_3 and SiO_2 versus Al_2O_3 percentage content (wt) were also drawn in order to verify the effect of these oxides in grouping. The results are given figures 5.15 and 5.16.

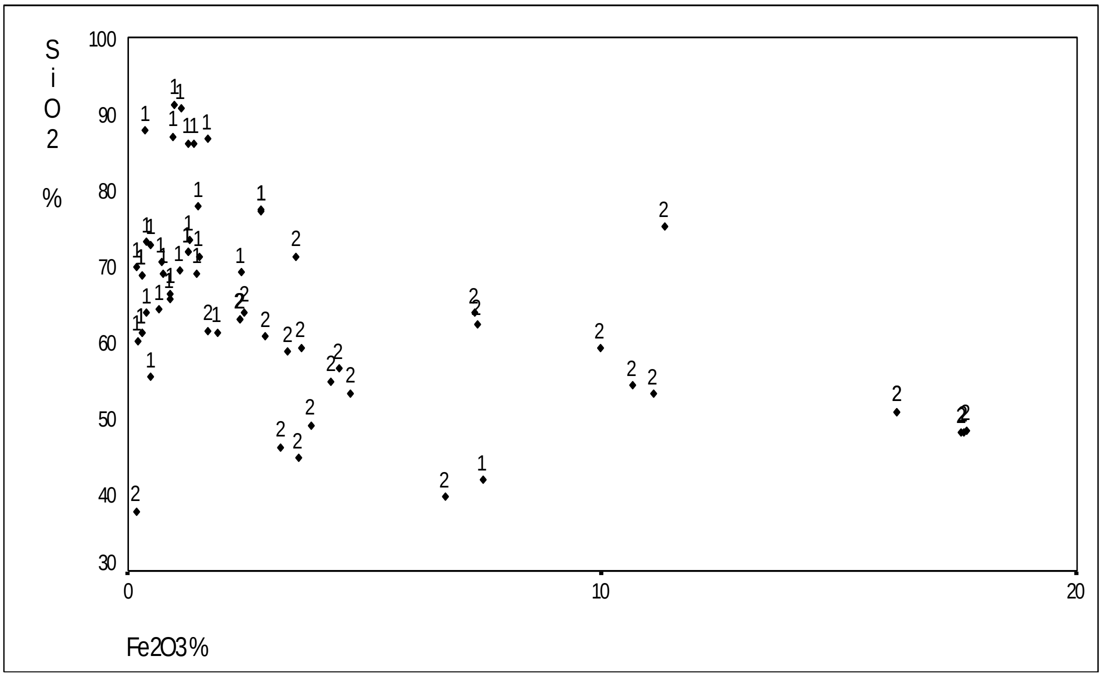

Figure 5.15: SiO_2 versus Fe_2O_3 percentage content (wt) for slip composition of 61 samples.

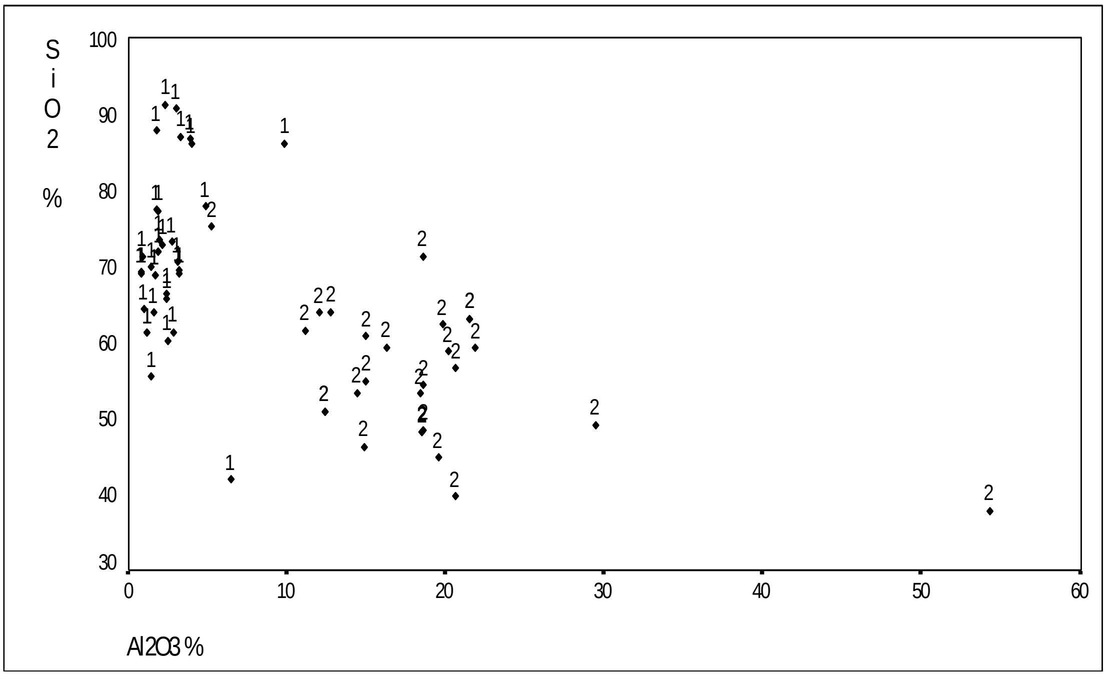

Figure 5.16: SiO_2 versus Al_2O_3 percentage content (wt) for slip composition of 61 samples.

5.2.2 Cluster Analysis (CA) of Slip Composition

CA was applied to the slip composition of 61 ceramic samples on the basis of Euclidean distance. The same chemical constituents were used as in the case of PCA in order to classify the samples. Dendograms obtained by the clustering for the Single and Complete Linkage Methods are given the figures 5.17 and 5.18.

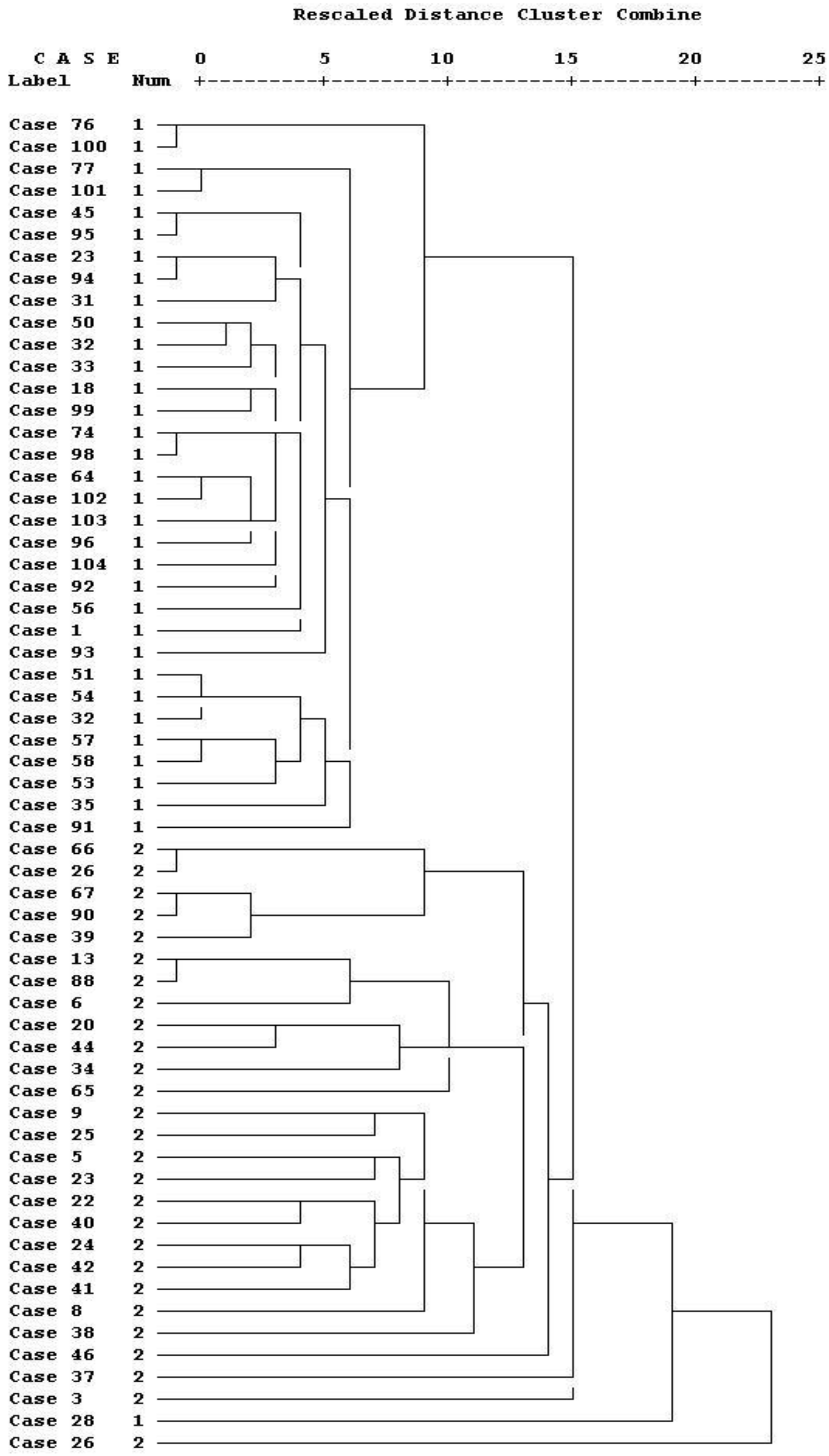

Figure 5.17: Dendogram showing the results of clustering slip composition data of 61 samples based of Single Linkage.

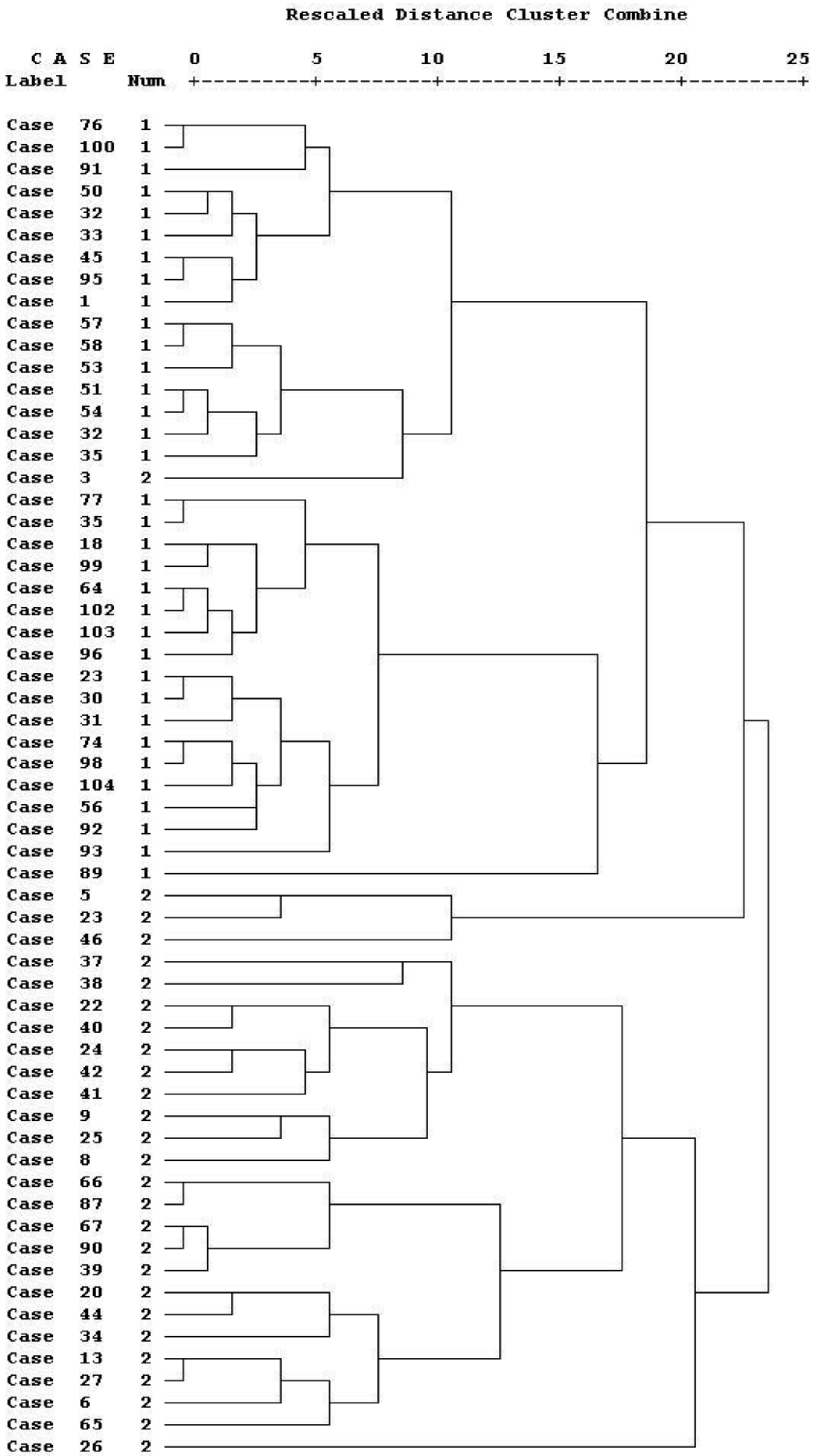

Figure 5.18: Dendogram showing the results of clustering slip composition data of 61 samples based of Complete Linkage.

Dendogram showing the results of clustering variables for slip composition of 61 ceramic samples are also given in the figures 5.19 and 5.20.

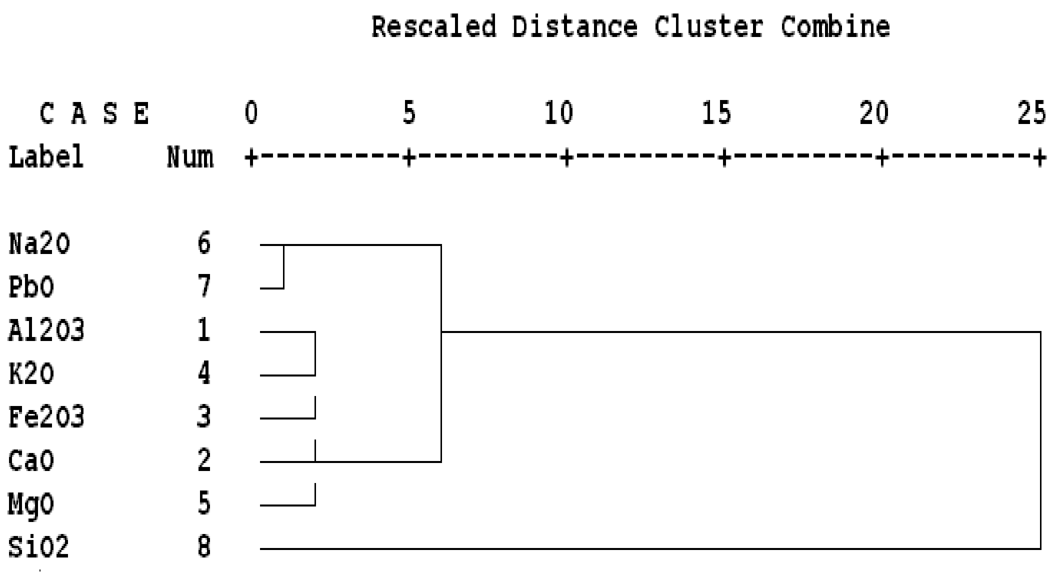

Figure 5.19: Dendogram showing the results of clustering variables for slip composition of 61 ceramic samples based of Single Linkage.

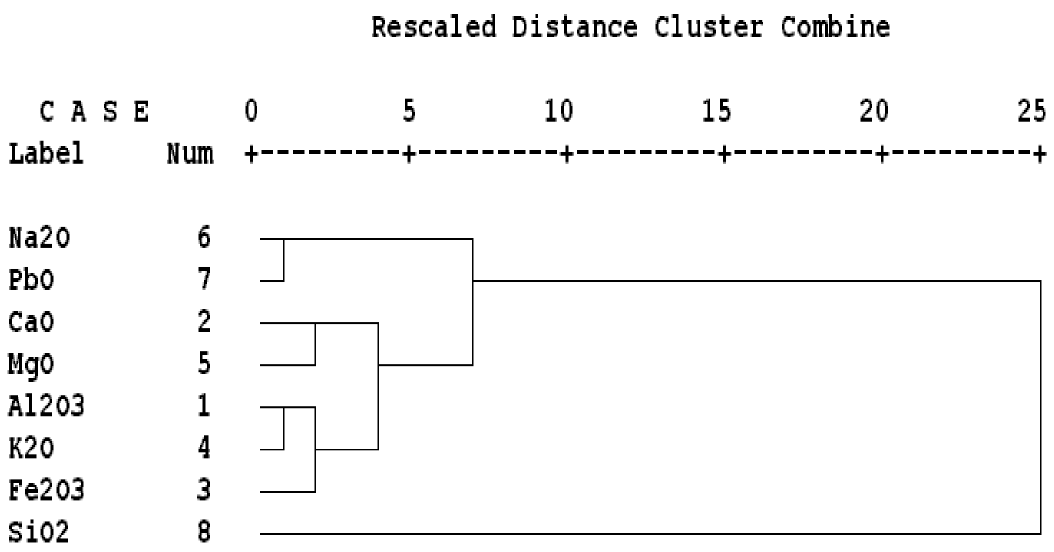

Figure 5.20: Dendogram showing the results of clustering variables for slip composition of 61 ceramic samples based of Complete Linkage.

5.3 Chemometric Analysis of Glaze Composition

5.3.1 Principle Component Analysis (PCA) of Glaze Composition

PCA was applied to the glaze composition of 75 ceramic samples whose value of oxide % is given in Table B.4 The correlation matrix and the eigen values, the percentages of variances, and cumulative percentages corresponding to the each principal components are shown in the following Table 5.7 and 5.8, respectively. A plot of principal component 1 and 2 showing the relationship between samples (SP) and impact of each variable (LP) are shown in figures 5.21 and 5.22.

Table 5.7. Correlation Matrix for Glaze Composition Data of 75 Samples

	Al_2O_3	**CaO**	**Fe_2O_3**	**K_2O**	**MgO**	**Na_2O**	**P_2O_5**	**PbO**	**SiO_2**	**SnO**
Al_2O_3	1.00000	0.61863	0.32179	0.39140	0.68082	-0.19507	0.52061	-0.46089	-0.13170	**-0.35880**
CaO		1.00000	0.57308	0.53435	0.50940	-0.25634	0.28958	-0.35329	-0.19754	-0.18643
Fe_2O_3			1.00000	0.37794	0.24894	-0.20463	0.14226	-0.26119	-0.15828	-0.25790
K_2O				1.00000	0.15598	0.32923	0.07714	-0.34616	-0.25706	-0.20988
MgO					1.00000	-0.21113	0.39662	-0.33213	-0.10407	-0.13179
Na_2O						1.00000	-0.13007	-0.15818	-0.15140	-0.00270
P_2O_5							1.00000	-0.52968	0.24960	-0.19380
PbO								1.00000	-0.63667	0.32003
SiO_2									1.00000	-0.24147
SnO										1.00000

Table 5.8. The eigen values, the percentages of variances, and cumulative percentages corresponding to the each principal components for Glaze Composition Data of 75 Samples

Variable	**Communality**	**PC**	**Eigenvalue**	**% of Variance**	**Cumulative Pct.**
Al_2O_3	1.00000	1	3.56053	35.6	35.6
CaO	1.00000	2	1.83130	18.3	53.9
Fe_2O_3	1.00000	3	1.45113	14.5	68.4
K_2O	1.00000	4	1.00136	10.0	78.4
MgO	1.00000	5	0.76292	7.6	86.1
Na_2O	1.00000	6	0.51546	5.2	91.2
P_2O_5	1.00000	7	0.44373	4.4	95.7
PbO	1.00000	8	0.23011	2.3	98.0
SiO_2	1.00000	9	0.20346	2.0	100.0
SnO	1.00000	10	0.00000	0.0	100.0

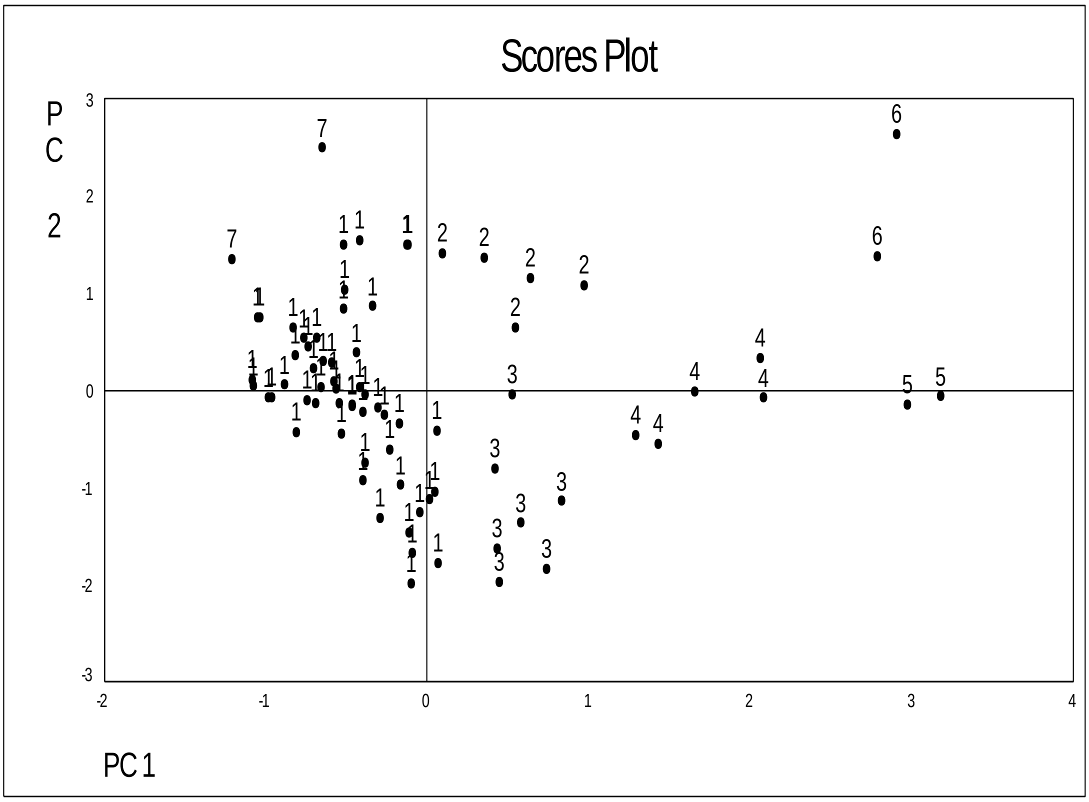

Figure 5.21: Scores plot showing the results of PCA of glaze composition data of 75 samples for PC1 and PC2.

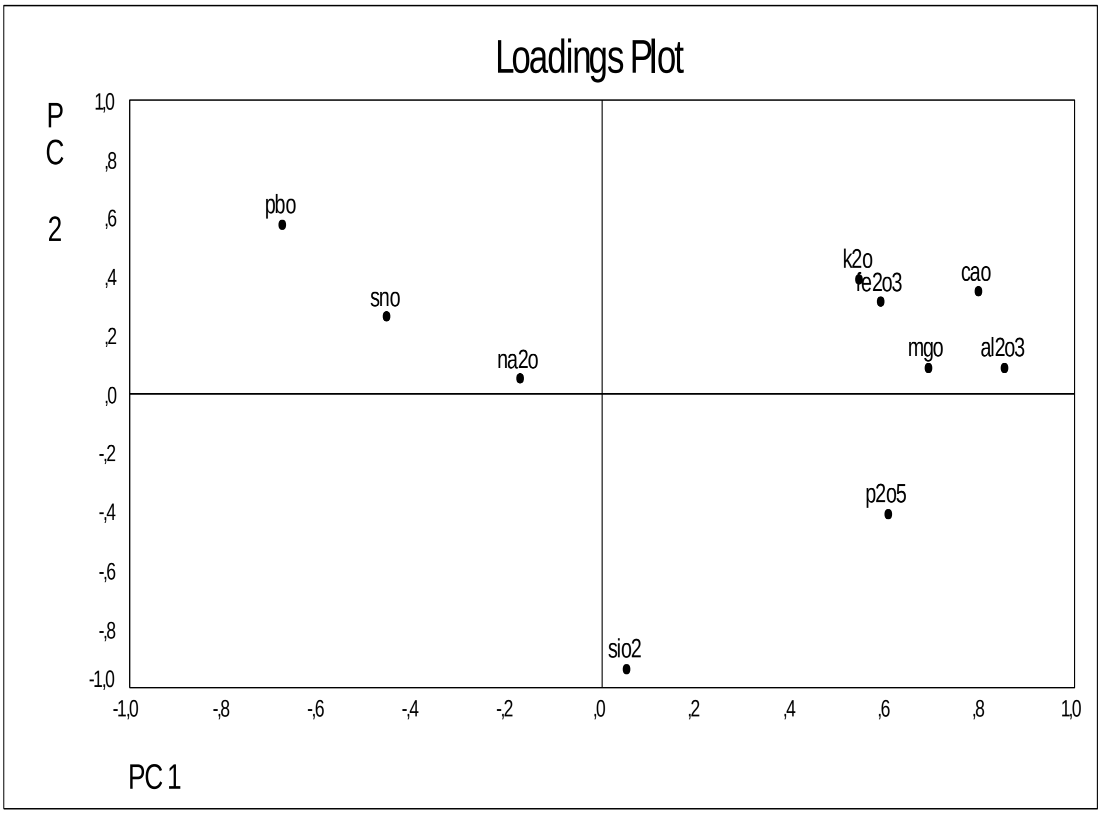

Figure 5.22: Loadings plot showing the results of PCA of glaze composition data of 75 samples for PC1 and PC2.

A graphical visualizing in three coordinate system, PC1, PC2, and PC3, was also performed for these ceramics. PC Loadings for each of principal components are seen in Table 5.9. Scores and loadings plots for three component system are given in the following figures 5.23 and 5.24.

Table 5.9. Values of Principal Component Loadings for Glaze Composition Data of 75 Samples

	PC 1	**PC 2**	**PC 3**
Al_2O_3	0.85419	0.08729	-0.13457
CaO	0.79875	0.34838	-0.08930
Fe_2O_3	0.59269	0.31249	-0.00696
K_2O	0.54606	0.39030	0.61267
MgO	0.69382	0.09040	-0.33125
Na_2O	-0.17144	0.05083	0.86866
P_2O_5	0.60856	-0.40754	-0.15273
PbO	-0.67373	0.57471	-0.33173
SiO_2	0.05451	-0.93613	0.02174
SnO	-0.45325	0.26240	-0.22692

In all figures 5.21 and 5.23 the numbers 1, 2, 3, 4, 5, 6, and 7 represents the samples as follows;

1: 12, 14-19, 28, 31-33, 39, 50, 52, 53, 55-58, 64, 68-75, 79, 80, 82, 87, 89, 93-104, 106, 114-117

2: 8, 10, 66, 81

3: 1, 5, 49, 51, 54, 78

4: 40, 41, 47, 88

5: 9, 45

6: 29, 106

7: 3, 30

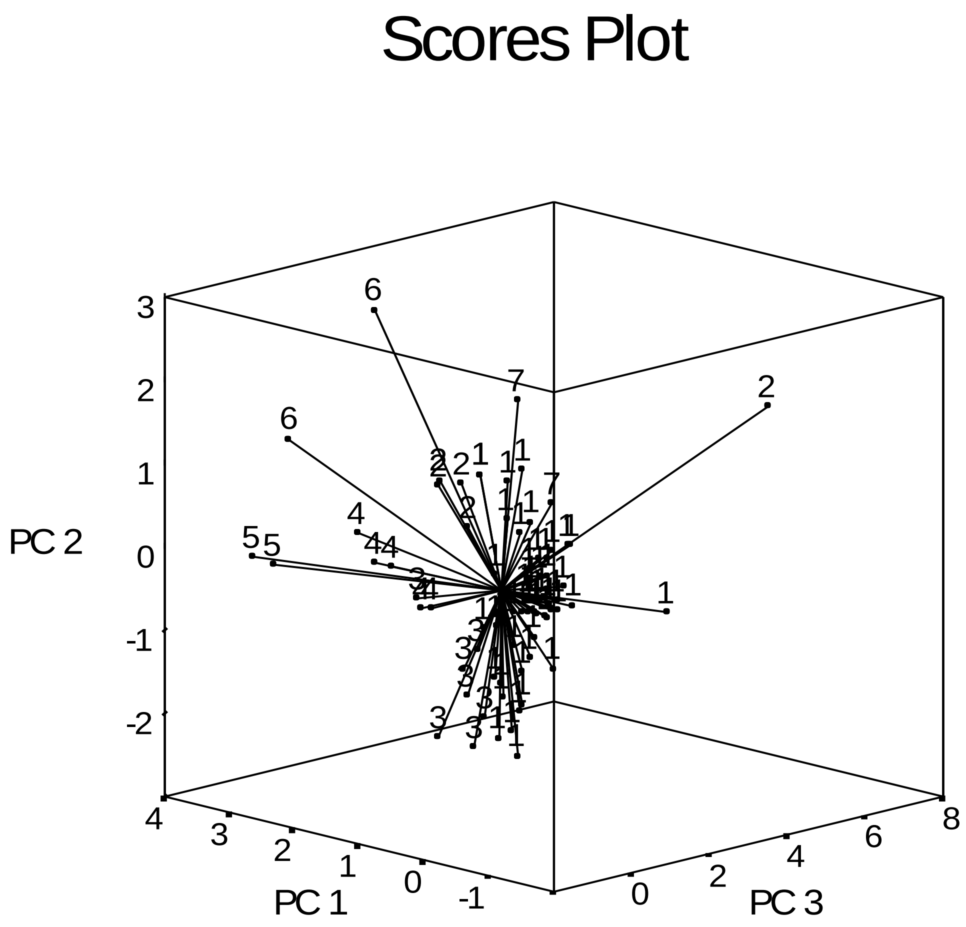

Figure 5.23: Scores plot showing the results of PCA of glaze composition data of 75 samples for PC1, PC2, and PC3.

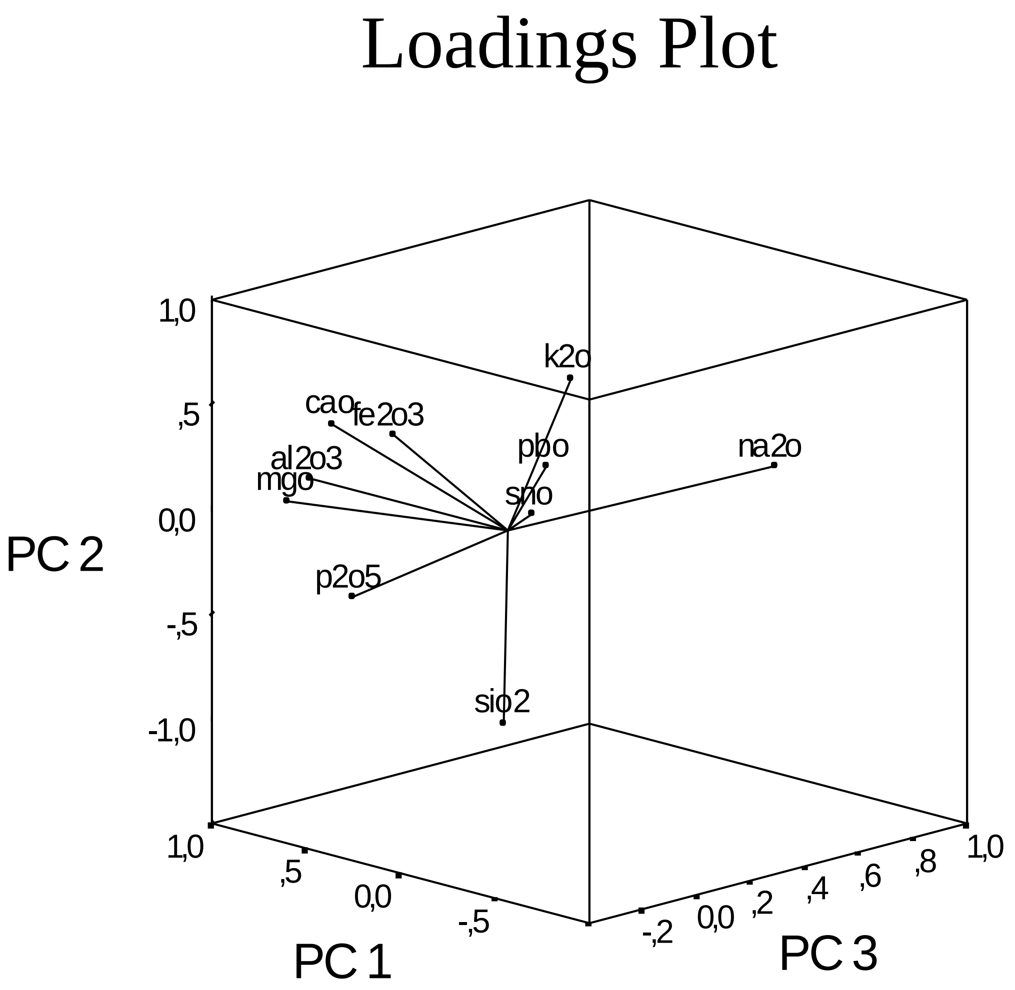

Figure 5.24: Loadings plot showing the results of PCA of glaze composition data of 75 samples for PC1, PC2, and PC3.

5.3.2 Cluster Analysis (CA) of Glaze Composition

CA was applied to the glaze composition of 75 ceramic samples on the basis of Euclidean distance. The same chemical constituents were used as in the case of PCA for clustering the samples. Dendograms obtained by the clustering for the Single and Complete Linkage Methods are given the figures 5.25 and 5.26.

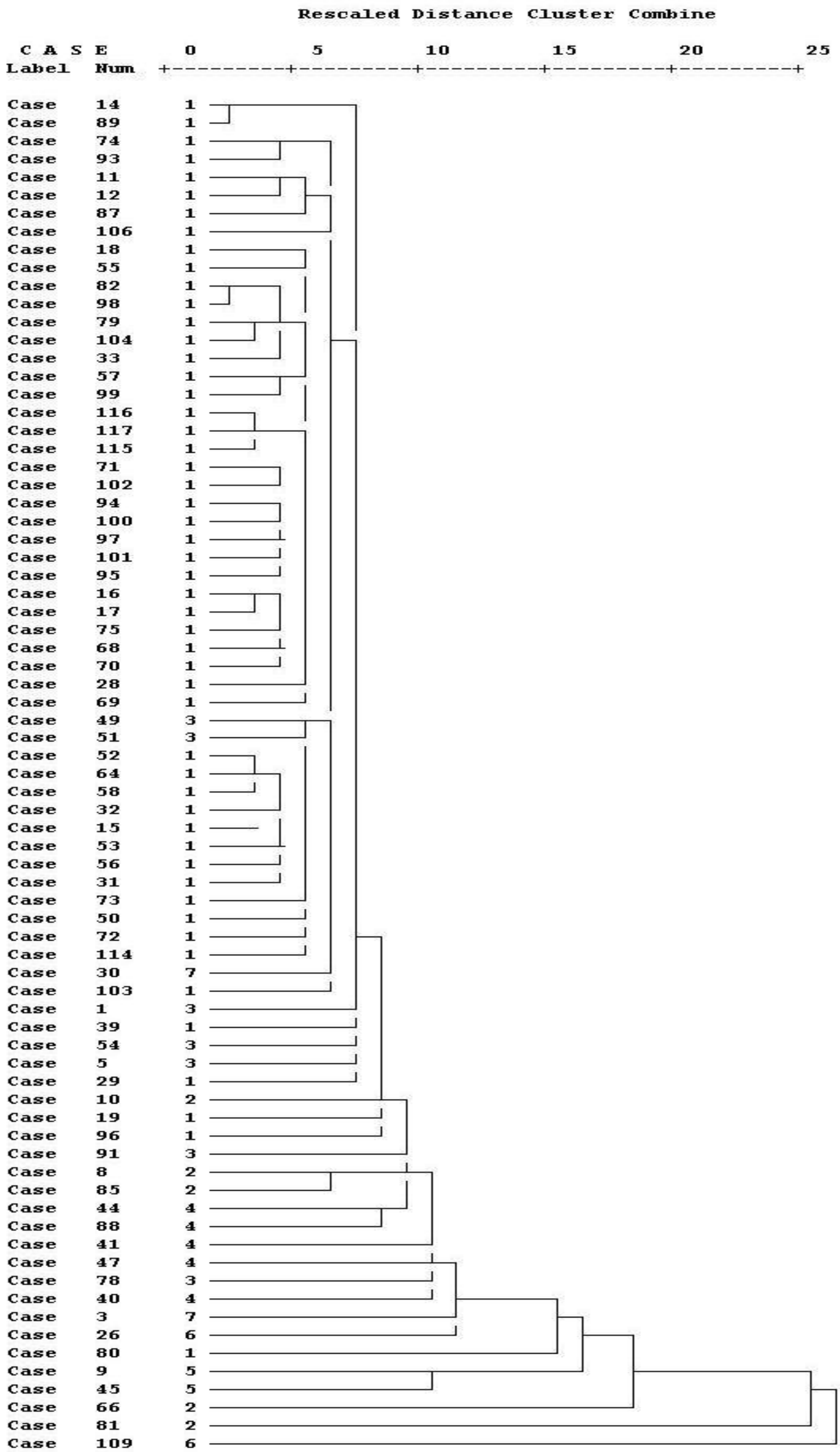

Figure 5.25: Dendogram showing the results of clustering glaze composition data of 75 samples based of Single Linkage.

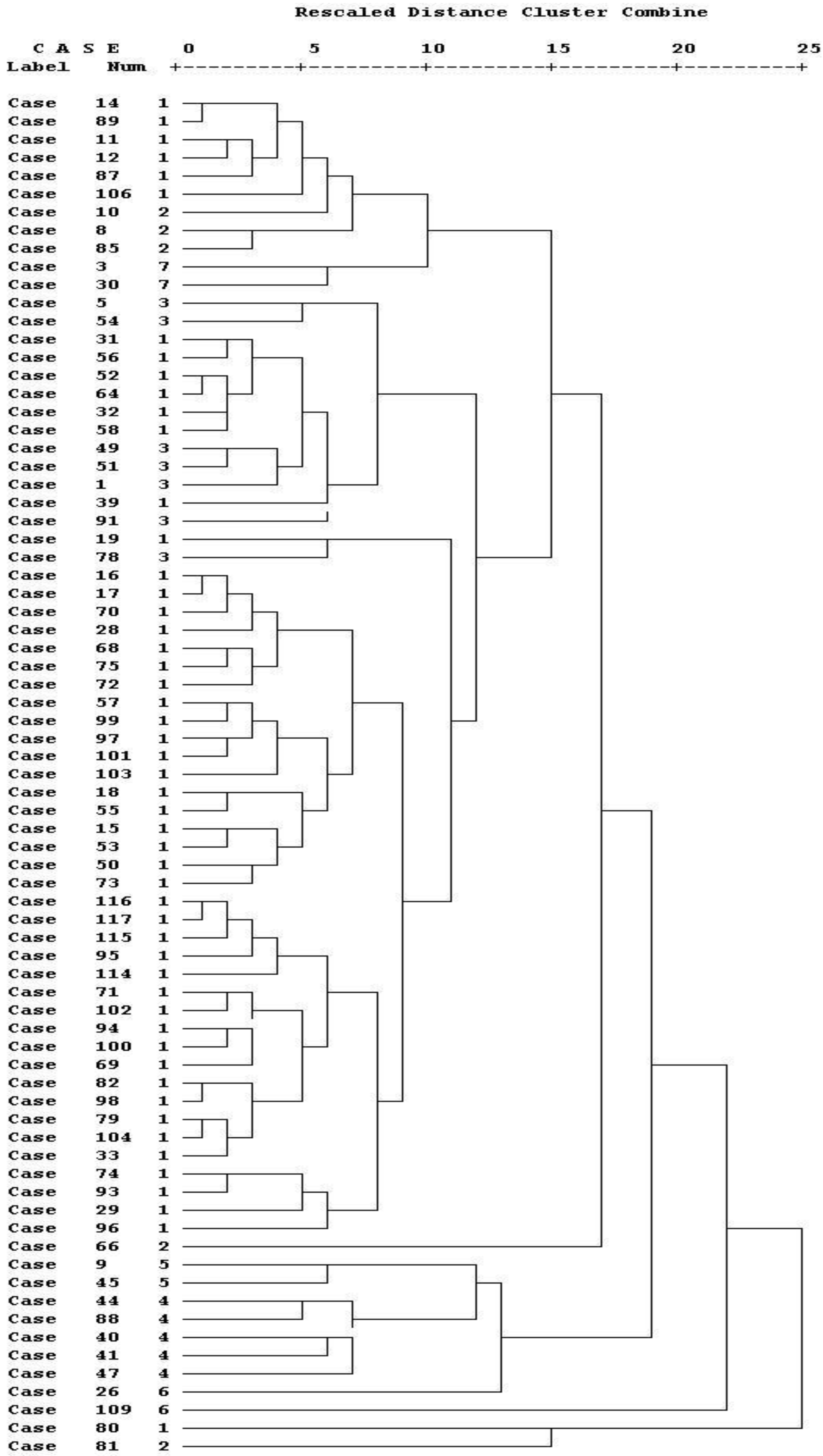

Figure 5.26: Dendogram showing the results of clustering glaze composition data of 75 samples based of Complete Linkage.

Dendogram showing the results of clustering variables for glaze composition of 75 ceramic samples are also given in the figures 5.27 and 5.28.

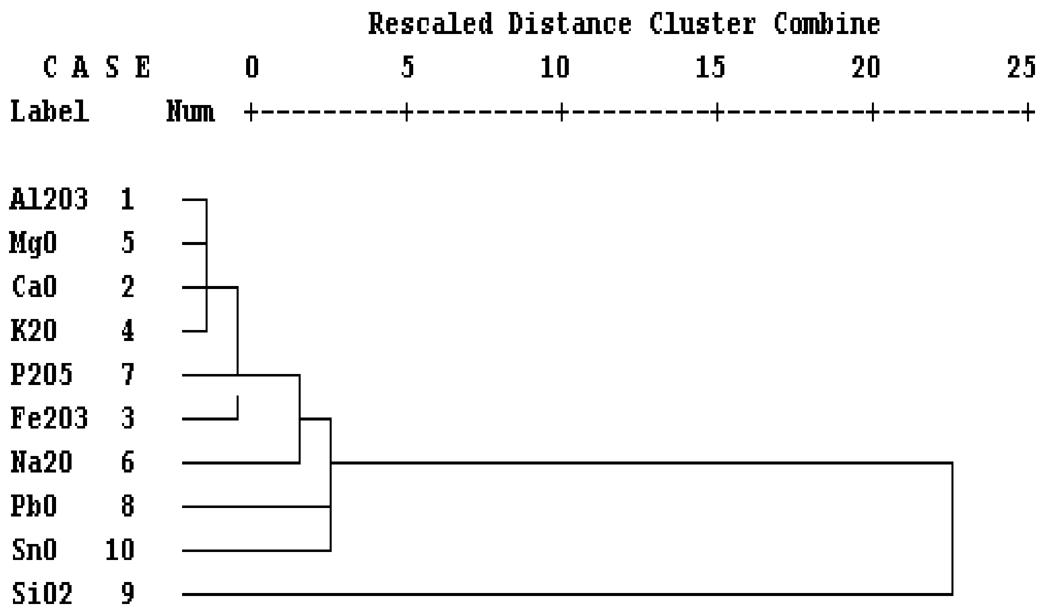

Figure 5.27: Dendogram showing the results of clustering variables for glaze composition of 75 ceramic samples based of Single Linkage.

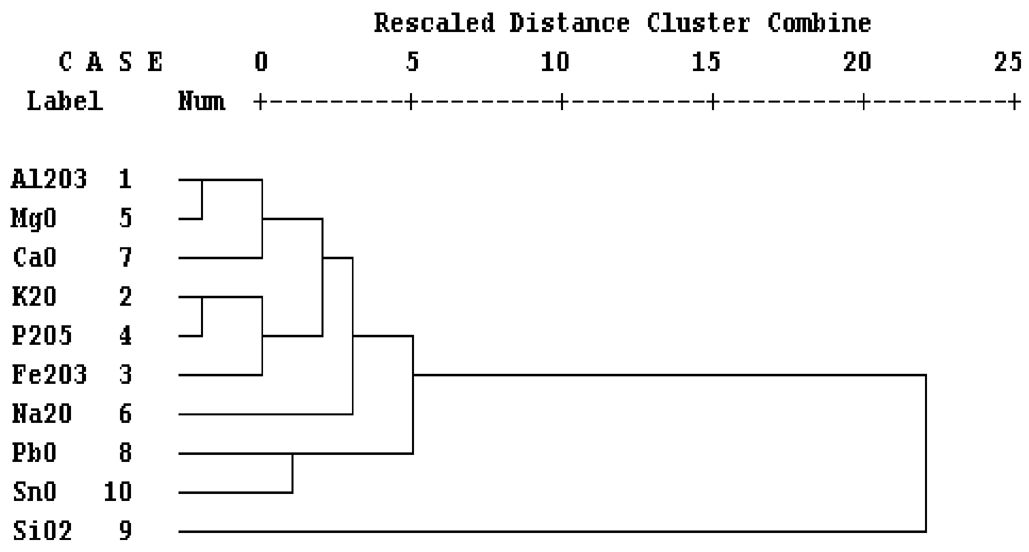

Figure 5.28: Dendogram showing the results of clustering variables for glaze composition of 75 ceramic samples based of Complete Linkage.

5.4 Chemometry of Glaze Data from Tulun's, Amara's, and Tite's Studies

The data of glaze composition from Tulun's together with Amara's and Tite's (Tulun et. al., 2002, Amara, 2003; Tite, 1989) were classified depending on the elemental oxides of glazes (Na_2O, MgO, Al_2O_3, SiO_2, K_2O, CaO, Fe_2O_3, PbO, SnO) by the application of PCA and CA.

5.4.1 Principle Component Analysis (PCA) of Glaze Data From from Tulun's, Amara's, and Tite's Studies

The scores and loadings diagrams of PCA, indicating PC1 and PC2, for Tulun's, Amara's, and Tite's glaze data are (Table B.5 and B.6) given in figures 5.29 and 5.30. The correlation matrix and the eigen values, the percentages of variances, and cumulative percentages corresponding to the each principal components are shown in the following Table 5.10 and 5.11, respectively.

Table 5.10. Correlation Matrix for Glaze Data of Tulun's, Amara's, and Tite's samples

	Al_2O_3	CaO	MgO	Na_2O	P_2O_5	PbO	SiO_2	SnO	Fe_2O_3	K_2O
Al_2O_3	1.00000	0.63547	0.45612	-0.22400	0.53748	-0.48977	-0.05925	-0.38918	0.34672	0.40798
CaO		1.00000	0.27414	-0.27384	0.31784	-0.39262	-0.08047	-0.21973	0.57678	0.55346
MgO			1.00000	-0.20906	0.24909	-0.22798	-0.27294	-0.20371	0.23032	0.03440
Na_2O				1.00000	-0.15633	-0.11194	-0.14230	0.06703	-0.23102	0.30373
P_2O_5					1.00000	-0.53913	0.26753	-0.23345	0.16844	0.10173
PbO						1.00000	-0.63654	0.33332	-0.28843	-0.37671
SiO_2							1.00000	-0.21662	-0.12245	-0.14151
SnO								1.00000	-0.29530	-0.20980
Fe_2O_3									1.00000	0.38086
K_2O										1.00000

Table 5.11. The eigen values, the percentages of variances, and cumulative percentages corresponding to the each principal components for Glaze Data of Tulun's, Amara's, and Tite's samples

Variable	Communality	PC	Eigenvalue	% of Variance	Cumulative Pct.
Al_2O_3	1.00000	1	3.50605	35.1	35.1
CaO	1.00000	2	1.72862	17.3	52.3
MgO	1.00000	3	1.43334	14.3	66.7
Na_2O	1.00000	4	0.97687	9.8	76.4
P_2O_5	1.00000	5	0.82433	8.2	84.7
PbO	1.00000	6	0.58097	5.8	90.5
SiO_2	1.00000	7	0.48304	4.8	95.3
SnO	1.00000	8	0.23939	2.4	97.7
Fe_2O_3	1.00000	9	0.21592	2.2	99.9
K_2O	1.00000	10	0.11470	0.1	100.0

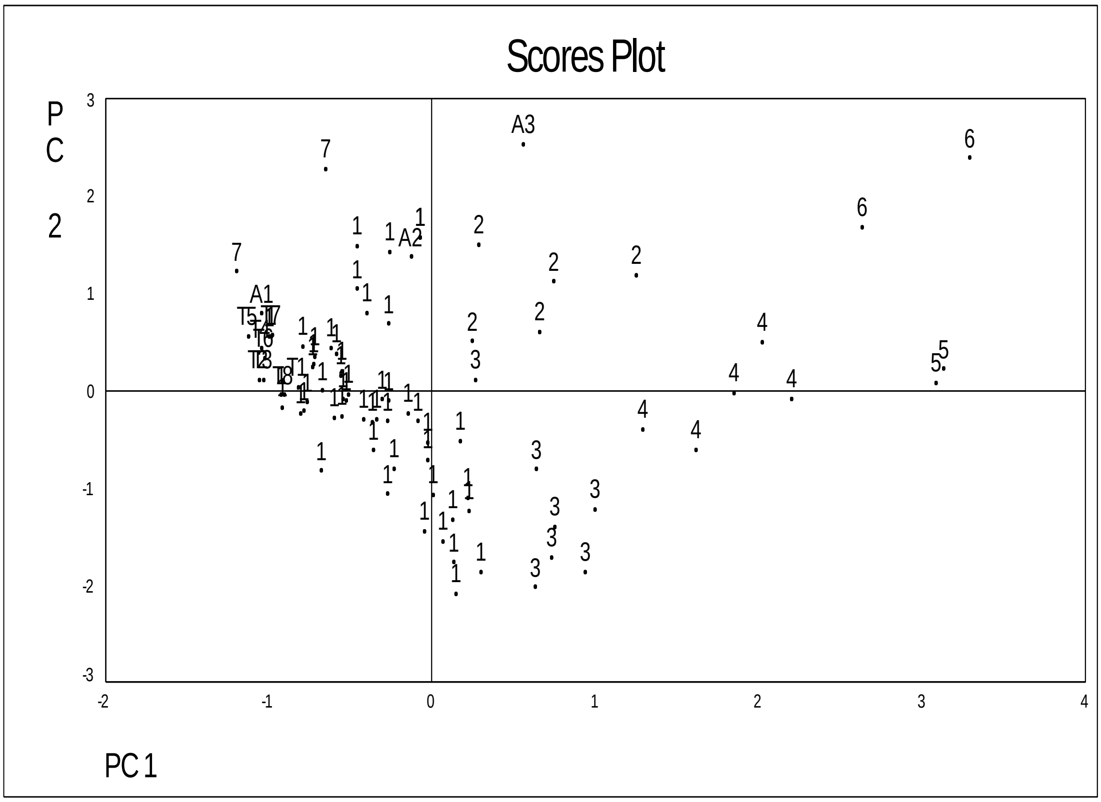

Figure 5.29: Scores plot showing the results of PCA of glaze data of Tulun's, Amara's, and Tite's samples for PC1 and PC

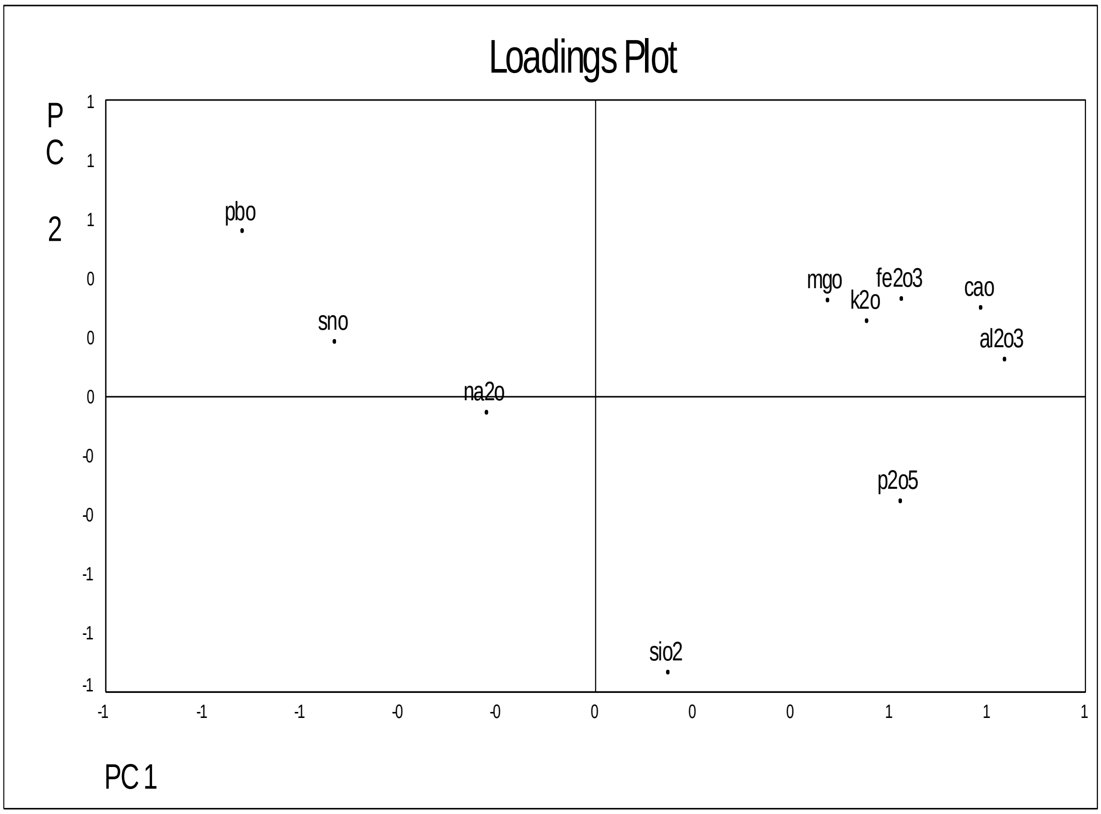

Figure 5.30: Loadings plot showing the results of PCA of glaze data of Tulun's, Amara's, and Tite's samples for PC1 and PC2

A graphical visualizing in three coordinate system, PC1, PC2, and PC3, was also performed for these ceramics. PC Loadings for each of principal components are seen in Table 5.12. Scores and loadings plots for three component system are given in the following figure 5.31 and 5.32.

Table 5.12. Values of Principal Component Loadings for Glaze Data of Tulun's, Amara's, and Tite's samples

	PC 1	**PC 2**	**PC 3**
Al_2O_3	0.83648	0.12538	-0.10328
CaO	0.78835	0.30096	0.04312
MgO	0.47639	0.32626	-0.38838
Na_2O	-0.22063	-0.05473	0.83584
P_2O_5	0.62494	-0.35429	-0.20232
PbO	-0.71860	0.55736	-0.22437
SiO_2	0.14876	-0.93181	-0.04813
SnO	-0.53044	0.18394	-0.00210
Fe_2O_3	0.62552	0.33114	0.01578
K_2O	0.55454	0.25487	0.69102

The number 1, 2, 3, 4, 5, 6, and 7 in figure 5.29 and figure 5.31 represents the same samples given in figures figures 5.21 and 5.23. The points, A1-A3, and T1-T8 shows the Amara's and Tite's samples, respectively.

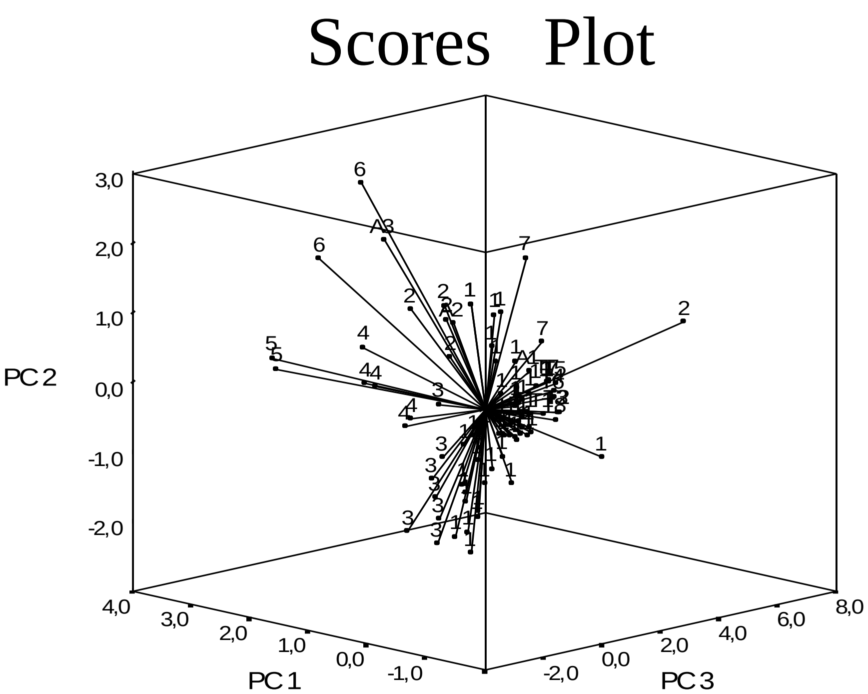

Figure 5.31: Scores plot showing the results of PCA of glaze data of Tulun's, Amara's, and Tite's samples for PC1, PC2 and PC3

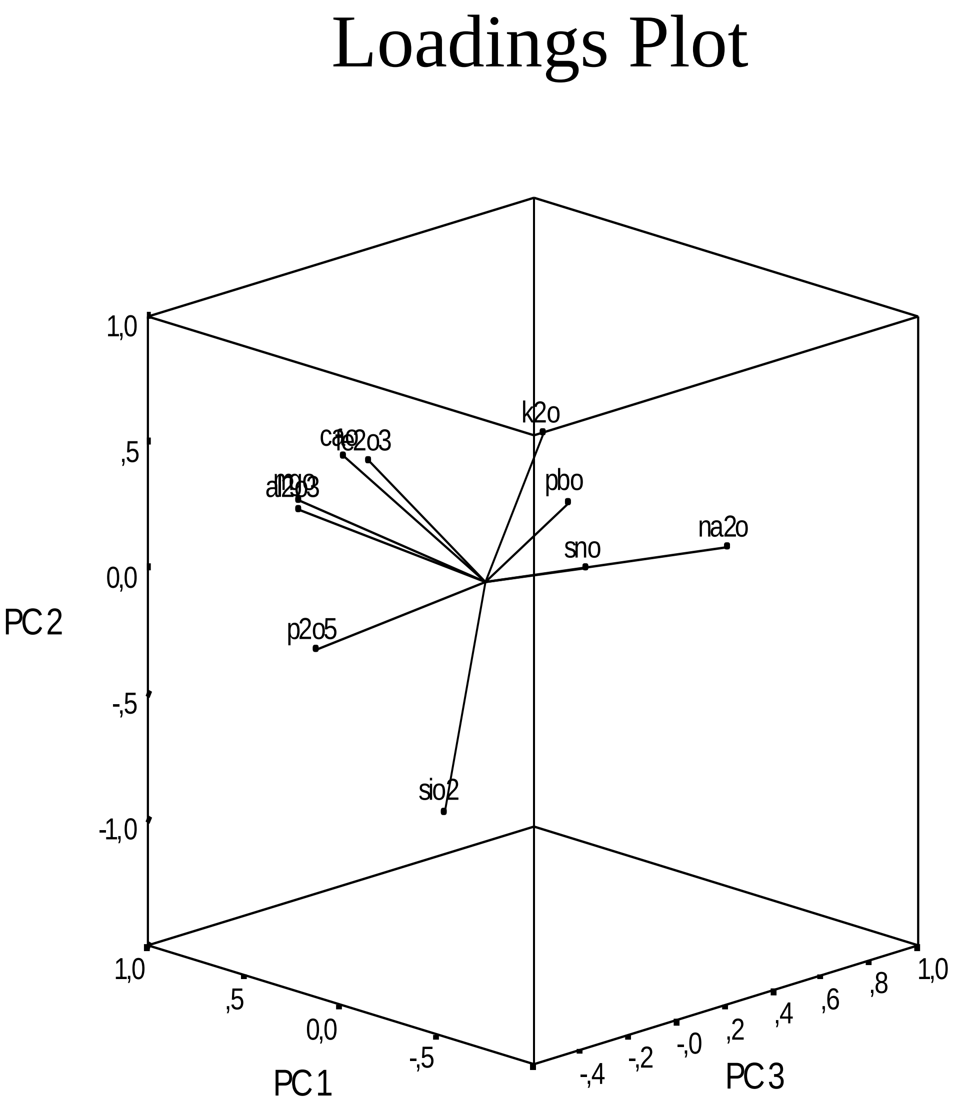

Figure 5.32: Loadings plot showing the results of PCA of glaze data of Tulun's, Amara's, and Tite's samples for PC1, PC2 and PC3

5.4.2 Cluster Analysis (CA) of Glaze Data From from Tulun's, Amara's, and Tite's Studies

CA was performed on the basis of Euclidean distance. Dendograms obtained by the clustering for the Single and Complete Linkage Methods are given the following figures 5.33 and 5.34.

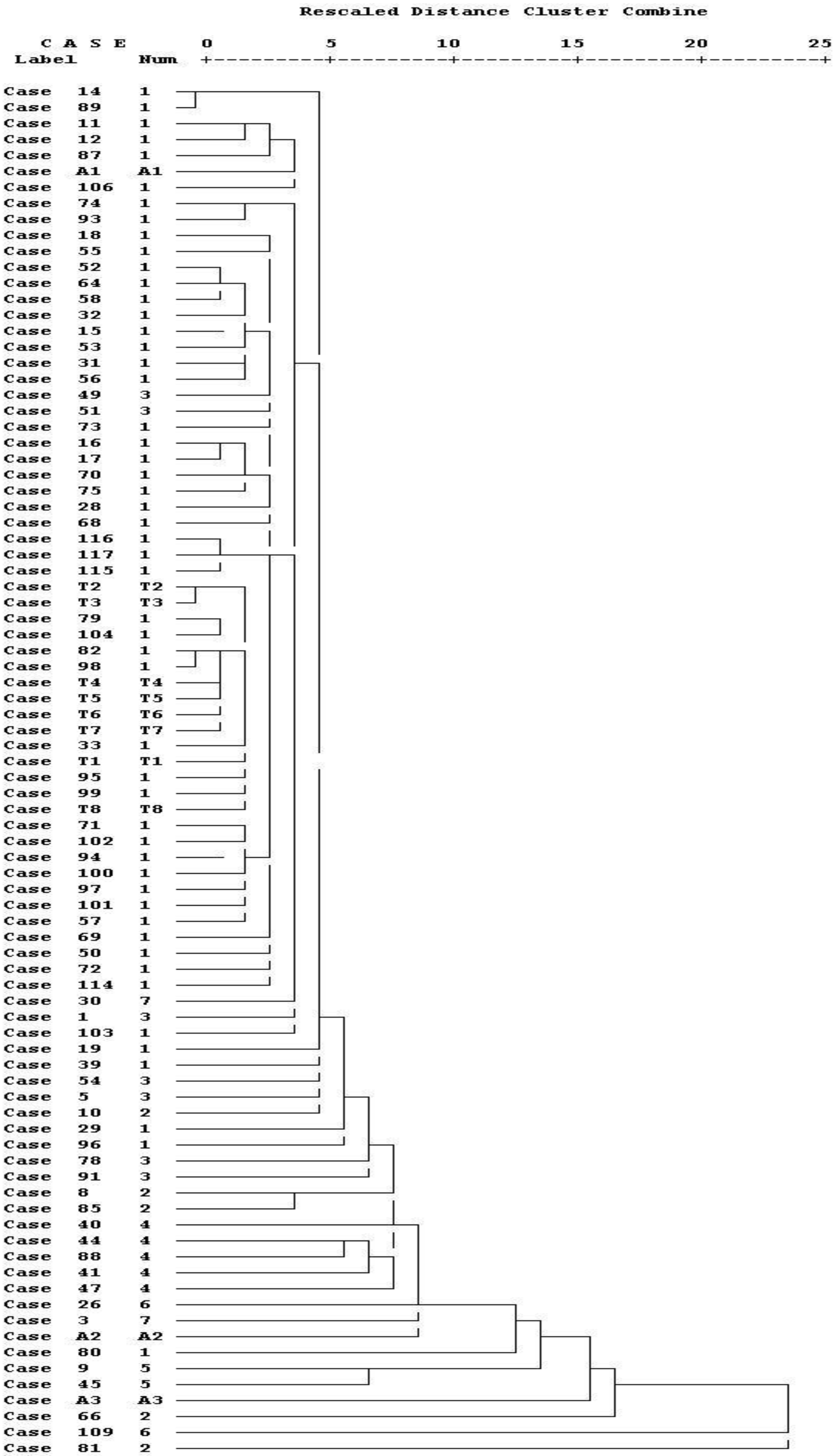

Figure 5.33: Dendogram showing the results of clustering glaze composition data from Tulun's, Amara's, and Tite's studies based of Single Linkage.

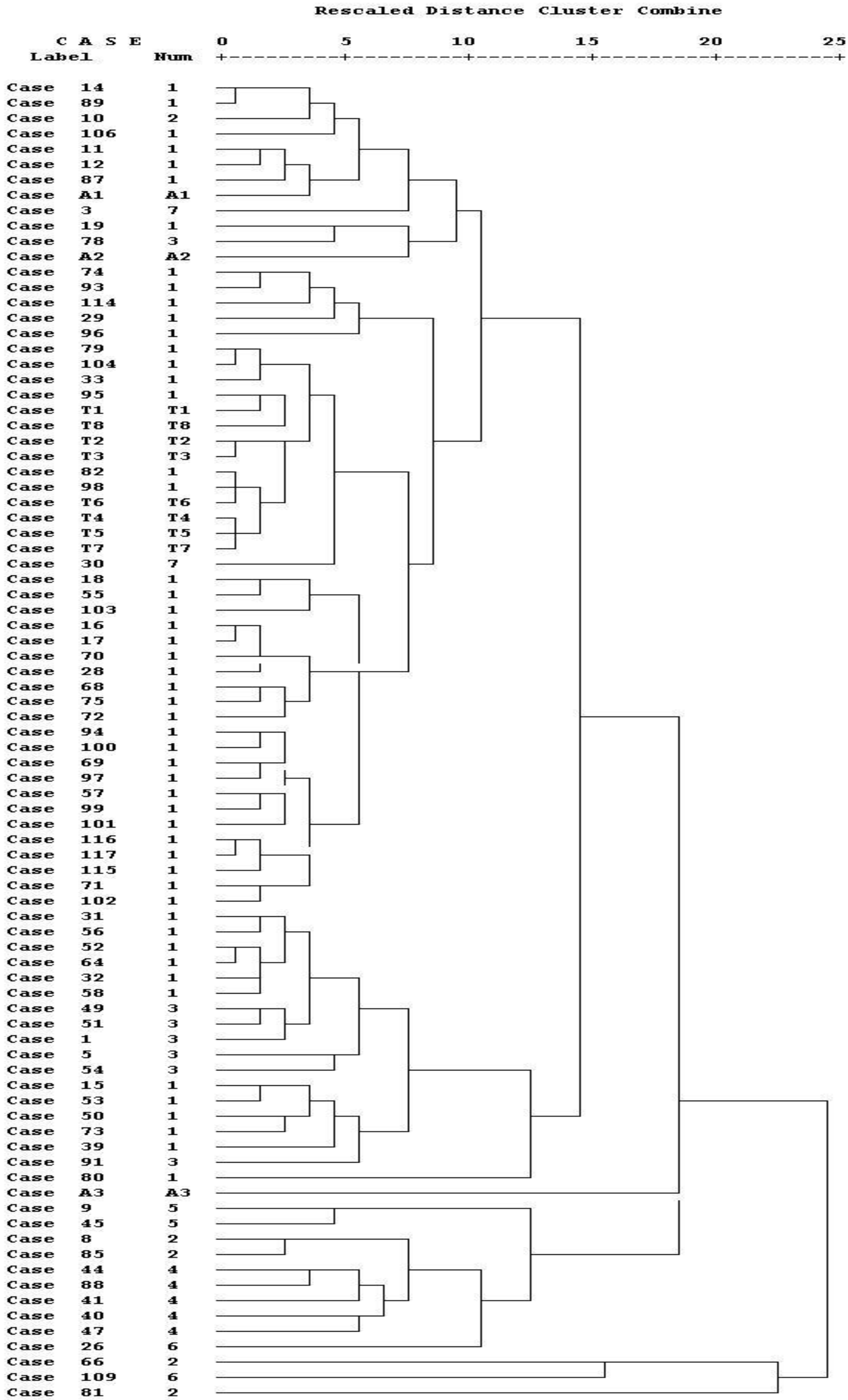

Figure 5.34: Dendogram showing the results of clustering glaze composition data from Tulun’s, Amara’s, and Tite’s studies on based of Complete Linkage.

Dendogram showing the results of clustering variables for glaze composition data from Tulun's, Amara's, and Tite's studies are also given in the figures 5.35 and 5.36.

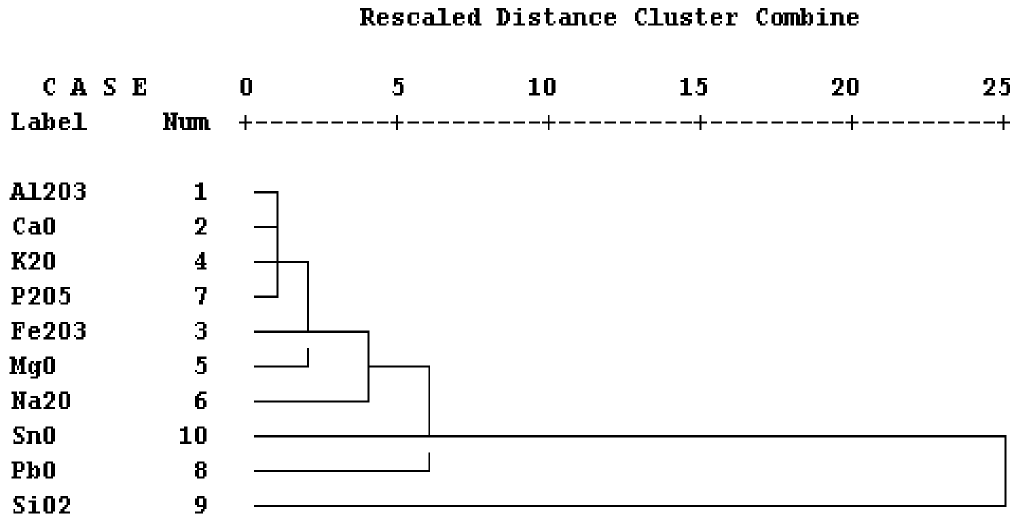

Figure 5.35: Dendogram showing the results of clustering variables glaze composition data from Tulun's, Amara's, and Tite's studies based of Single Linkage.

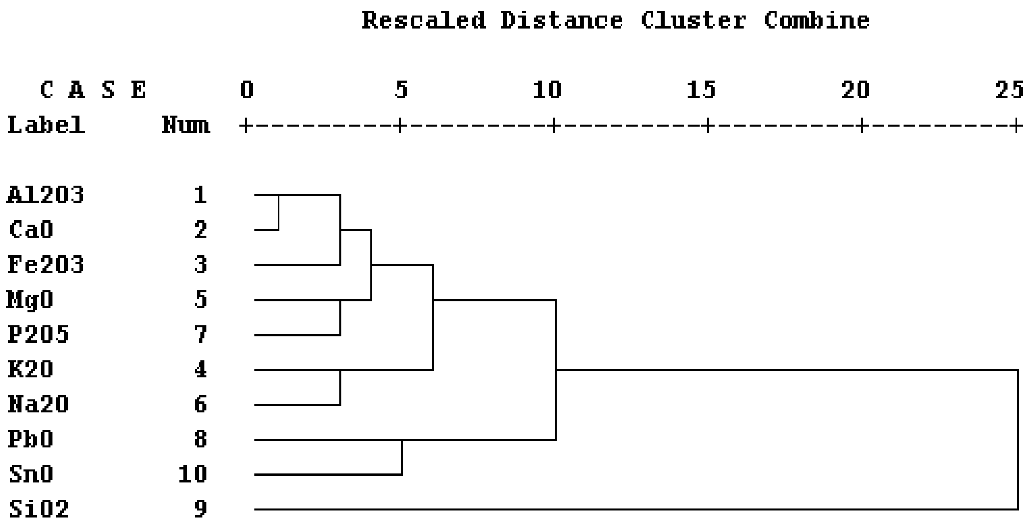

Figure 5.36: Dendogram showing the results of clustering variables glaze composition data from Tulun's, Amara's, and Tite's studies based of Complete Linkage.

5.5 Chemometric Analysis of Porosity Characteristics

5.5.1 Principle Component Analysis (PCA) of Porosity Characteristics

The PCA of 40 ceramic samples was carried out regarding their porosity characteristics. Apparent and bulk density, % porosity, and total pore volume were the main variables used in classification (Table B.7). The correlation matrix and the eigen values, the percentages of variances, and cumulative percentages corresponding to the each principal components are shown in the following Table 5.13 and 5.14, respectively. The visual aspects of PCA results showing two principle components scores and loadings plots are given in figures 5.37 and 5.38.

Table 5.13. Correlation Matrix for Porosity Data of 40 Samples

	Apparent Density	Bulk Density	Pore Diameter	Total Pore Volume
Apparent Density	1.00000	-0.04105	-0.09140	0.19290
Bulk Density		1.00000	-0.27329	-0.24741
Pore Diameter			1.00000	-0.13886
Total Pore Volume				1.00000

Table 5.14. The eigen values, the percentages of variances, and cumulative percentages corresponding to the each principal components for Porosity Data of 40 Samples

Variable	Communality	PC	Eigenvalue	% of Variance	Cumulative Pct.
Apparent Density	1.00000	1	1.37822	34.5	34.5
Bulk Density	1.00000	2	1.16336	29.1	63.5
Pore Diameter	1.00000	3	0.93953	23.5	87.0
Total Pore Volume	1.00000	4	0.51889	13.0	100.0

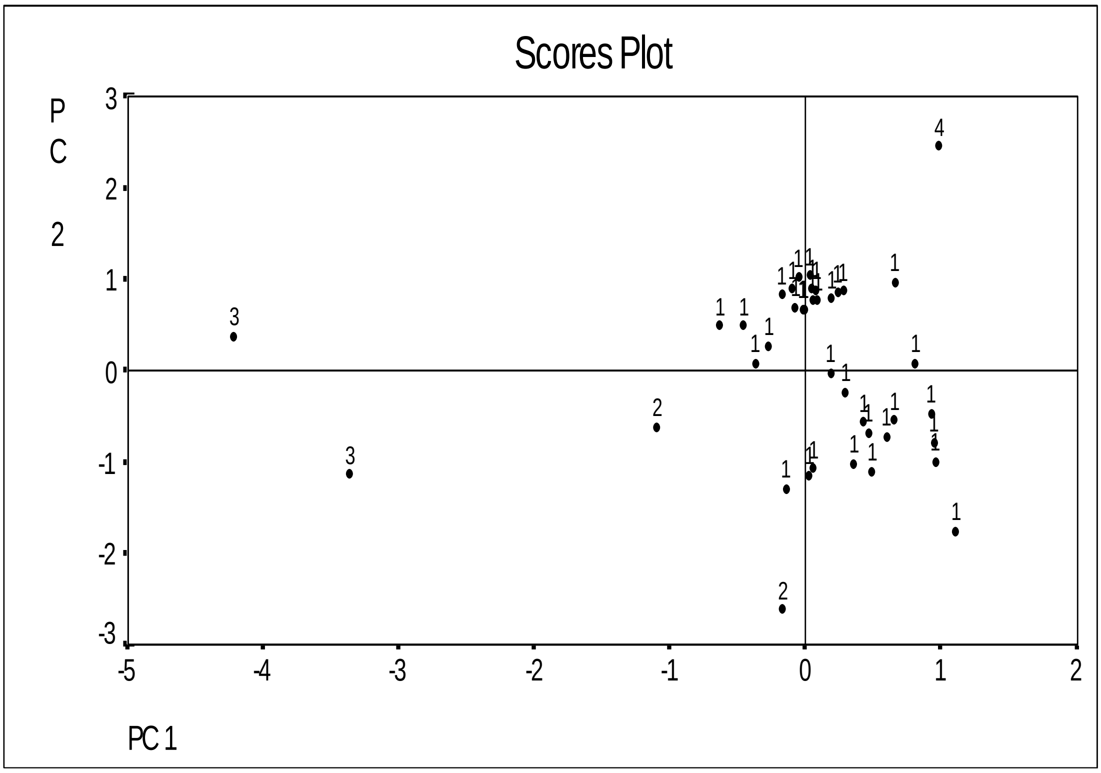

Figure 5.37: Scores plot showing the results of PCA of porosity data of 40 samples for PC1 and PC2.

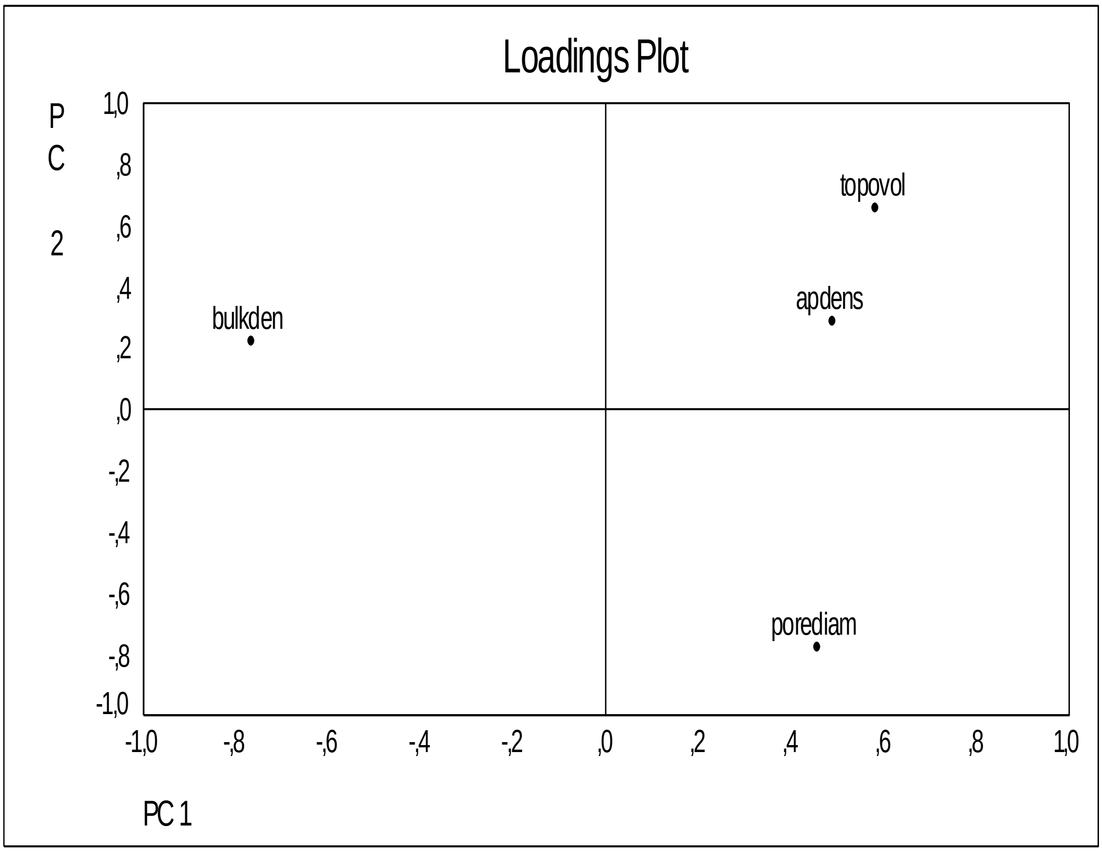

Figure 5.38: Loadings plot showing the results of PCA of porosity data of 40 samples for PC1 and PC2.

A graphical visualizing in three coordinate system, PC1, PC2, and PC3, was also performed for these ceramics. PC Loadings for each of principal components are seen in Table 5.15. Scores and loadings plots for three component system are given in the following figure 5.39 and 5.40.

Table 5.15. Values of Principal Component Loadings for Porosity Data of 40 Samples

	PC 1	PC 2	PC 3
Apparent Density	0.49138	0.28819	0.79722
Bulk Density	-0.76590	0.22403	0.44222
Pore Diameter	0.45795	-0.77281	0.20866
Total Pore Volume	0.58348	0.65793	-0.25469

In figures 5.37 and 5.39, the samples 21 and 31 were indicated by number 2, the samples 3 and 66 were indicated by number 3, number 4 indicated sample 4 and the rest of samples were indicated by number 1.

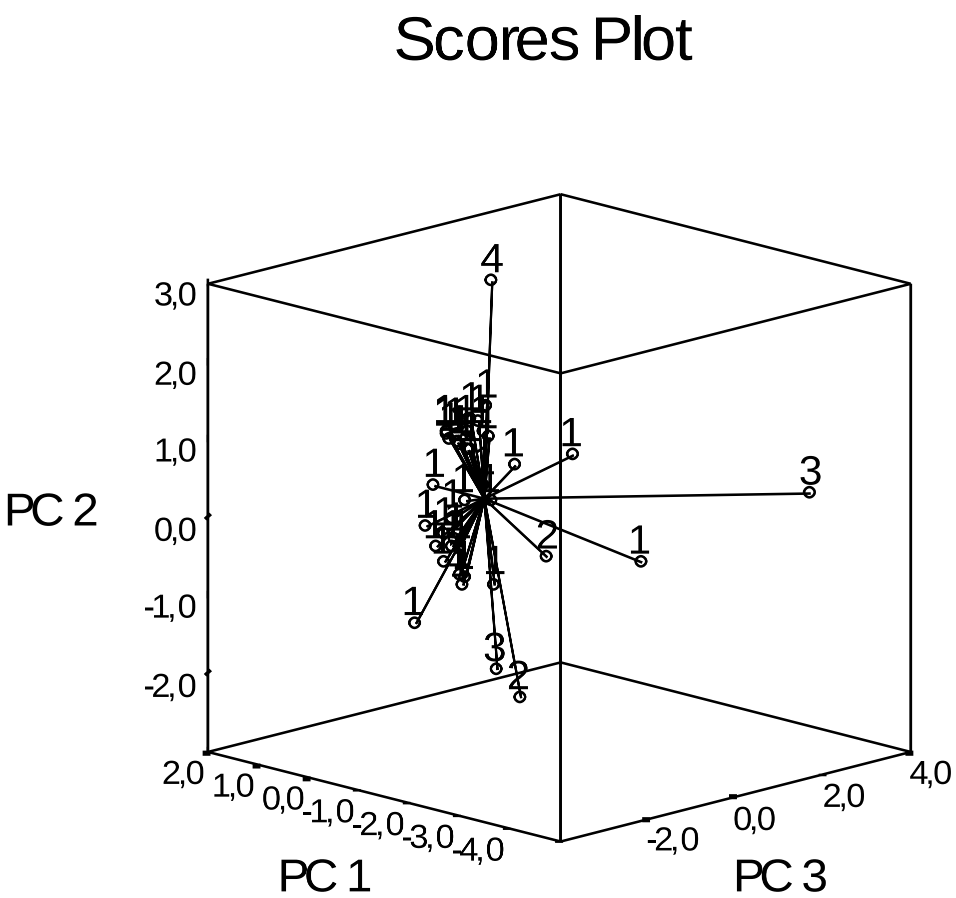

Figure 5.39: Scores plot showing the results of PCA of porosity data of 40 samples for PC1, PC2 and PC3.

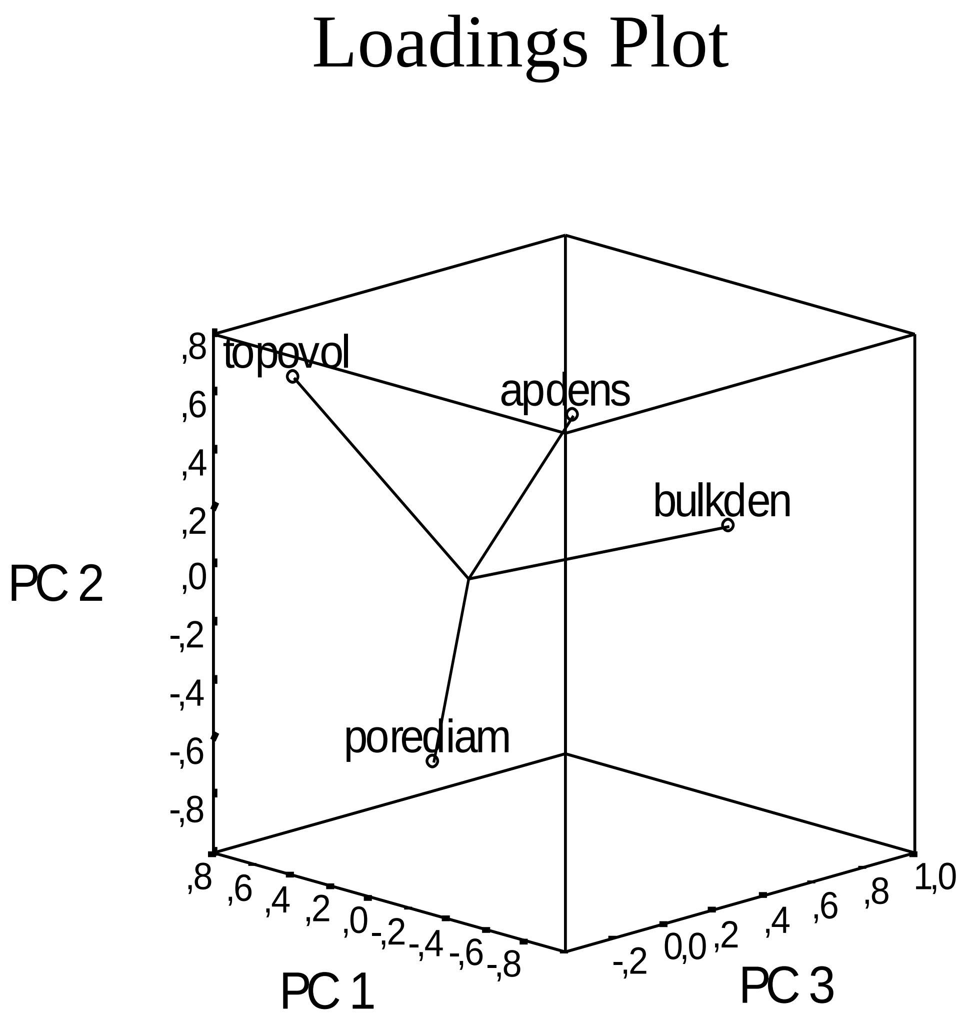

Figure 5.40: Loadings plot showing the results of PCA of porosity data of 40 samples for PC1, PC2 and PC3.

5.5.2 Cluster Analysis (CA) of Porosity Characteristics

CA was performed for the porosity characteristics of 40 ceramic samples on the basis of Euclidean distance. The same chemical constituents were used as in the case of PCA. Dendograms of obtained by the clustering for the Single and Complete Linkage Methods are given the figures 5.41 and 5.42.

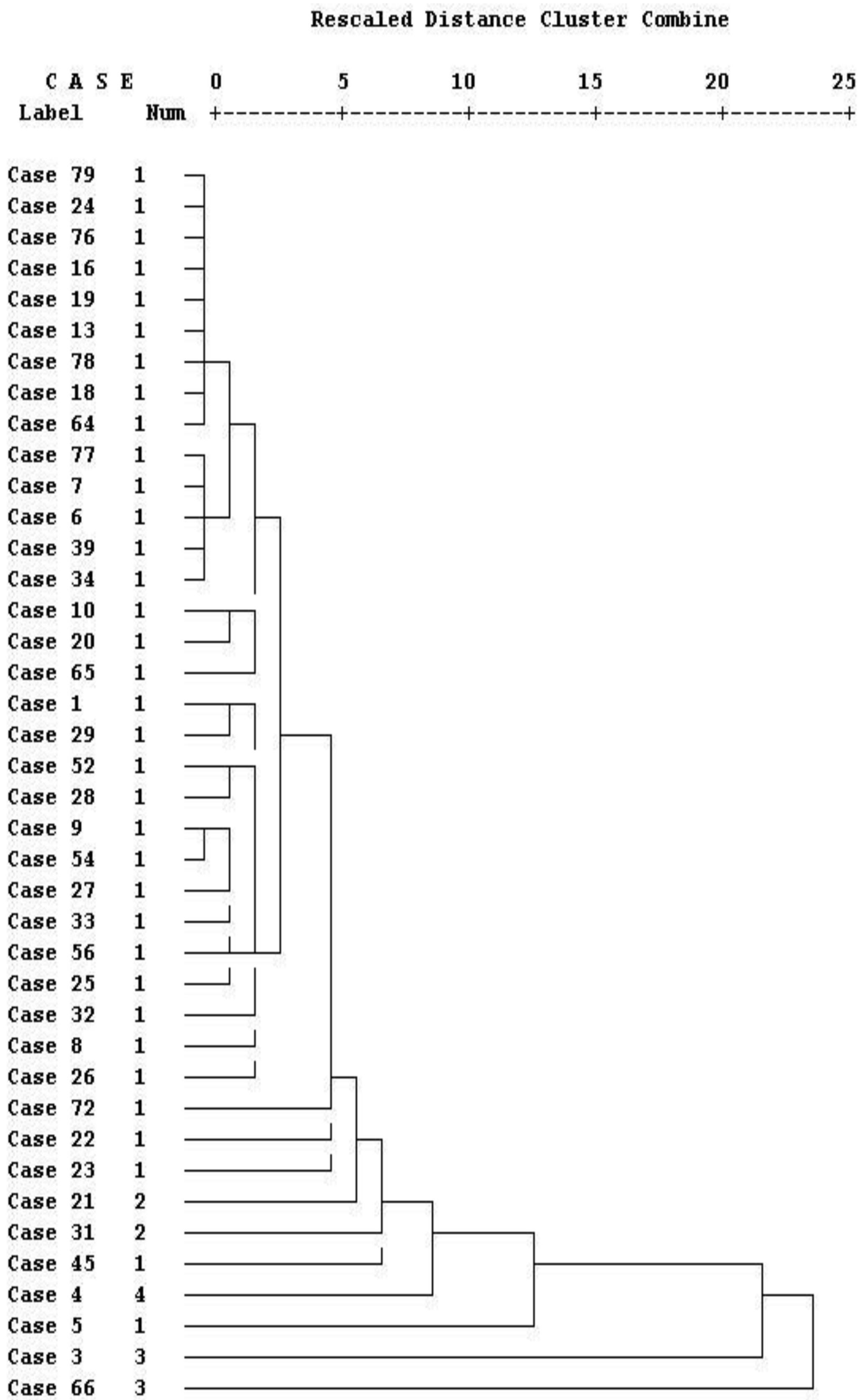

Figure 5.41: Dendogram showing the results of clustering porosity data of 40 samples based of Single Linkage.

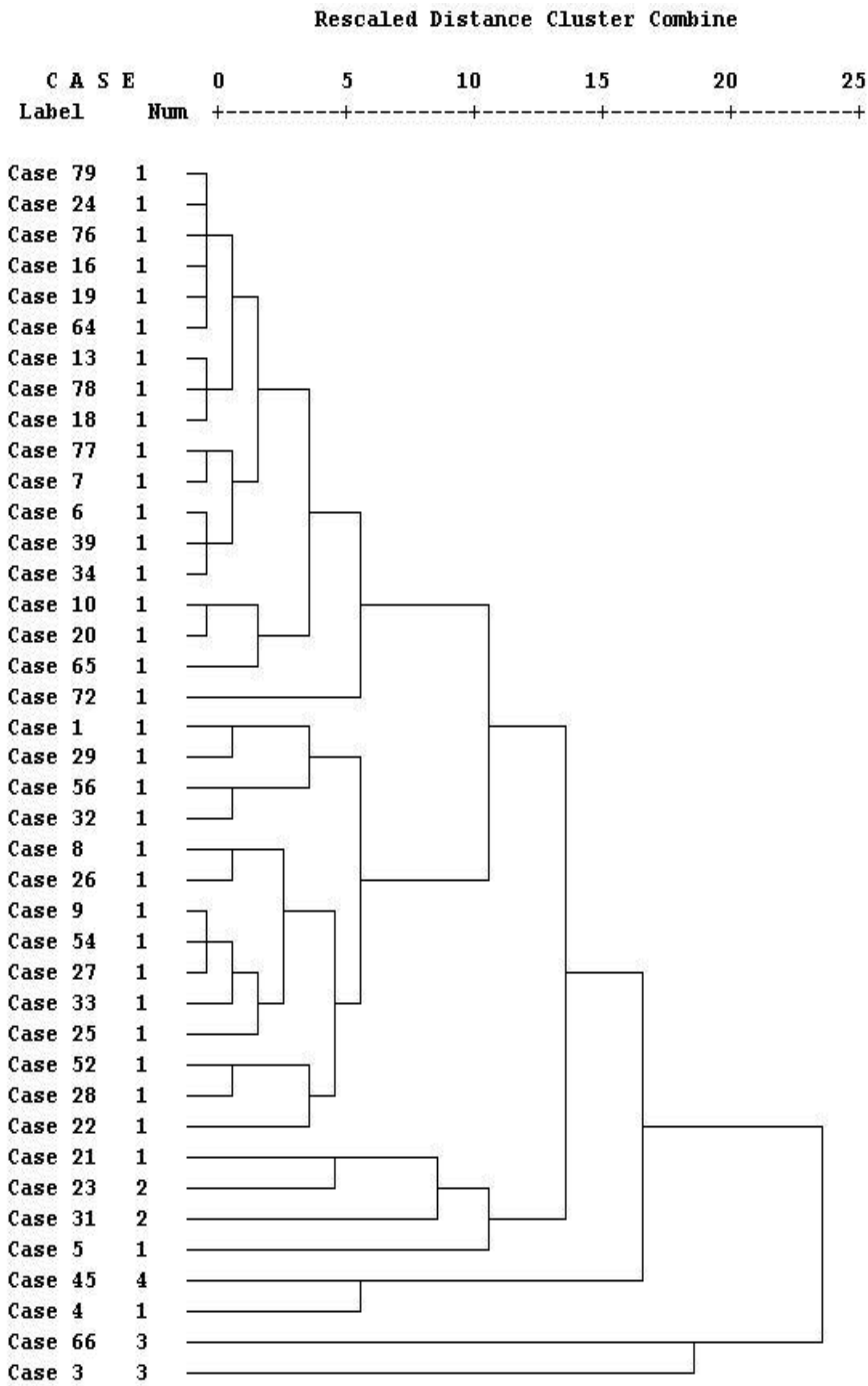

Figure 5.42: Dendogram showing the results of clustering porosity data of 40 samples based of Complete Linkage.

Dendogram showing the results of clustering variables for porosity data of 40 ceramic samples are also given in the figures 5.43 and 5.44.

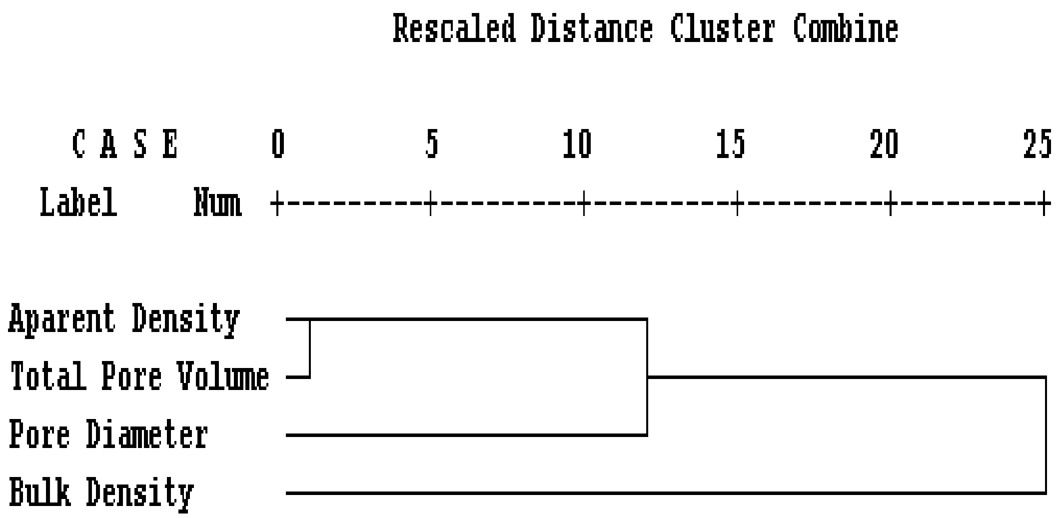

Figure 5.43: Dendogram showing the results of clustering variables for porosity data of 40 ceramic samples based of Single Linkage.

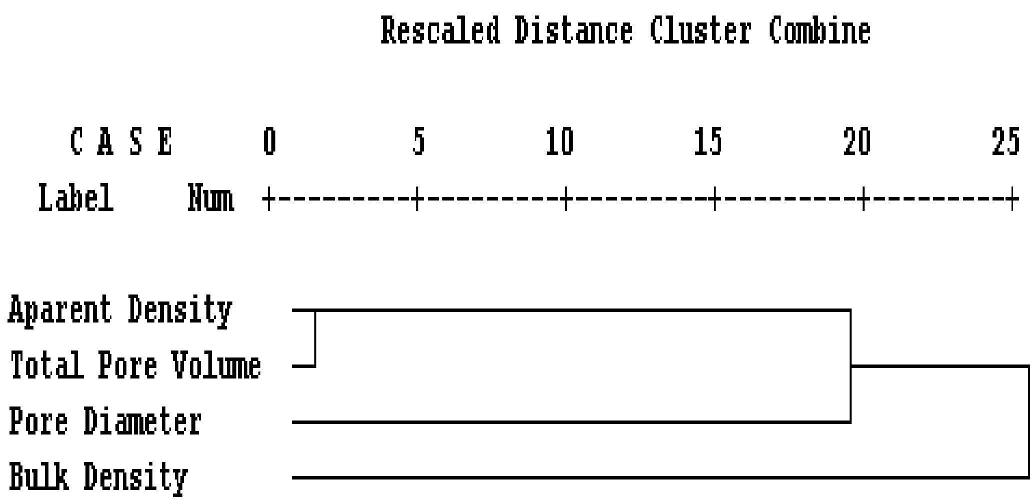

Figure 5.44: Dendogram showing the results of clustering variables for porosity data of 40 ceramic samples based of Complete Linkage.

5.6 Chemometric Analysis of Soluble Salts

5.6.1 Principal Component Analysis (PCA) of Soluble Salts

PCA was applied to the soluble salts content of 23 ceramic samples (Table 4.7). The correlation matrix and the eigen values, the percentages of variances, and cumulative percentages corresponding to the each principal components are shown in the following Table 5.16 and 5.17, respectively. A plot of principal component 1 and 2 showing scores and loadings are shown in figures 5.45 and 5.46. The amounts of each anion with respect to temperature and time duration (except PO_4^{3-} and SO_4^{2-} for 20^oC) were the variables in order to classify the samples.

Table 5.4. Correlation Matrix for Soluble Salts Data of 23 Samples

	Cl^- 20^OC	**Cl^- 25 ^OC**	**Cl^- 30 ^OC**	**NO_3^- 20 ^OC**	**NO_3^- 25 ^OC**	**NO_3^- 30 ^OC**	**PO_4^{3-} 25 ^OC**	**PO_4^{3-} 30 ^OC**	**SO_4^{2-} 25 ^OC**	**SO_4^{2-} 30 ^OC**
Cl^- 20^OC	1.00000	0.99714	0.98726	0.89619	0.80385	0.81052	-0.13689	0.17812	0.39189	0.24895
Cl^- 25 ^OC		1.00000	0.99416	0.89276	0.79874	0.80671	-0.11625	0.21768	0.37456	0.21745
Cl^- 30 ^OC			1.00000	0.87703	0.79254	0.81576	-0.08586	0.27159	0.35572	0.17334
NO_3^- 20 ^OC				1.00000	0.93760	0.85497	-0.09111	0.08326	0.29542	0.11955
NO_3^- 25 ^OC					1.00000	0.95913	-0.02070	0.01453	0.21093	0.03215
NO_3^- 30 ^OC						1.00000	-0.00794	0.01251	0.18656	0.04208
PO_4^{3-} 25 ^OC							1.00000	0.48853	-0.22118	-0.01913
PO_4^{3-} 30 ^OC								1.00000	-0.05779	-0.24607
SO_4^{2-} 25 ^OC									1.00000	0.59364
SO_4^{2-} 30 ^OC										1.00000

Table 5.5. The eigen values, the percentages of variances, and cumulative percentages corresponding to the each principal components for Soluble Salts Data of 23 Samples

Variable	**Communality**	**PC**	**Eigenvalue**	**% of Variance**	**Cumulative Pct.**
Cl^- 20^OC	1.00000	1	5.60101	56.0	56.0
Cl^- 25 ^OC	1.00000	2	1.76965	17.7	73.7
Cl^- 30 ^OC	1.00000	3	1.25655	12.6	86.3
NO_3^- 20 ^OC	1.00000	4	0.73594	7.4	93.6
NO_3^- 25 ^OC	1.00000	5	0.37631	3.8	97.4
NO_3^- 30 ^OC	1.00000	6	0.13263	1.3	98.7
PO_4^{3-} 25 ^OC	1.00000	7	0.11841	1.2	99.9
PO_4^{3-} 30 ^OC	1.00000	8	0.00689	0.1	100.0
SO_4^{2-} 25 ^OC	1.00000	9	0.00213	0.0	100.0
SO_4^{2-} 30 ^OC	1.00000	10	0.00048	0.0	100.0

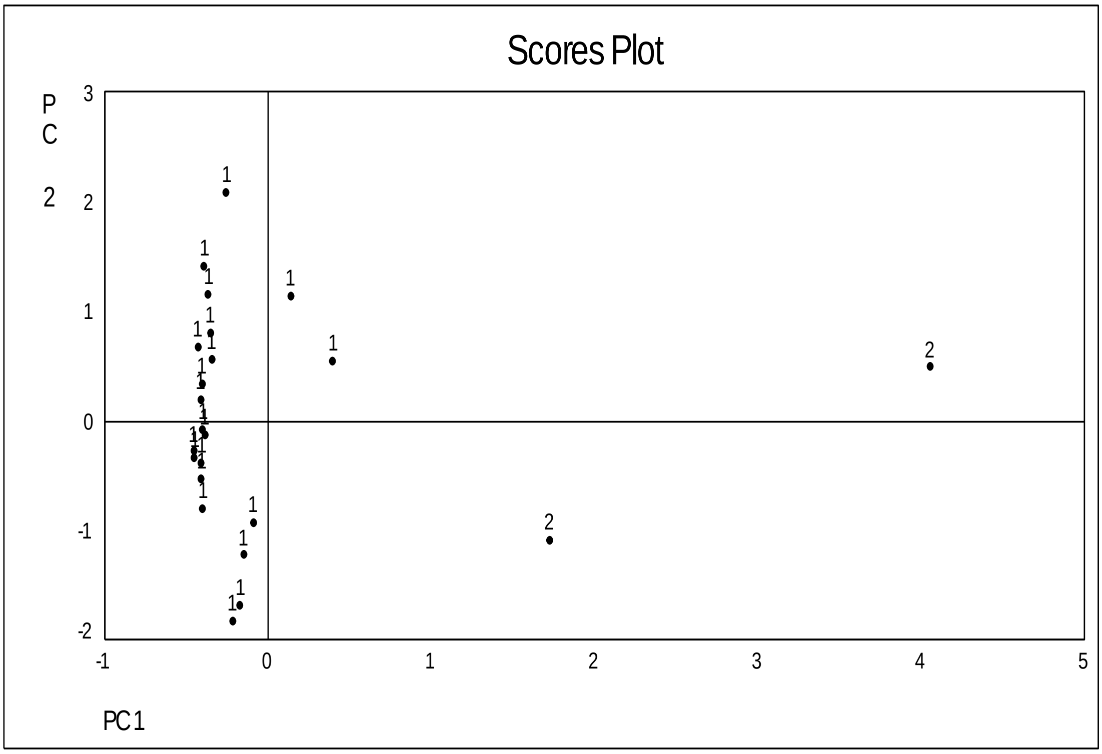

Figure 5.45: Scores plot showing the results of PCA of soluble salts data of 23 samples for PC1 and PC2.

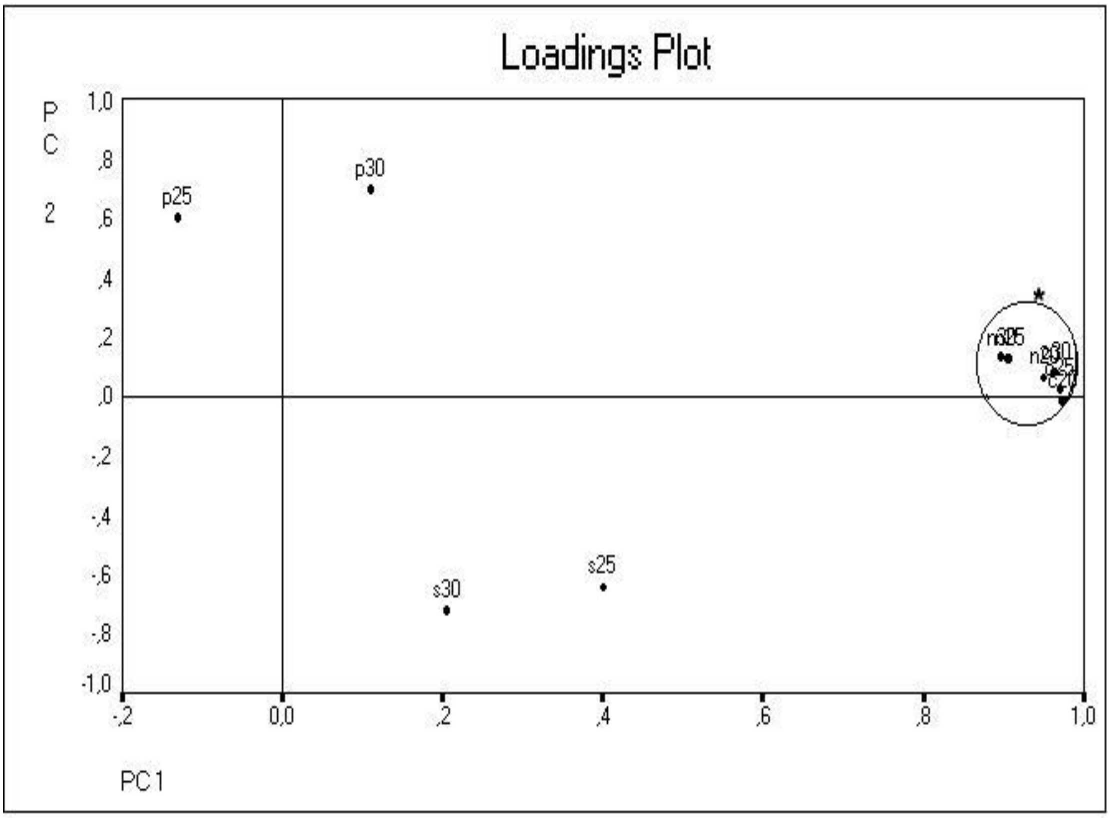

Figure 5.46: Loadings plot showing the results of PCA of soluble salts data of 23 samples for PC1 and PC2.

A graphical visualizing in three coordinate system, PC1, PC2, and PC3, was also performed for these ceramics. PC Loadings for each of principal components are seen in Table 5.18. Scores and loadings plots for three component system are given in the following figure 5.47 and 5.48.

Table 5.18. Values of Principal Component Loadings for Soluble Salts Data of 23 Samples

	PC 1	PC 2	PC 3
Cl^- 20^OC	0,97439	-0,01525	0,05112
Cl^- 25^OC	0,97164	0,02548	0,05918
Cl^- 30^OC	0,96534	0,08103	0,07004
NO_3^- 20^OC	0,95040	0,05735	-0,11819
NO_3^- 25^OC	0,90716	0,12382	-0,22161
NO_3^- 30^OC	0,89795	0,13089	-0,21136
PO_4^{3-} 25^OC	-0,10212	0,61935	0,56591
PO_4^{3-} 30^OC	0,13546	0,70028	0,53695
SO_4^{2-} 25^OC	0,40734	-0,62499	0,46852
SO_4^{2-} 30^OC	0,21999	-0,67959	0,55651

In figures 5.45 and 5.47, samples 25 and 26 were indicated by number 2 and the rest of samples by number 1. In figures 5.46 and 5.48, p25, p30, s25, s30 represents the phosphates and sulphates at 25^{o}C and 30^{o}C respectively. * Shows c20, c25, c30, n20, n25, and n30 that indicates the chlorides at 20^{o}C, 25^{o}C, and 30^{o}C and nitrates at 20^{o}C, 25^{o}C, and 30^{o}C in the same manner.

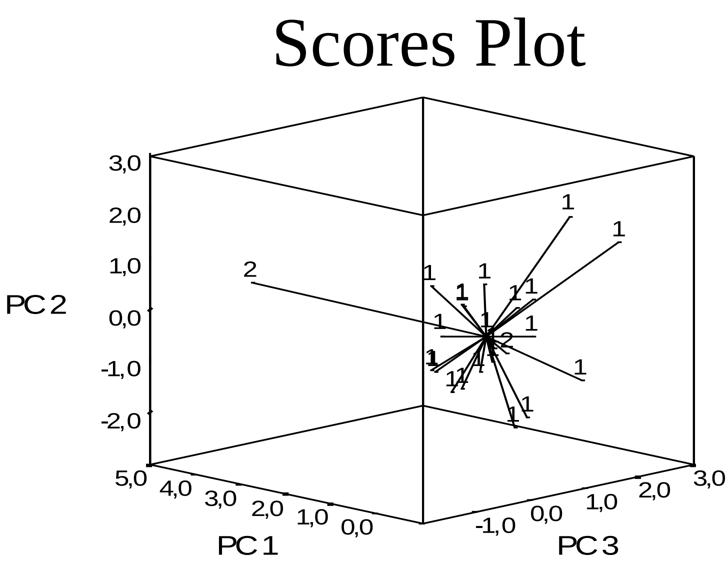

Figure 5.47: Scores plot showing the results of PCA of soluble salts data of 23 samples for PC1, PC2 and PC3

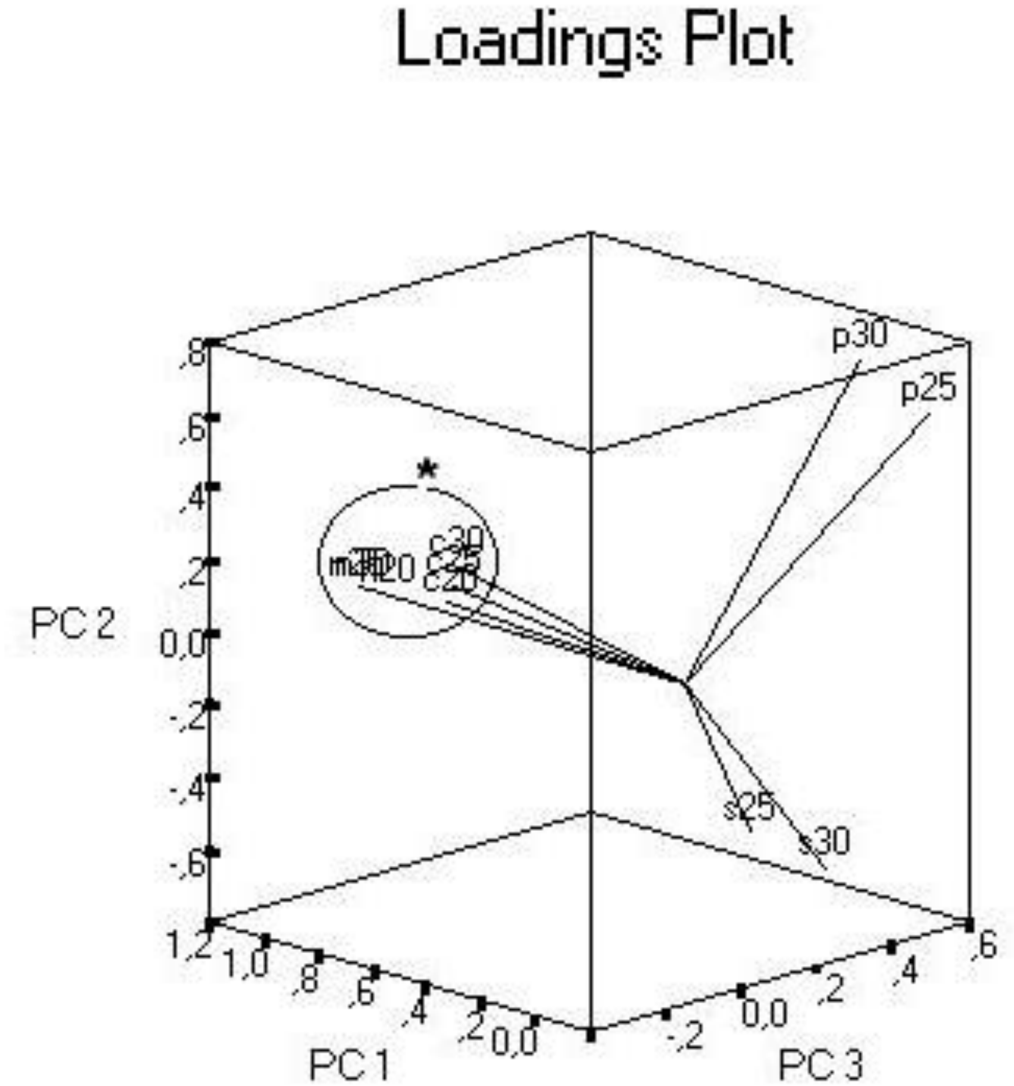

Figure 5.48: Scores plot showing the results of PCA of soluble salts data of 23 samples for PC1, PC2 and PC3

5.6.2 Cluster Analysis (CA) of Soluble Salts

CA was applied to the soluble salt content of 23 ceramic samples on the basis of Euclidean distance. The same variables were used as in the case of PCA in order to classify the samples. Dendograms obtained by the clustering for the Single and Complete Linkage Methods are given the figures 5.49 and 5.50.

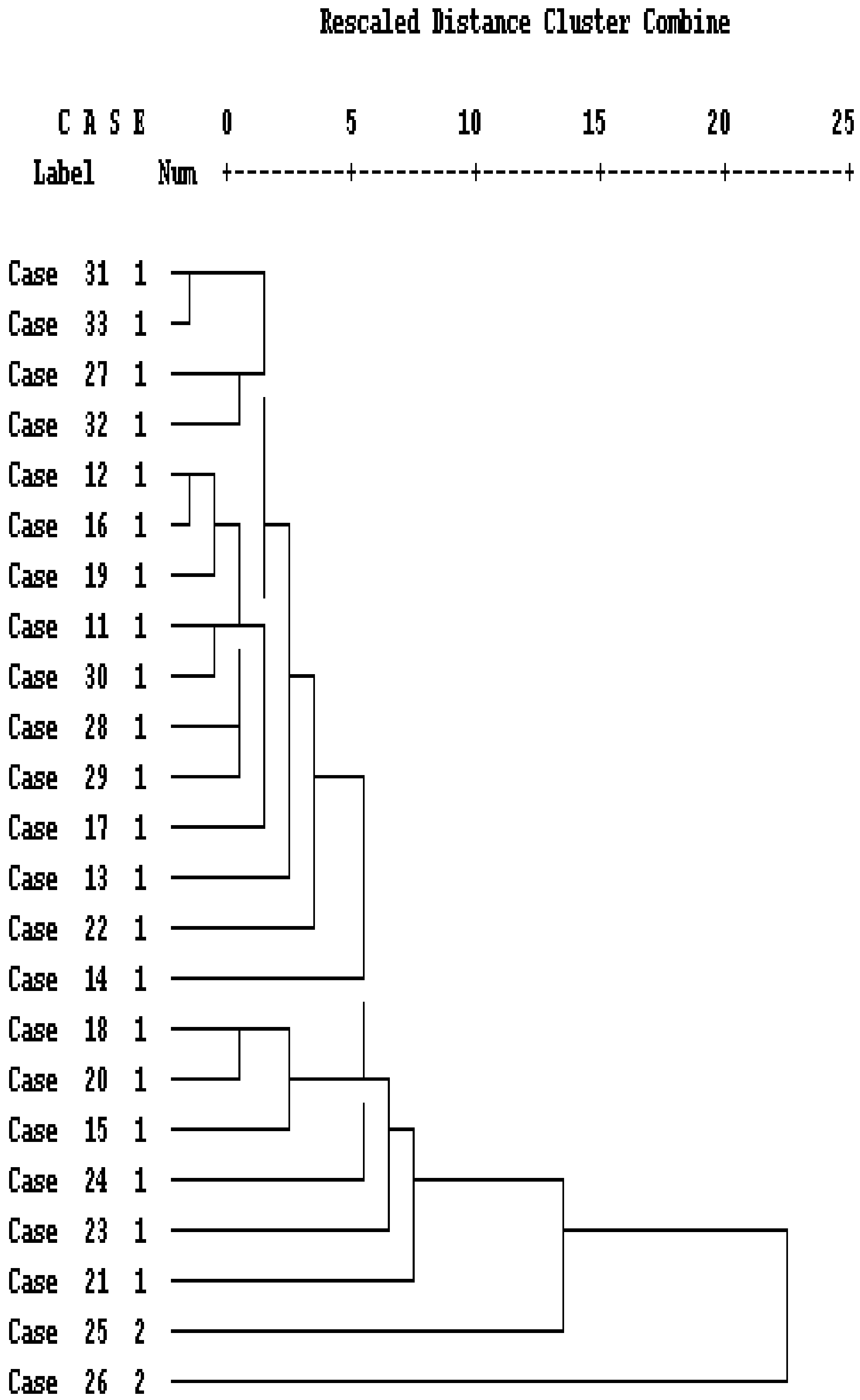

Figure 5.49: Dendogram showing the results of clustering soluble salts data of 23 samples based of Single Linkage.

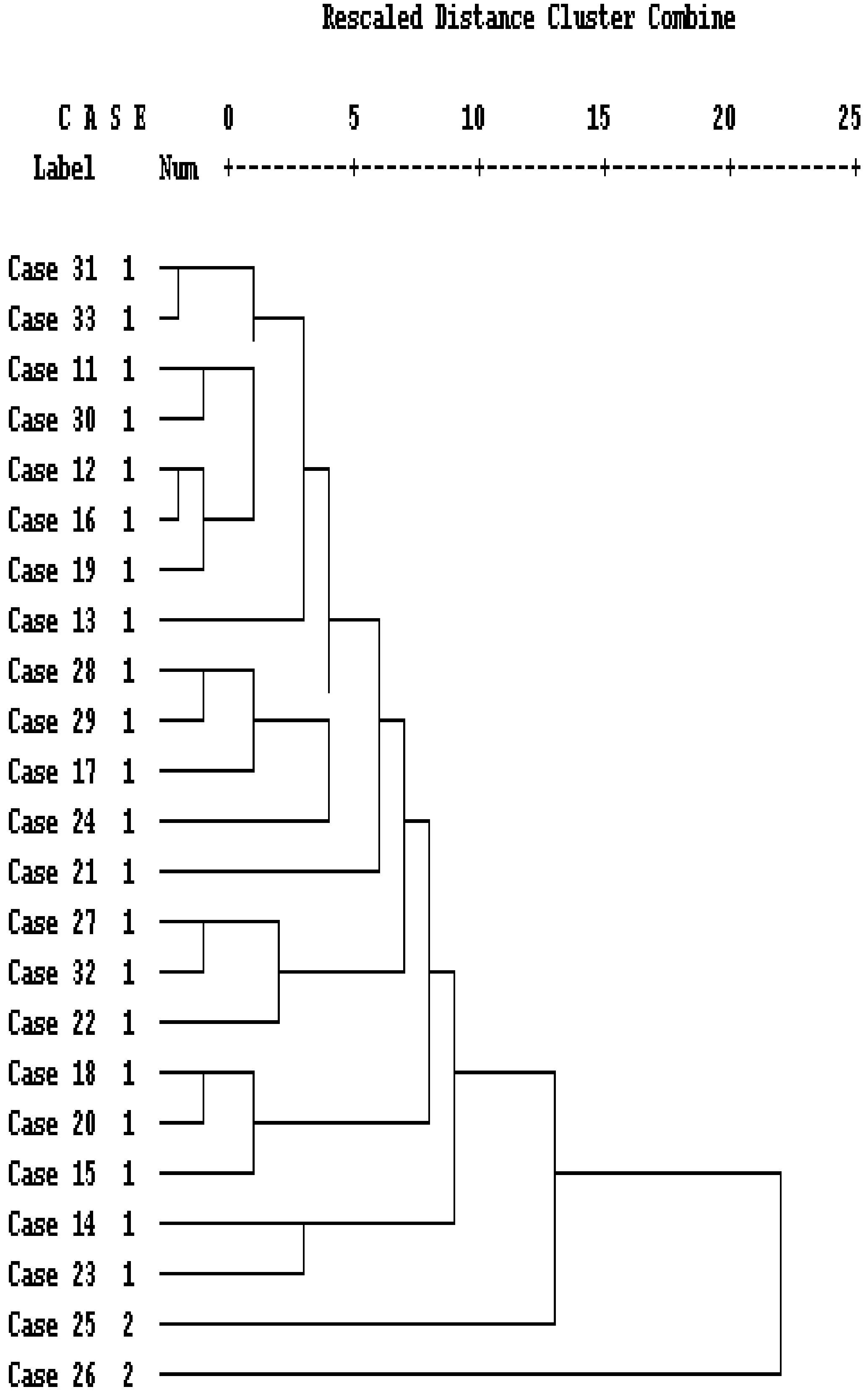

Figure 5.50: Dendogram showing the results of clustering soluble salts data of 23 samples based of Complete Linkage.

Dendogram showing the results of clustering variables for soluble salts data of 23 ceramic samples are also given in the figures 5.51 and 5.52.

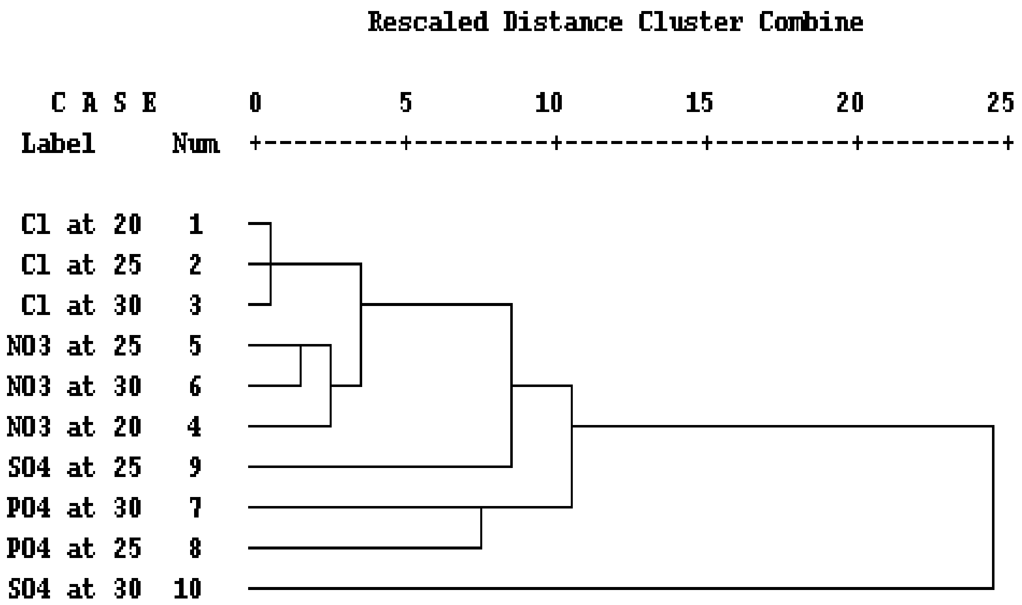

Figure 5.51: Dendogram showing the results of clustering variables for soluble salts data of 23 ceramic samples based of Single Linkage.

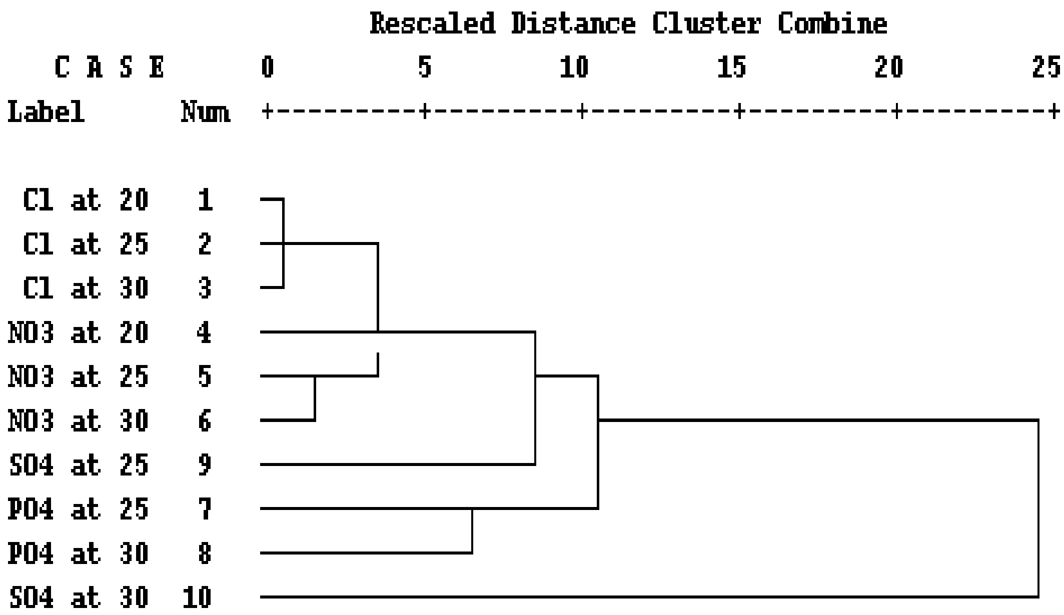

Figure 5.52: Dendogram showing the results of clustering variables for soluble salts data of 23 ceramic samples based of Complete Linkage.

6. RESULTS and DISCUSSIONS

6.1 Results of Experimental Part

6.1.1 Soluble Salts

The concentration of chloride varied with in a large range at 20^{o}C for almost all soaking time except the samples of 1, 7, and 8 (Table 4.1). This result can be seen clearly from the curves that concentration in linear function of time (Figures A.1-A.6). Unlinear relation between concentration and time, and temperature reveals the inhomogeneity in composition of some samples. The soluble amount of chloride was higher than the solubility of rest of the anions.

In general, it was considered that chloride content became constant at high temperatures of 25^{o}C, 30^{o}C, and 35^{o}C for the 10, 15, and 25 days duration.

Almost all samples contained phosphate after the temperature of 25^{o}C for all period of time except 1 and 7 (Table 4.3). The concentration of phosphate was lower than chloride but higher than nitrate and suphate. Phosphate has special property since phosphorous is among the mobile elements of earth crust. Therefore, it might also be originated by the environmental contamination as well as its occurrence within glaze paste in some samples. It has been known that bone ash was added to the glaze paste towards the end of 16th century in some atelier.

The extracted amount of nitrate was lower than chloride and phosphate. It showed constant values, generally, between the temperature of 20^{o}C and 25^{o}C for all duration of time (Table 4.4).

Sulphate was detected after the experiment carried out at 35^{o}C within 10 and 15 days duration. The soluble amount of sulphate became constant at 35^{o}C in the samples of 3, 8, and 9 (Table 4.5). The rest of the samples' concentrations were changed slightly. Sulphate is less probable to be found in glaze and body pastes.

The results of cation analysis showed that concentrations of sodium, potassium, calcium, and magnesium slightly increased at 30^{o}C and 35^{o}C for every soaking period of time.

6.1.2 Saturation Coefficient

It is know that the sample whose saturation coefficient is below 0.75 gives good assurance of durability. Nevertheless, there are old ceramic examples with excellent duraibility having values above 0.75. Saturation coefficient for sample 6 was found to be 0.9423 for 110 ^{o}C that was an average value, and it was found to be 1.2510 for 220 ^{o}C that was greater than the 0.75. This result showed that the proportions of large pores to small ones are high.

6.1.3 Weight Lost of Ceramic by Acid and Base Attack

In figure 4.4, it was obviously seen that the weight lost of sample increases when it was immersed in acid and base solutions. In other words, it was observed that the weight lost as a function of time is slightly dependent on pH of the solution. However, the increase in the weight lost was in the same ratio in water and acid solution. This conclusion can be verified by the slopes of the lines, which were nearly close to each other for water, chloride, sulphiric, and sodium hydroxide solutions.

6.2 Results of Chemometry Analysis

6.2.1 Results for Body Composition

The PCA (Principle Component Analysis) of body composition for 107 samples (Table B.2) was performed using chemical constituents, Na_2O, MgO, Al_2O_3, SiO_2, K_2O, CaO, Fe_2O_3, and PbO. These elements led to obtain three major categories (Figure 5.1). The first group of samples represented by 1, mainly comprised of Blue and White, Monochrome glazed, Golden Horn, and Damascus types of tile samples belonging to different centuries whereas the second group, 2, consisted of Sigrafitto and Miletus types. The last third group was both Sgrafitto and Monochrome glazed type of samples. In other words it overlapped with groups 1 and 2. In addition, samples from 104 to 109, signed by 4, in figure 5.1, were apart from the rest of samples. It can be concluded from the loadings plot that distinction of these samples from the others was due to the content of Fe_2O_3 (figure 5.2). The samples from 104 to

109 contain the highest amount of Fe_2O_3 compared to the other samples. In more detail, these results can be seen in detail on the scores and loadings plot of three coordinate systems, PC1-PC2-PC3 (Figures 5.3 and 5.4). The diagrams of PC1-PC2 and PC1-PC2-PC3 showed the similar results. Na_2O, MgO, and SiO_2 were the main oxides contributing the separation of samples, indicated by 1, from the others, indicated 2, 3, 4, and 5. Thus, loadings plot of PCA for body composition can be also illustrated by SiO_2 versus Fe_2O_3 and SiO_2 versus Al_2O_3 diagrams in which the samples were separated well depending on the ratio of these oxides (Figures 5.2, 5.5 and 5.6). Dendograms of Cluster Analysis confirmed all these results. The third group of samples obtained by PCA clustered together in the dendograms with the first and second groups of PCA results (Figure 5.7 and 5.8). Although sample 44, signed by 5, fell into a different subset in those dendograms, it matched with the second group of sample due to the ratios of SiO_2 -Fe_2O_3 and SiO_2-Al_2O_3 (Figures 5.5 and 5.6). (It was very close to the group 2 in dendograms also). In addition, it can be obviously seen in figures 5.9 and 5.10 that K_2O, CaO, and Fe_2O_3, grouping around the positive side of the first principal axis formed a tight subgroup. Figures 5.9 and 5.10 also shows that dendograms for clustering variables of body composition confirmed with loadings plots of PCA (figures 5.2 and 5.4).

6.2.2 Results for Slip Composition

The PCA of slip composition for 61 samples (Table B.3) was performed using chemical constituents, Na_2O, MgO, Al_2O_3, SiO_2, K_2O, CaO, Fe_2O_3, PbO, SnO, and P_2O_5. It is evident from figure 5.11 that there is a distinct separation of two groups as indicated by 1 and 2 which did not distinguish types of slips as in the case of body. The first group, 1, was separated well from the rest of the samples which of those were grouped around the positive side of first first PC axis in the scores plot (Figure 5.11). As shown in figure 5.12 (Loading Plot), the variables of MgO, Al_2O_3, K_2O and Fe_2O_3 were the main oxides for the separation of two groups. In addition, the amount of Na_2O and PbO, and for some of the samples SiO_2 were higher in the set of samples indicated by 1, which grouped around the negative side of the first PC axis (Figure 5.11). In three coordinate systems for scores and loading plots, PC1-PC2-PC3, was illustrated well the classification and showed the groups 1 and 2 in different directions (Figure 5.13). In this illustration, MgO, Al_2O_3, K_2O and Fe_2O_3 were in the same direction (Figure 5.14). The results of PCA can be verified by the plot of SiO_2 versus Fe_2O_3 and SiO_2 versus Al_2O_3 in which the samples were separated depending on the ratio of these oxides (Figures 5.15 and 5.16). These results are also seen apparently in the dendograms in which group 1 and 2 were clustered in different subgroups (Figures 5.17 and 5.18). In addition, grouping of MgO, Al_2O_3, K_2O and Fe_2O_3, and Na_2O and PbO as different subsets of the same cluster in the dendograms for clustering variables of slip composition showed confirmation of PCA (Figures 5.19 and 5.20).

6.2.3 Results for Glaze Composition

The PCA of glaze composition for 75 samples (Table B.4) was performed using chemical constituents Na_2O, MgO, Al_2O_3, SiO_2, K_2O, CaO, Fe_2O_3, PbO, SnO, and P_2O_5. Classification of ceramics depending on their glaze composition can be concluded that there is no distinctive separation between them. This clearly is shown in the scores plot of PCA (Figure 5.21). Although the variables were shown classified in the loadings plots (Figure 5.22) as if they could perform an effect on samples, they did not have an evident effect on samples to cause classification. By other words, the effects of each variable on samples were in the same level and seem similar. The three coordinate diagrams for loadings and scores plot confirmed this result by showing the uniform distribution of each samples and variables towards the sides of the cube as a sphere suggesting that they were not been greatly affected by each other (Figures 5.23 and 5.24). Distribution of the samples and common effect of each variable on samples were also seen in dendograms. As shown in figures 5.25, 5.26, 5.27, and 5.28, almost all samples (and variables) make a group under the same cluster.

6.2.4 Results for Glaze Composition from Tulun's, Amara's, and Tite's studies

These data were classified depending on the elemental oxides of glazes (Na_2O, MgO, Al_2O_3, SiO_2, K_2O, CaO, Fe_2O_3, PbO, SnO). Scores plot of PCA distinguishes groups in which Tite's samples (Table B.6) were closed to each other in the dense group revealed from Tulun's results, which was signed by 1 (Figure 5.29). Amara's samples (Table B.5) and Tulun's samples (Table B.4) were in the same group. Centuries of the ceramics in this group varied from 15th to the second half of 16th century. Loadings plot of PCA showed that a group with two members, signed by 5, differed from others with their CaO and Al_2O_3 content. The group 1 which was the largest one among the others was distinctive with its high amount of PbO and SnO (Figure 5.30). Besides MgO, K_2O, and Fe_2O_3 played roles to differentiate the same samples. These results can be seen in three-dimensional diagrams for scores and loadings plot of PCA (Figure 5.31 and 5.32). CA analysis confirmed the PCA results. Dendograms of samples showed that although both Amara's and Tite's samples were clustered together with Tulun's samples, their samples did not show any significant similarities in common with each other (Figure 5.33 and 5.34). In addition, MgO, Al_2O_3, K_2O, CaO, Fe_2O_3, PbO, and SnO as clustering variables performed a group in the dendograms (Figure 5.35 and 5.36).

6.2.5 Results for Porosity Data

The data of 40 samples (Table B.7) were classified depending on the porosity characteristics (bulk density, apparent density, pore diameter, total pore volume). Scores plot of PCA showed two groups mainly (Figure 5.37). Sample 3 and 66, signed by 3, were separated from the rest of the sample giving a different group. These samples have red pastes from the 13th and 14th century. Loadings plot of PCA indicated that these two samples separated from others as to their bulk density properties (Figure 5.38). The second group in the scores plot showed a dense part, which contains most of the samples. Ceramic in these groups are from the 12th, 15th, and 16th century. Apparent density and total pore volume were the reasons of their being a separate group than the rest of samples. Samples 4, indicated by 4 in the figures 5.37 and 5.39, stayed farther from the dense part. Apparent densities gives distinct position to sample 4 and left them out of the dense group. The same results can be easily interpreted from the three coordinate system diagrams of PC1-PC2-PC3 (Figures 5.39 and 5.40). Dendograms were also concluded the same result. In figure.5.41 and 5.42, the dense group indicated by 1 was clustered together. Dendograms showed the results that variables for porosity data confirmed the result of loadings plots (Figures 5.43 and 5.44).

6.2.6 Results for Soluble Salts

PCA of 23 ceramics depending on the contents of soluble salts (Table 4.7) showed that the distinctive appearances of sample 25 and 26, signed by 2, arisen due to the high amount of chloride and nitrate ions in all the given temperatures (Figures 5.45 and 5.46). Sample 25 contained less amount nitrate compare to the sample 26;

therefore, it took part near the group, which do not contain nitrate ions. These results can be easily seen from the three-dimensional PCA scores and loadings (Figures 5.47 and 5.48). Dendograms of CA also confirmed these results (Figures 5.49 and 5.50). In addition, these two ions (chloride and nitrate) had place in the same cluster of the dendograms depending on the variables (Figures 5.51 and 5.52).

7. CONCLUSION

Archaeo-Ceramics (wares and tiles) from different centuries and provenance were classified depending on the compositional groups of body and glaze parts, porosity data, and soluble salts content using Principal Component (PCA) and Cluster (CA) Analyses. The data of PCA and CA showed that the eight oxides, Na_2O, MgO, Al_2O_3, SiO_2, K_2O, CaO, Fe_2O_3 and PbO were responsible for the classification in body pastes. These elements led to obtain three major groups. The chemical composition of the both group indicated a difference in the production technology. The oxides of MgO, Al_2O_3, Fe_2O_3, SiO_2 and Na_2O were the main oxides contributing the separation, and were strongly correlated with first PC-Axis.

The PCA of glaze composition was performed using chemical oxides of Na_2O, MgO, Al_2O_3, SiO_2, K_2O, CaO, Fe_2O_3, PbO, SnO, and P_2O_5. The Loading plot showed that the largest proportion of the variance in the data was Al_2O_3, CaO, Fe_2O_3 and P_2O_5, which caused the distinct separation of two groups. Na_2O and K_2O were poor at separation in the glaze.

This result revealed that alkaline oxides were not used as flux in the glaze composition. It is also possible that the difference in the production technology in respect of elemental composition might arise depending on the particular production technology of different workshops.

Although the century and types of the samples were different, various samples was possible to be clustered in the same group. This result implied that quite similar raw materials might have been used in tiles and wares production.

Porosity characteristics, bulk density, apparent density, pore diameter, total pore volume were the main variables responsible for the grouping. Result of PCA showed two groups mainly which were separated from others in respect to their bulk density properties. In this classification it is certain that different firing temperatures played roles during the production process.

PCA of 23 ceramics depending on the contents of soluble salts resulted in two groups. High amount of chloride and nitrate ions in all the given temperatures were responsible for the classification. This result indicated that the main soluble ions penetrated through the samples were chloride and nitrate ions rather than phosphate and sulphate. By other words, particularly these ions (chloride and nitrate), coming from the seawater, rain, or rivers, accumulated within the pores of the samples during burials over years.

In addition the classification results with respect to the porosity and soluble salt data revealed that the same deterioration mechanism underwent in two separated groups.

Hierarchical agglomeration clustering applied on the standardized data by means of Single and Complete Linkage Methods on the basis of Euclidian Distance yielded almost the similar results with PCA, except some differences in the classification of subgroups. Three-dimensional visualizations of PCA and dendograms of CA were also confirmed all the results concluded

REFERENCES

Altun et al., 1997**.** Excavations Throw Light on Ceramics, The Story of Ottoman Tiles and Ceramics. Creative Publisher Istanbul.

Amara B. A., 2003. Le 'Rouge d' Iznik Données Technologiques Sur Une Production Tardire Du XVII^{e} Ciécle, Dissettation Thesis, Bordeaux, France.

Anderson, T. W., 1984. An Introduction to Multivariate Statistical Analysis, Wiley Series in Probability and Mathematical Statistics, Wiley.

Attanasio et al., 2001. The Possibility of Provenancing A Series of Bronze Punic Coins Found At Tharros (Western Sardinia) Using The Literature Lead Isotope Database, *Archaeometry*, **43**, 529-547.

Baxter, M. J., 1995. Standardization and Transformation in Principal Component Analysis, with Applications to Archeometry, *Applied Statistics,* **44**, 513-527.

Baxter, M. J., 2001. Statistical Modelling Artefact Compositional Data, *Archaeometry*, **43**, 131-147

Brereton, R.G., 1992. Multivariate Pattern Recognition in Chemometrics, Elsevier, Amsterdam.

Brereton, R.G., 2003. Chemometrics. Data Analysis for Laboratory and Chemical Plant. Wiley.

Butterworth, B., 1964. Frost Resistance of Bricks and Tiles: a review, *J. Br. Ceram. Soc*,.**1(2)**, 203-223.

Cini, N. and Tulun, T., 2002. Chemometric Analysis of SEM-EDAX Data for Archaeo-Ceramics, *3rd Aegean Analytical Chemistry Days*, Lesvos, Greece, September 29th and October 3rd.

Duda R. O. et al., 2001. Pattern Clasification, John Wiley and Sons Pub., USA.

Graham, R. G., 1993. Richard C. Graham, Data Analysis For The Chemical Sciences, John Wiley and Sons 1993.

Hall, M. E., 2001. Pottery Styles During The Early Jomon Period: Geochemical Perspectives on The Moroiso and Ukishima Pottery Styles, *Archaeometry*, **43**, 59-75.

Hecht, G., 1990 Mathematic in Chemistry. Printice Hall, New Jersey.

Heimann et al., 2001. Mineralogical and Chemical Investigation of Bloomery Slags From Prehistoric (8th Century BC to 4th Century AD) Iron Production Sites in Upper and Lower Lusatia, Germany, *Archaeometry*, **43**, 227-252.

Larsen, P. H. et al., 1999. The Influence of SiO_2 Addition to $2MgO-Al_2O_3-3.3P_2O_5$ Glass. *Journal of Non-Crystalline Solids*, **244**, 16-24.

Maesschalck, R. De et al., 2000. Tutorial, The Mahaonobis Distance, *Chemometrics and Intelligent Laboratory systems*, **20**, 1-18.

Mirti, P., et al., 1990. Roman Pottery From Audusta Praetoria (Aosta, Italy): A Provenance Study, *Archaeometry*, **32**, 2, 163-175.

Mirti, P. et al., 1994. On The Role of Major and Trace Elements in Provenancing Ceramic Material. A Case Study: Roman Terra Sigillata From Augusta Praetoria, *Fresenius J. Anal. Chem.*, **348**, 396-401.

Mirti, P., and David, P., 2001. Technological Characterization of Campanian Pottery of Type A, B, and C and of Regional Products From Ancient Calabria (South Italy), *Archaeometry*, **43**, 19-23.

Morgan E., 1997. Ed Morgan , Chemometrics: Experimental Design, John Wiley and Sons, London, Newyork

Odigure, J. O., 2002. Deterioration of Long –Serving Cement-Based Sandcrete Structures in Nigeria, Cement and Concrete Research, **32**, 1451-1455.

Papageorgiou, I., et al., 2001. Model Based Cluster Analysis of Artefact Compositional Data, *Archaeometry*, **43**, 571-588.

Rhodes, D., 1966. Clay and Glazes for the Potter, Chilton Book Co., Philadelphia and Newyork.

Rivera, J. and Karbhari, V.M., 2002. Cold-Temperature Simultaneous Aqueous Environment Related Degradation of Carbon/Vinylester Composites, *Composites part B.*, **33**,17-24.

Robinson, G. C., et al., 1977. Relation Between Physical Properties and Durability of Commercially Marketted Brick, *Am. Ceram. Soc. Bull.*, **56 (12)**, 1071-1076.

Storch, P., 1986. Curatorial Care and Handling of Ceramic Objects. Conservation Notes 15, Austin, Texas: Texas Memorial Museum.

Tite, M. S., 1989. Iznik Pottery : An Investigation of the Methods of Producion., *Archaeometry,* **31(2)**, 115-132.

Tulun et al., 2001. An Archaeometric Study On Ancient Iznik Ceramics, *1st Black Sea Basin Conference on Analytical Chemistry* Odessa, Ukraine, September, 11-15.

Tulun et al., 2002. A Multidisciplinary Study of Ancient Iznik Ceramics, Archaeolingua, Cental European Series 1, BAR International Series 1043 (II).

Yap, C. T., and Hua, Y., 1994. A study of Chinese Porcelain Raw Materials for Ding, Xing, Gongxing and Dehua Wares, *Archaeometry,* **36, 1**, 63-76.

APPENDIX A

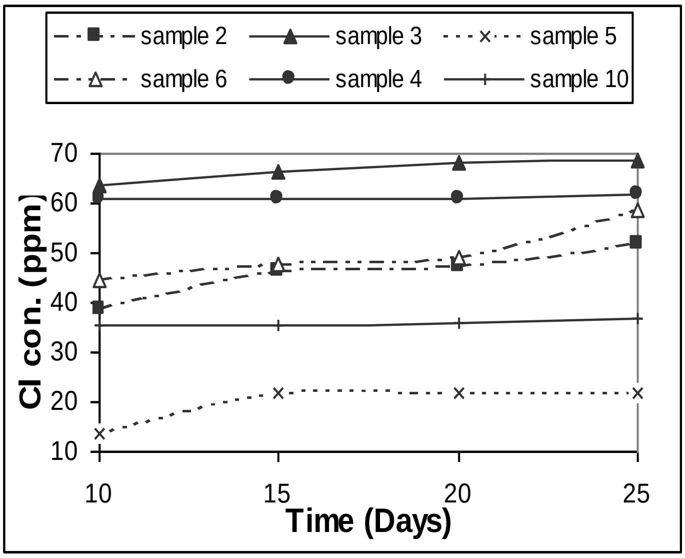

sample 2 y = 0,7922x + 32,164
R2 = 0,907

sample 3 y = 0,3252x + 60,924
R2 = 0,9279

sample 5 y = 0,483x + 11,21
R2 = 0,595

sample 6 y = 0,865x + 34,8
R2 = 0,8521

sample 8 y = 0,0648x + 59,896
R2 = 0,6

sample 10 y = 0,0756x + 34,662
R2 = 0,8909

Figure A.1: Cl^- % =f (time) for 20ºC concerning to samples 2, 3, 5, 6, 8, and 10

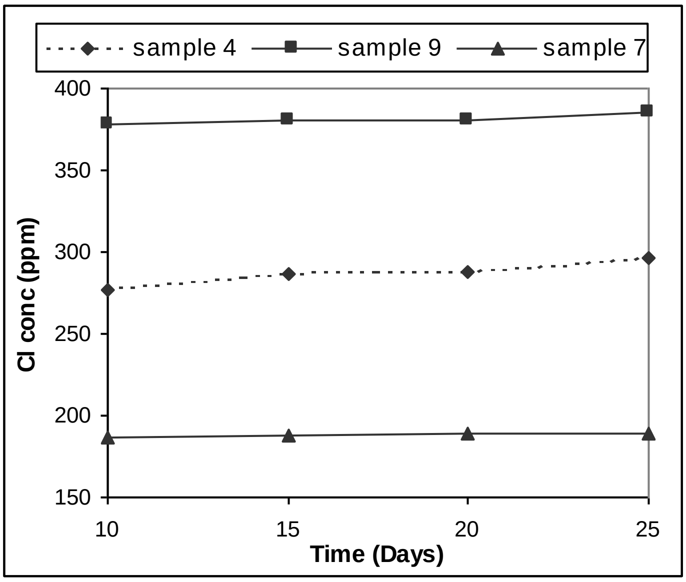

sample 4 y = 1,1714x + 266,48
R2 = 0,9114

sample 7 y = 0,1378x + 185,78
R2 = 0,7561

sample 9 y = 0,4392x + 373,85
R2 = 0,8555

Figure A.2: Cl^- % =f (time) for 20ºC concerning to samples 4, 7, and 9

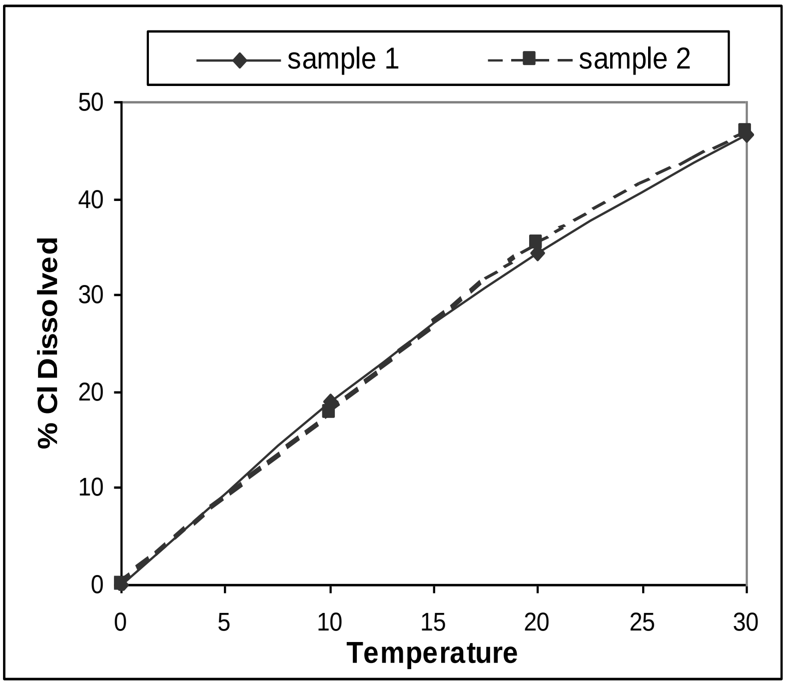

Sample 1 y = 1,5531x + 1,704

R2 = 0,9906

Sample 2 y = 1,5818x + 1,2723

R2 = 0,9908

Figure A.3:Cl^- % = f (t ^oC) for 20 days soaking period concerning to samples 1 and 2

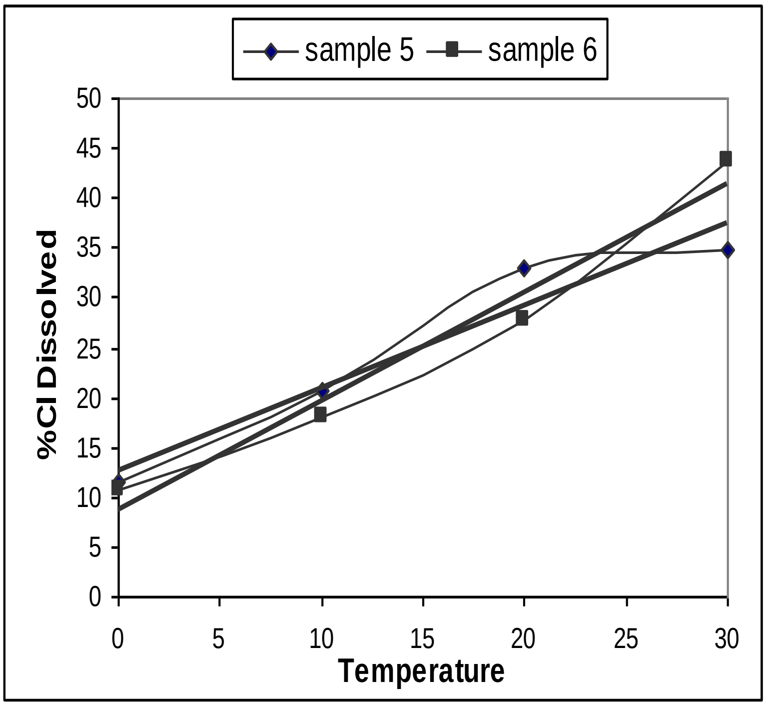

Sample 5 y = 0,8218x + 12,673

R2 = 0,9326

Sample 6 y = 1,0835x + 8,7478

R2 = 0,9676

Figure A.4:Cl^- % = f (t ^oC) for 20 days soaking period concerning to samples 5 and 6

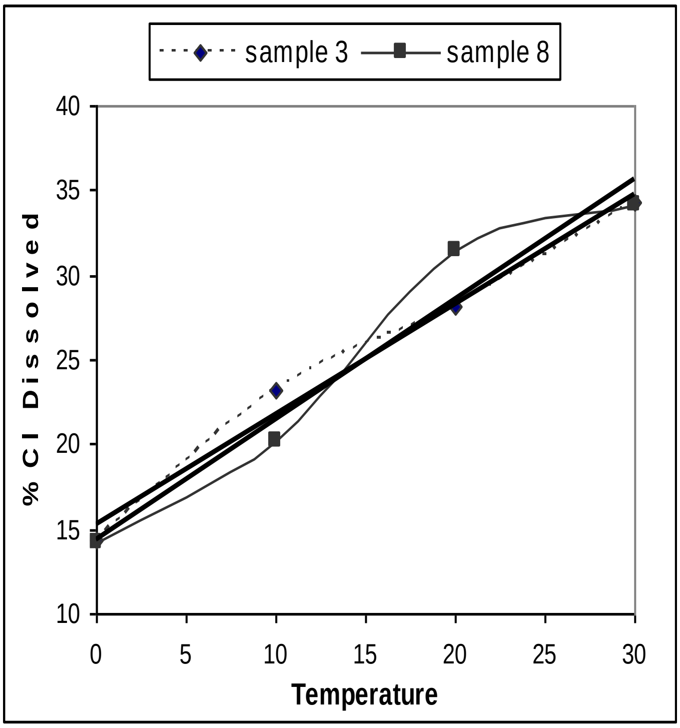

Sample 3 $y = 0{,}648x + 15{,}28$

$R2 = 0{,}9843$

Sample 8 $y = 0{,}7104x + 14{,}344$

$R2 = 0{,}9546$

Figure A.5:Cl^- % = f (t °C) for 20 days soaking period concerning to samples 3 and 8

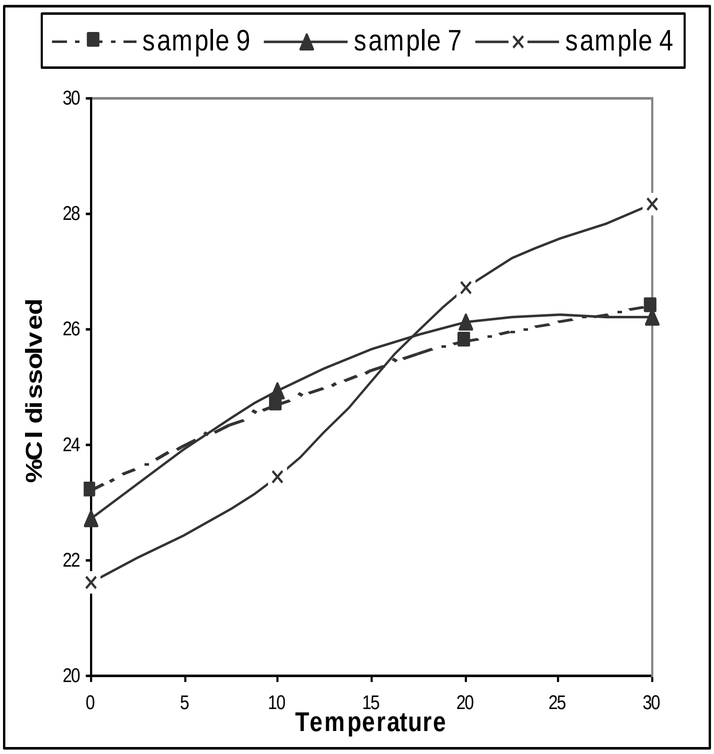

Sample 4 $y = 0{,}2293x + 21{,}56$
$R2 = 0{,}9785$

Sample 7 $y = 0{,}1156x + 23{,}265$
$R2 = 0{,}8558$

Sample 9 $y = 0{,}1071x + 23{,}394$
$R2 = 0{,}9642$

Figure A.6: Cl^- % = f (t °C) for 20 days soaking period concerning to samples 4, 7, and 9

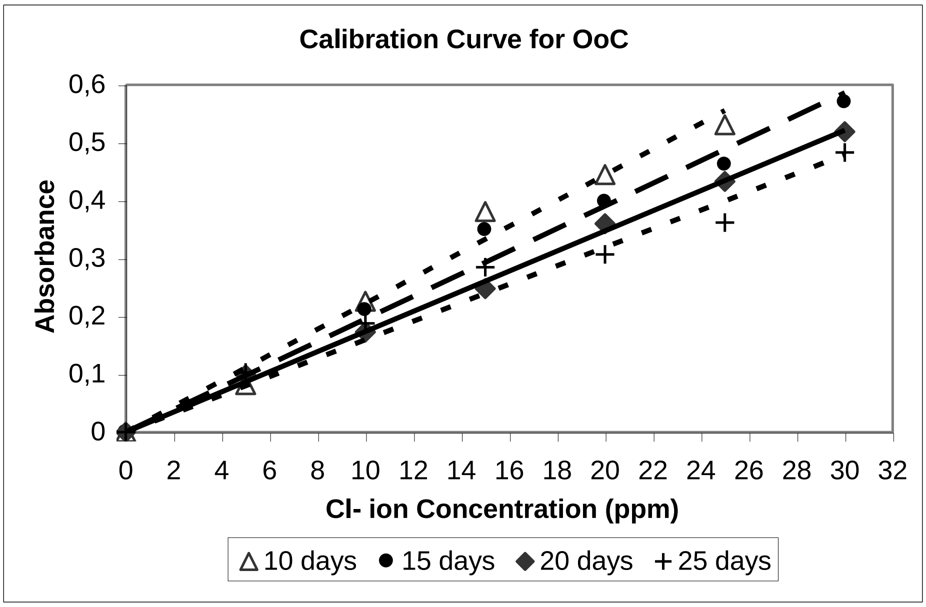

Δ...$y = 0.0222x$ $R^2 = 0.9831$ •- - -$y = 0.0195x$ $R^2 = 0.9784$ ♦ —— $y = 0.0174x$ $R^2 = 0.9977$ +- - - $y = 0.016x$ $R^2 = 0.9688$

Figure A.7: Calibration curve of Cl^- analysis for 0ºC

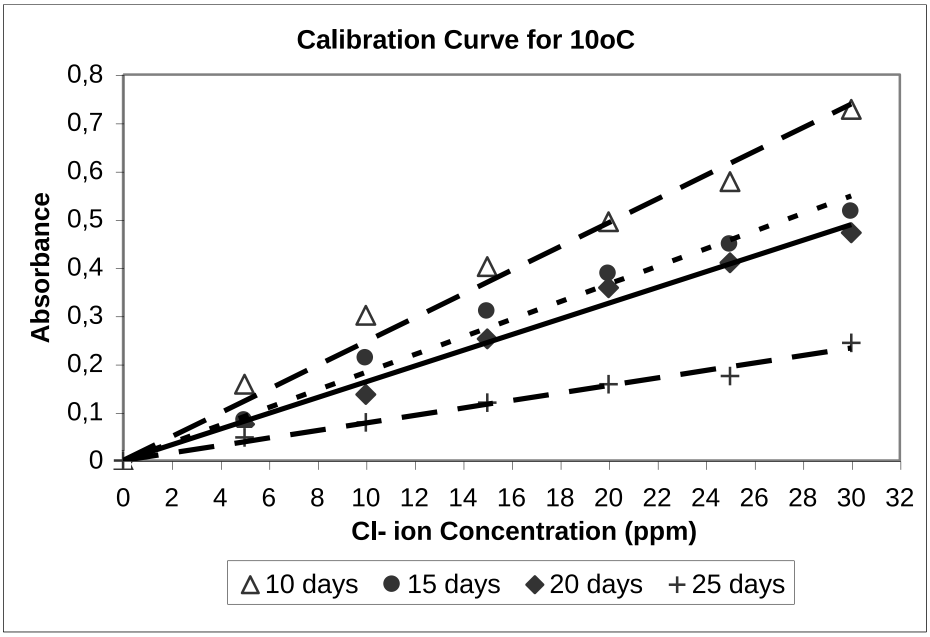

Δ...$y = 0.0246x$ $R^2 = 0.9818$ •- - -$y = 0.0183x$ $R^2 = 0.9829$ ♦ —— $y = 0.0163x$ $R^2 = 0.9891$ +- - - $y = 0.078x$ $R^2 = 0.9856$

Figure A.8: Calibration curve of Cl^- analysis for 10ºC

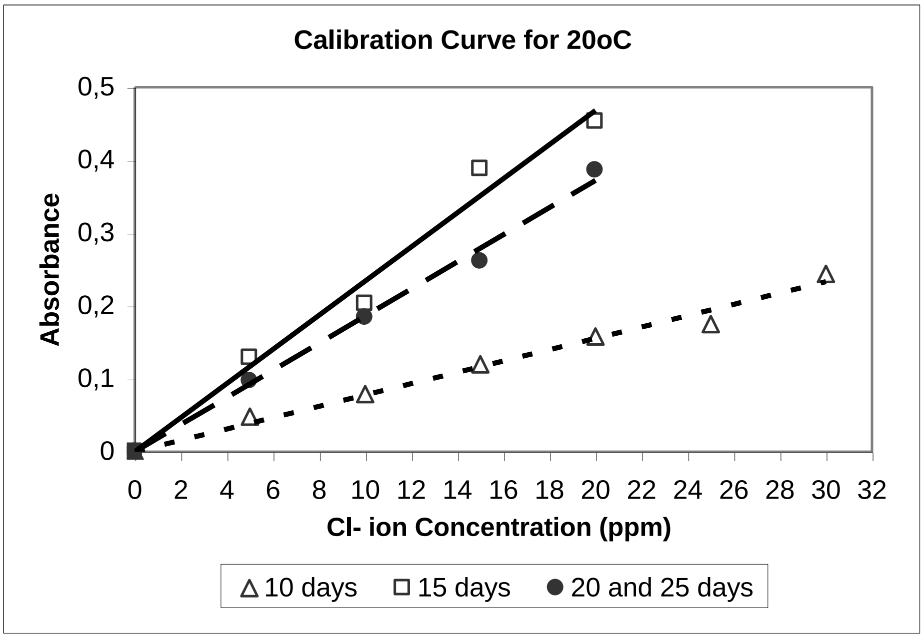

Δ- - - $y = 0.0078x$ $R^2 = 0.9856$ ● - - - $y = 0.0186x$ $R^2 = 0.9939$ □ ▬▬ $y = 0.0234x$ $R^2 = 0.9805$

Figure A.9: Calibration curve of Cl^- analysis for 20ºC

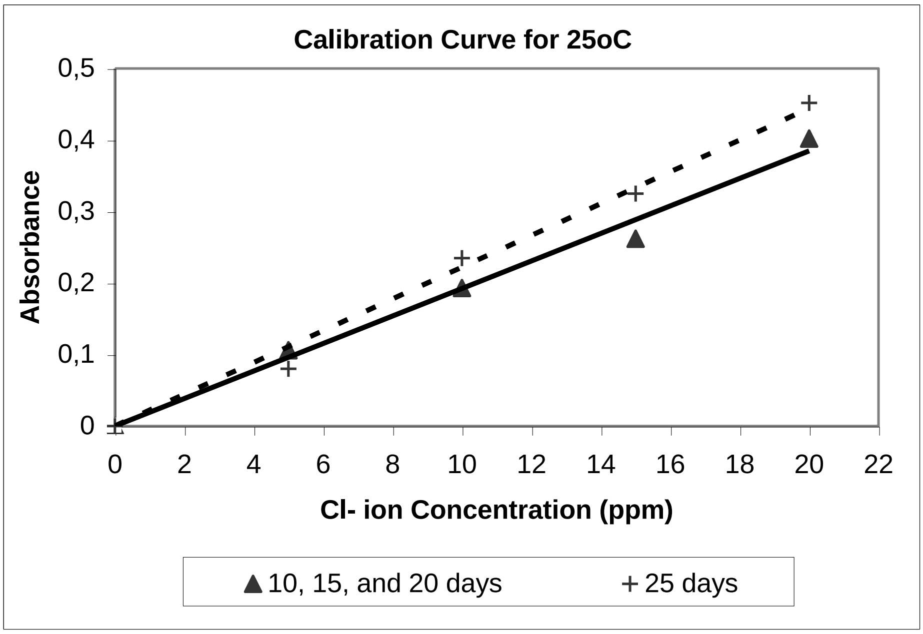

▲ ▬▬ $y = 0,0192x$ $R^2 = 0,9882$ +- - - $y = 0,0222x$ $R^2 = 0,9905$

Figure A.10: Calibration curve of Cl^- analysis for 25ºC

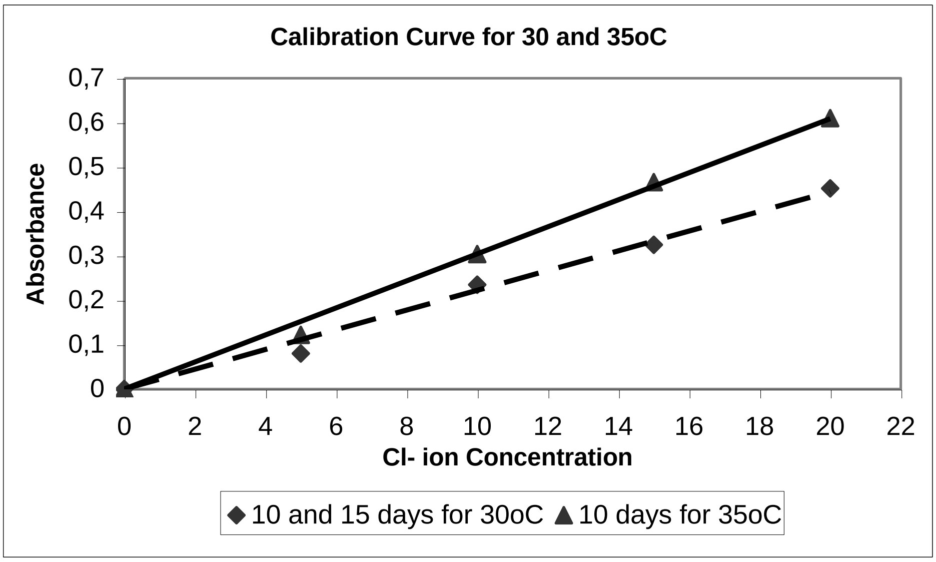

♦- - - $y = 0,0222x$ $R^2 = 0,9905$

▲ —— $y = 0,0305x$ $R^2 = 0,9959$

Figure A.11: Calibration curve of Cl^- analysis for 30ºC and 35ºC

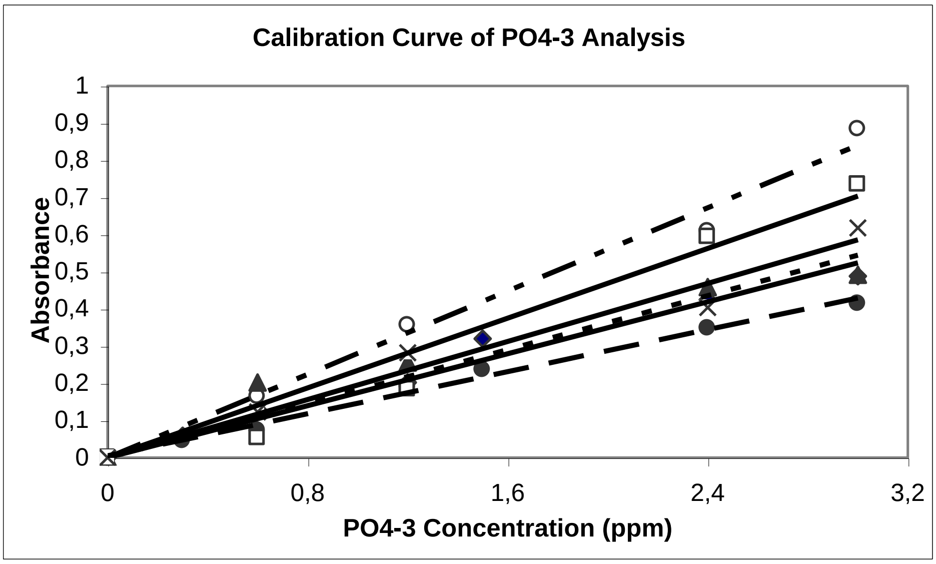

♦—— $y = 0,1747x$ $R^2 = 0,9736$	●– – – $y = 0,1437x$ $R^2 = 0,9918$	○— - - — $y = 0,2801x$ X $R^2 = 0,9872$
x—— $y = 0,1954x$ $R^2 = 0,9676$	□—— $y = 0,2345x$ $R^2 = 0,9564$	▲- - - - $y = 0,1815x$ $R^2 = 0,9171$

Figure A.12: Calibration curve of PO_4^{3-} analysis. ♦——: 10, 15, 20 days for 10ºC; ●– – –: 25 days for 10ºC, 10 and 15 days for 20ºC;○— - - — -: 20 and 25 days for 20ºC, 10, 15, 20, and 25 days for 25ºC; x——: 10 and 15 days for 30ºC □——: 20 and 25 days for 30ºC, 10 and 15 days for 35ºC; ▲- - - -: 20 and 25 days for 35ºC

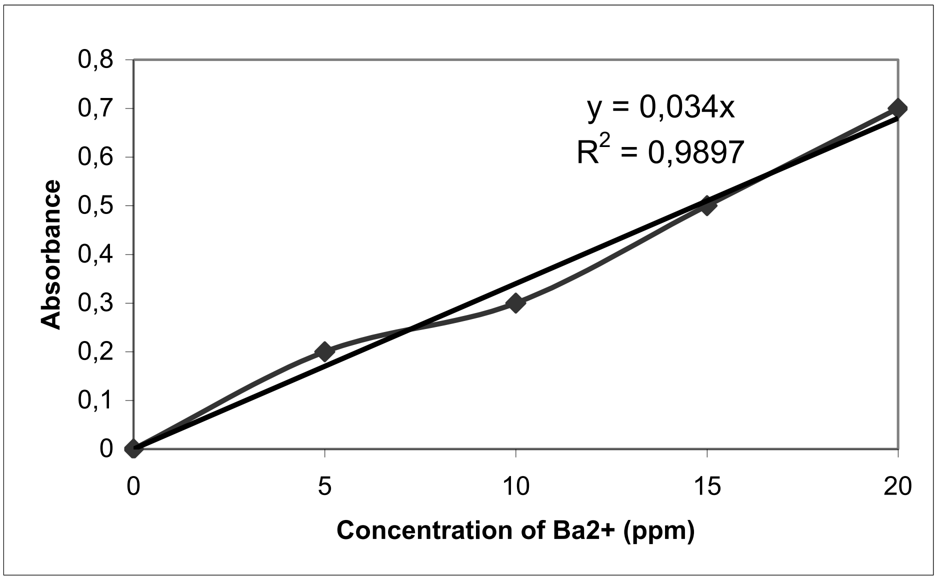

Figure A.13: Calibration curves of SO_4^{2-} analysis by flame spectroscopy

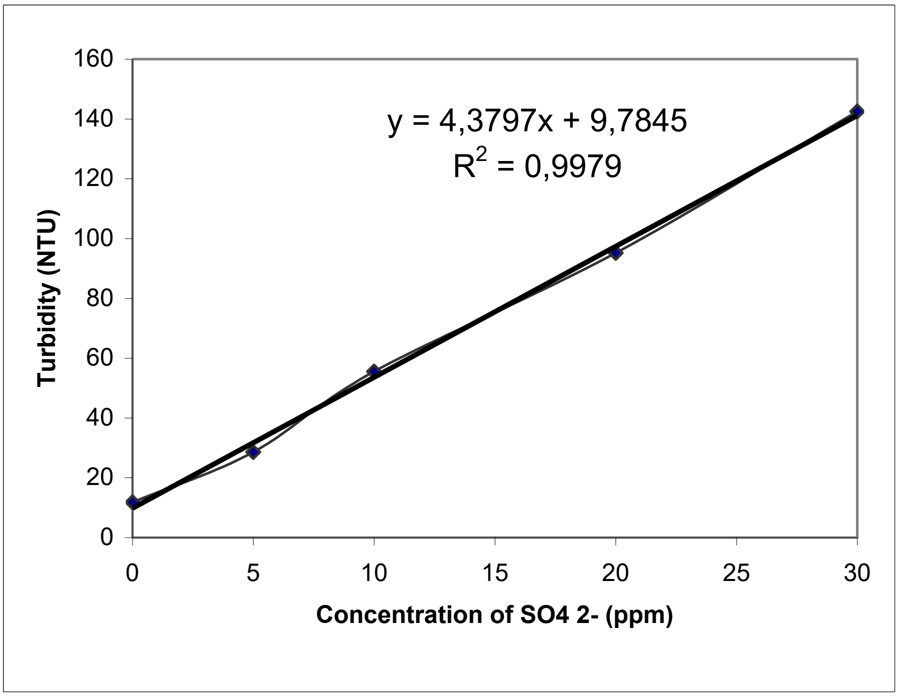

Figure A.14: Calibration curves of SO_4^{2-} analysis by Turbidimetry

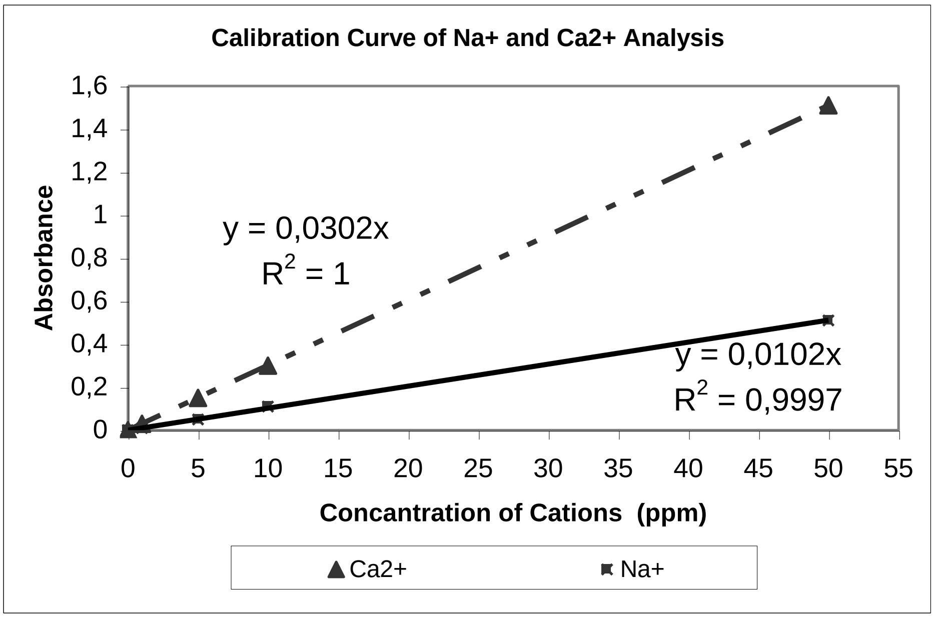

Figure A.15: Calibration curves of Na^{+} and Ca^{2+} analysis for 10 and 15 days immersion at 30°C.

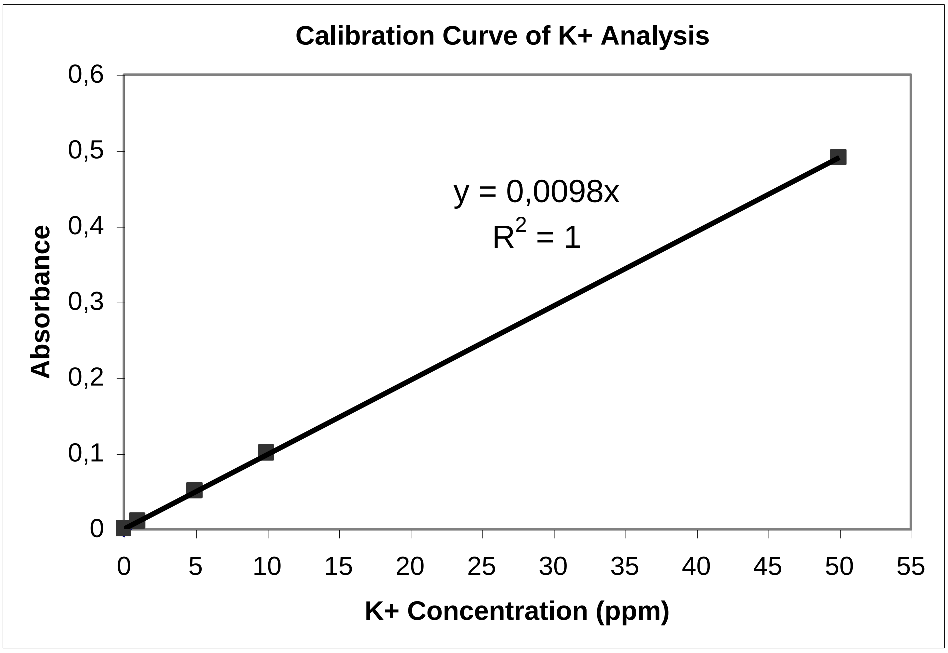

Figure A.16: Calibration curves of K^{+} analysis for 10 and 15 days immersion at 30°C

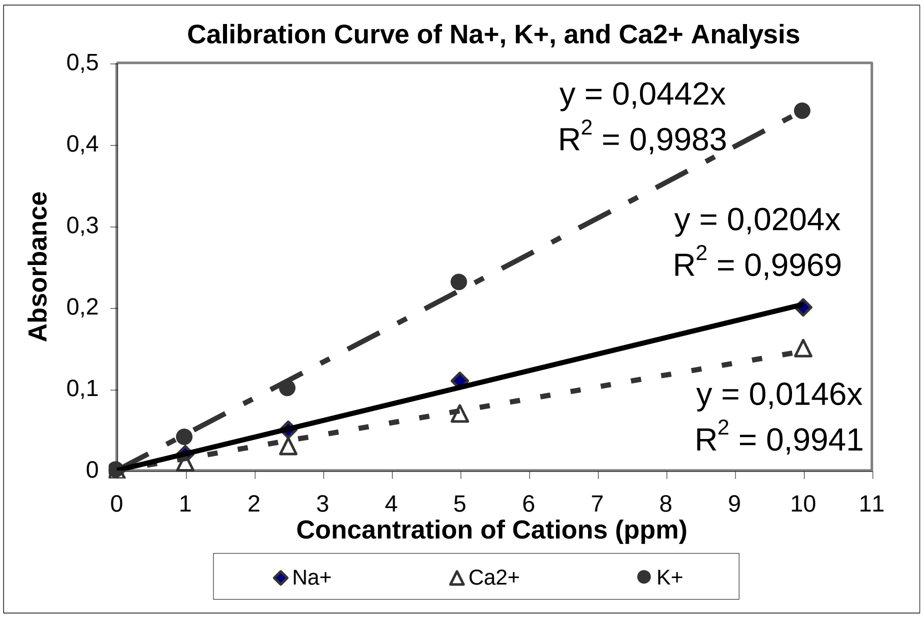

Figure A.17: Calibration curves of Na^+, K^+, and Ca^{2+} analysis in both 20 and 25 days immersion at 30°C, and 10 and 15 days immersion at 35°C.

APPENDIX B

Table B.1. Descriptions of Ceramics

Sample No	Century	Description
1	XV-XVI	ware-piece, monochrome glaze
2	-	red paste, ware-bottom piece, monochrome glaze
3	-	fired red paste, brick piece with glaze
4	-	red paste, ware-side piece with slip and without glaze
5	XV	red paste, ware-body piece, Miletus with glaze
6	XII, Seljuk	red paste, ware-body piece, print technique,
7	-	red paste, ware-body piece, without slip and glaze
8	XIII-XIV	red paste, ware-body piece, Sgrafitto with glaze
9	XV	red paste, ware-piece, Miletus with glaze,
10	-	fired red paste, brick piece with glaze
11	-	red paste, ware-piece, green glazed
12	XIII-XIV	red paste, ware-piece, Sgrafitto with glaze
13	XIV	red paste, ware-piece, slip with glaze
14	XV	red paste, ware-piece, Miletus with glaze
15	XVI, 1.Half	red paste, ware-piece, Damascus with glaze
16	XVI, 2.Half	white paste, ware-piece, Rhodes
17	XVI, 2.Half	white paste, ware-bottom piece, Rhodes
18	XVI, 2.Half	white paste, tile, Rhodes,
19	XVI, 2.Half	white paste, tile, Rhodes,
20	XII, Seljuk	red paste, ware-body piece, print technique
21	XII, Seljuk	red paste, ware-side piece, print technique
22	XIII-XIV	red paste, ware-side piece, Sgrafitto with glaze
23	XIV	red paste, ware-piece, slip without glaze
24	XIV	red paste, ware-piece, slip with glaze
25	XV	red paste ware-piece, Miletus without glaze,
26	XV	red paste, ware-body piece, Miletus with glaze
27	XV-XVI	white paste, ware- bottom piece, without slip and glaze

Table B.1. Descriptions of Ceramics (Continued)

28	XV-XVI	white paste, ware- body piece, monochrome glaze
29	XV-XVI	white paste, ware- body piece, monochrome glaze
30	XV-XVI	white paste, ware- bottom piece, monochrome glaze
31	XV-XVI	white paste, ware- side piece, Blue and White
32	XVI, 1.Half	white paste, ware- body piece, Golden Horn
33	XVI, 2.Half	white paste, ware-piece, Rhodes
34	-	fired red paste, kiln piece
35	-	fired red paste, kiln piece
36	-	red paste, ware-body piece, without slip and glaze
37	-	red paste, ware-body piece, slip without glaze
38	-	red paste, ware-body piece, slip without glaze
39	-	red paste, ware-piece, monochrome glaze
40	-	red paste, ware-side piece, monochrome glaze
41	-	red paste, ware-handle piece, monochrome glaze
42	XIII-XIV	red paste, ware-side piece, Sgrafitto without glaze
43	XIII-XIV	red paste, ware-side piece, Sgrafitto without glaze
44	XIII-XIV	red paste, ware-piece, Sgrafitto with glaze
45	XV	red paste, ware- body piece, slip with glaze
46	XV	red paste, ware- body piece, Miletus without glaze
47	XV	red paste, ware- body piece, Miletus with glaze
48	XV-XVI	white paste, ware-body piece, without slip and glaze
49	XV-XVI	white paste, ware- body piece, monochrome glaze
50	XV-XVI	white paste, ware- body piece, Blue and White
51	XV-XVI	white paste, ware- body piece, Blue and White
52	Beginning of XVI	white paste, ware- body piece, Blue and White
53	XVI, 1.Half	white paste, ware- body piece, Golden Horn
54	XVI, 1.Quarter	white paste, ware-piece, Damascus with glaze
55	XVI, 2.Half	white paste, ware- bottom piece, Rhodes
56	XVI, 2.Half	white paste, ware- body piece Rhodes
57	XVI, 2.Half	white paste, ware- side piece, Rhodes
58	XVI, 2.Half	white paste, ware- side piece, Rhodes
59	-	red paste, fired red paste, kiln piece
60	-	red paste, fired red paste, kiln piece
61	-	red paste, fired red paste, kiln piece

Table B.1. Descriptions of Ceramics (Continued)

62	-	red paste, fired red paste, kiln piece
63	-	red paste, ware- body piece, without slip and glaze
64	-	red paste, ware- body piece, slip without glaze
65	XIII-XIV	red paste, ware- side piece, Sgrafitto without glaze
66	XIII-XIV	red paste, ware- bottom piece, Sgrafitto with glaze
67	XV	red paste, ware- body piece, Miletus without glaze
68	XV	red paste, ware-bottom piece, Miletus with glaze
69	XV-XVI	white paste, ware- side piece, monochrome glaze
70	XV-XVI	white paste, ware- side piece, Blue and White
71	Beginning of XVI	white paste, ware- bottom piece, Blue and White
72	XVI, 1.Half	white paste, ware- bottom piece, Golden Horn
73	XVI, 2.Half	white paste, ware- body piece, Rhodes
74	XVI, 2.Half	white paste, ware- body piece, Rhodes
75	XVI, 2.Half	white paste, ware- bottom piece, Rhodes
76	XVI, 2.Half	white paste, tile piece, Rhodes
77	XVI, 2.Half	white paste, tile piece, Rhodes
78	-	red body, Kiln waster
79	XVI, 2.Half	white paste, tile piece, Rhodes
80	XVI, 2.Half	white paste, tile piece, Rhodes
81	XVI, 2.Half	white paste, tile piece, Rhodes
82	XVI, 2. Half	white paste, tile piece, Blue and White
83	-	red body, Kiln waster
84	-	white slip, ware-body piece, t-glaze without paint
85	-	red body, ware-body piece, sherd green glaze without slip and paint
86	XIII-XIV	red body, ware-side piece, white slip, sgrafitto without glaze
87	XIII-XIV	red body, ware-body piece, sgrafitto with thin slip, t-glaze flow technique
88	XIV	red body, ware-body piece, without glaze white paint
89	XIV	red body, ware-body piece, white slip, t-glaze
90	XV	red body, white slip, Miletus without glaze
91	XV	red body, ware-bottom piece, Miletus with white slip, t-glaze

Table B.1. Descriptions of Ceramics (Continued)

92	XV-XVI	white body, ware-side piece, monochrome glazed without slip
93	XV-XVI	white body, ware-side piece, white slip, t-glaze, Blue and White
94	XVI, 1. Half	white body, ware-bottom piece, white slip, t-glaze, Golden Horn
95	XVI, 2. Half	white body, ware-body piece, white slip, t-glaze, Damascus
96	XVI, 2. Half	white body, ware-body piece, white slip, t-glaze, Rhodes
97	XVI, 2. Half	white body, ware-body piece, white slip, t-glaze, Rhodes
98	XVI, 1. Half	white body, tile piece, white slip, t-glaze, Blue and White
99	XVI, 2. Half	white body, tile piece, white slip, t-glaze, Rhodes
100	-	white body, tile piece, Rhodes
101	XVI, 2. Half	white body, tile piece, white slip, t-glaze, Rhodes
102	XVI, 2. Half	white body, tile piece, white slip, t-glaze, Rhodes
103	XVI, 2. Half	white body, tile piece, white slip, t-glaze, Rhodes
104	-	white body, tile piece, Rhodes
105	-	red body without glaze

Table B.2. Body Composition (for 107 samples)

Sample No	Na_2O	MgO	Al_2O_3	SiO_2	K_2O	CaO	Fe_2O_3	PbO
1	3.11	1.75	4.89	74.70	1.22	4.75	3.25	nd
3	0.38	0.13	4.16	93.28	0.51	0.50	0.58	nd
5	1.39	2.53	10.73	36.00	1.89	38.99	3.67	nd
6	0.37	0.68	1.45	96.55	0.00	0.28	0.19	nd
7	0.95	2.48	8.60	29.58	1.79	50.86	3.16	nd
8	1.93	3.70	12.89	41.88	2.80	26.47	6.11	nd
9	1.03	1.59	14.44	71.78	2.41	2.05	5.48	nd
11	1.13	2.37	18.26	56.19	2.77	7.55	9.99	nd
12	0.87	1.82	14.62	49.84	3.50	10.31	16.37	nd
13	1.23	2.94	16.93	54.90	3.05	8.55	10.97	nd
14	1.24	3.86	18.13	52.20	2.87	11.18	9.69	nd
15	1.88	3.75	19.76	57.50	2.66	6.89	6.78	nd
16	2.85	1.18	3.40	85.92	0.94	2.61	1.18	1.40
17	3.01	1.44	4.31	83.35	1.05	3.23	2.33	1.28
18	3.60	2.20	4.30	76.52	1.10	4.80	2.80	2.20
19	3.80	1.80	4.20	81.43	1.06	2.80	1.91	2.61
20	0.93	1.92	16.22	42.38	2.02	26.76	4.94	nd
22	0.87	0.76	11.19	66.17	0.04	12.43	7.37	nd
23	1.56	2.96	14.85	71.42	3.04	1.91	3.50	nd
24	2.03	2.38	16.49	50.56	3.64	8.15	10.70	nd
25	1.35	2.75	16.10	57.45	2.52	5.51	13.09	nd
26	1.96	3.72	16.39	53.37	2.48	8.51	10.66	nd
27	5.52	2.23	4.87	74.17	0.82	1.99	1.15	nd
28	0.89	1.06	3.43	88.45	0.67	2.00	1.21	nd
29	0.91	0.35	7.09	65.35	2.55	3.03	4.18	nd
30	2.77	1.78	9.09	71.48	0.85	5.14	5.92	nd
31	5.02	3.23	4.71	76.34	0.84	2.99	2.42	nd
32	2.12	1.04	3.57	83.23	1.01	2.94	3.16	nd
33	2.17	1.34	2.81	76.10	0.88	10.80	2.13	nd
34	1.05	5.61	9.52	66.78	1.28	7.22	7.13	nd
35	1.15	3.37	16.67	55.37	2.60	10.35	8.58	nd
36	0.36	0.21	1.00	97.70	0.02	0.13	0.30	nd

Table B.2. Body Composition (for 107 samples) (Continiued)

37	nd	nd	6.16	81.57	6.63	0.00	0.00	nd
38	nd	nd	7.80	87.72	1.34	0.00	0.89	nd
39	2.29	0.49	12.10	82.12	0.97	0.34	0.72	nd
40	2.03	4.46	12.22	54.70	1.58	1.01	1.50	nd
41	0.69	1.95	20.91	42.23	1.37	23.86	7.31	nd
42	0.55	4.19	11.37	63.90	2.80	4.81	3.42	nd
43	1.76	2.53	13.26	68.89	1.82	2.93	4.77	nd
44	1.68	3.22	16.75	44.01	1.41	5.07	5.93	nd
45	1.52	1.76	10.68	56.45	3.90	8.46	13.91	nd
46	1.28	3.91	21.29	56.89	2.10	6.09	6.56	nd
47	1.35	3.27	16.30	42.77	2.20	17.02	13.95	nd
48	2.10	3.56	6.77	77.72	2.41	1.21	2.98	nd
49	3.44	1.32	6.11	71.85	1.57	3.47	4.14	nd
50	3.02	1.29	3.88	80.14	0.94	3.48	3.11	nd
51	2.34	1.60	5.20	61.51	1.90	11.20	6.24	nd
52	1.64	1.44	7.97	77.85	1.59	4.09	3.19	nd
53	2.73	1.99	6.54	73.15	1.80	4.80	4.09	nd
54	2.61	1.52	4.46	78.74	1.28	4.41	3.62	nd
55	3.31	1.68	3.38	80.53	1.25	2.18	2.37	nd
56	2.82	1.26	0.03	77.87	1.18	5.15	4.27	nd
57	1.72	0.78	3.22	76.07	1.31	5.59	8.62	nd
58	3.04	1.30	4.01	73.09	0.90	9.12	3.76	nd
59	1.37	3.05	18.17	55.36	3.02	9.14	8.62	nd
60	1.57	3.33	17.32	57.14	2.75	7.98	7.55	nd
61	1.69	3.05	17.21	58.18	3.16	7.90	7.69	nd
62	1.43	2.79	16.33	50.03	3.38	12.59	9.70	nd
63	1.11	1.85	16.07	66.21	2.76	4.79	5.99	nd
64	1.47	2.95	19.38	57.07	3.03	6.91	8.30	nd
65	1.46	4.03	16.52	53.94	2.55	9.69	1.,65	nd
66	1.24	2.40	15.74	49.74	3.75	9.77	14.64	nd
67	1.37	4.02	19.80	51.68	3.70	7.56	11.28	nd
68	1.62	3.10	18.67	55.71	3.52	7.37	6.95	nd
69	3.54	2.65	4.39	75.83	0.81	7.95	1.64	2.61

Table B.2. Body Compositon (for 107 samples) (Continiued)

70	3.56	1.27	4.07	84.78	0.98	2.18	1.38	1.66
71	2.93	2.16	5.11	77.32	1.08	6.20	3.77	1.07
72	3.30	1.15	3.66	81.05	3.86	0.40	1.29	1.49
73	3.68	2.10	3.51	85.28	0.56	2.26	0.63	1.70
74	2.83	1.87	4.02	81.50	0.91	3.75	1.78	3.02
75	1.73	2.08	17.00	68.62	1.13	3.92	3.94	nd
76	3.10	1.12	7.80	76.50	1.63	5.01	2.80	2.23
83	1.40	2.80	16.30	50.00	3.30	12.60	9.70	nd
84	1.50	2.90	19.40	57.10	3.00	6.90	8.30	nd
85	1.10	2.40	18.30	56.20	2.80	7.50	10.00	nd
86	1.50	4.00	16.50	52.90	2.50	9.70	10.60	nd
87	1.20	2.40	15.70	49.70	3.70	9.80	14.60	nd
88	1.20	2.90	16.90	54.90	3.00	8.50	10.90	nd
89	1.20	3.90	18.10	52.10	2.90	11.20	9.70	nd
90	1.40	4.00	19.50	51.70	3.50	7.60	11.30	nd
91	1.90	3.70	19.80	57.50	2.70	6.90	6.80	nd
92	3.50	2.60	4.40	75.80	0.80	7.90	1.60	2.60
93	3.60	1.30	4.00	84.70	1.00	2.20	1.40	1.70
94	3.30	1.10	3.70	81.00	1.30	3.90	2.60	1.50
95	2.80	1.20	3.00	85.90	0.90	2.60	1.20	1.40
96	3.70	2.10	3.50	85.30	0.60	2.30	0.60	1.70
97	2.80	1.90	4.00	81.50	0.90	3.70	1.80	3.00
98	2.30	1.10	6.50	81.00	1.00	2.30	1.60	1.30
99	3.00	0.90	6.00	83.60	0.60	2.40	1.80	1.00
100	3.60	2.00	4.30	78.00	1.10	4.80	1.50	3.60
101	3.00	1.10	7.80	76.50	1.60	5.00	2.80	2.20
102	3.80	1.80	4.20	81.40	1.00	2.80	1.90	2.60
103	3.90	1.40	3.80	84.20	1.10	3.20	1.40	0.80
104	3.20	1.30	6.50	80.40	1.00	3.40	1.40	2.30
105	0.22	0.96	9.79	42.16	5.34	13.71	22.60	nd
106	0.19	0.97	10.00	42.20	5.00	17.27	20.45	nd
107	0.16	1.05	9.31	39.95	5.45	16.43	20.29	nd
108	0.08	1.00	10.24	43.77	5.55	13.38	21.81	nd
109	0.29	1.27	8.76	39.93	5.19	16.48	22.39	nd
110	2.34	5.53	19.35	56.41	2.36	5.85	6.40	nd

Table B.2. Body Compositon (for 107 samples) (Continiued)

111	nd	4.73	19.89	51.77	2.95	7.82	10.00	nd
112	nd	5.38	9.93	72.02	0.89	4.34	1.43	nd
113	nd	2.26	3.27	87.92	0.44	2.04	1.30	nd
114	nd	2,18	4.40	85.09	0.67	2.23	0.57	2.10
115	nd	2.80	3.82	83.01	0.80	3.19	1.58	2.68
116	nd	2.56	3.65	85.51	0.72	2.58	1.06	1.88
117	nd	2.27	3.58	85.44	0.75	2.28	1.11	3.16

Table B.3. Slip Composition (for 61 samples)

Sample No	Na_2O	MgO	Al_2O_3	SiO_2	K_2O	CaO	Fe_2O_3	PbO
1	4.90	0.30	1.80	67.80	1.00	4.20	1.20	11.10
3	0.37	0.71	5.23	74.51	0.57	6.40	11.21	nd
5	1.54	3.98	17.74	51.38	2.47	8.57	10.68	nd
6	1.50	1.70	12.21	61.12	3.90	7.50	2.35	5.12
8	1.51	2.29	19.25	44.23	3.74	19.18	3.55	4.87
9	1.00	1.81	16.61	32.09	1.69	21.99	5.39	nd
13	0.68	2.00	20.81	61.02	3.98	5.83	2.29	nd
18	11.00	0.70	0.90	71.10	0.70	4.20	1.50	12.80
20	1.21	0.61	21.00	56.93	4.96	1.71	9.56	nd
22	1.66	3.22	20.39	55.83	2.06	11.07	4.40	nd
23	1.07	2.81	18.18	53.11	2.26	9.78	10.38	nd
24	0.96	2.99	14.04	52.08	2.05	20.73	4.59	nd
25	2.01	2.08	14.33	44.58	2.68	27.51	3.12	nd
26	3.07	0.60	50.84	35.53	1.26	2.20	0.17	nd
31	6.07	0.00	0.96	61.76	0.53	0.60	0.64	25.39
32	2.09	1.04	3.78	83.62	1.13	3.07	1.62	nd
33	5.03	0.61	3.12	67.66	1.14	1.90	1.06	16.84
34	0.98	0.10	18.19	69.76	4.45	0.87	3.48	nd
35	0.47	0.59	9.83	85.96	1.02	0.43	1.41	nd
37	0.14	0.34	29.16	48.79	0.95	15.87	3.82	nd
38	0.43	0.54	9.35	51.60	2.52	17.87	1.42	nd
39	0.60	0.00	15.60	40.60	4.10	7.60	14.80	0.40
40	2.51	2.79	15.46	56.33	1.83	12.46	3.47	nd
41	0.90	1.93	14.36	58.31	1.23	16.36	2.79	nd
42	0.66	2.01	13.57	49.73	2.05	18.52	3.88	nd
44	0.91	0.83	19.15	60.34	4.91	3.38	7.12	nd
45	4.40	0.80	1.90	76.80	1.10	1.90	2.80	9.60
46	1.61	5.71	11.34	60.25	1.74	6.66	6.88	nd
50	6.24	1.01	2.73	72.26	0.86	1.11	0.40	14.11
51	1.90	1.03	3.92	84.65	1.04	3.17	1.26	1.22
53	1.99	0.26	1.76	85.59	0.61	1.57	0.36	5.25
54	1.68	1.11	3.28	85.68	1.04	2.90	0.95	1.79
56	6.01	0.97	2.80	60.21	0.71	1.57	1.85	23.91

Table B.3. Slip Composition (for 61 samples) (Continiued)

57	1.54	0.40	2.95	88.32	0.55	1.71	1.10	0.81
58	1.93	0.64	2.33	89.35	0.41	1.59	0.97	0.65
64	7.90	0.60	3.00	63.80	1.00	1.10	0.70	14.20
65	3.43	1.81	19.89	58.05	6.21	5.99	3.34	0.00
66	1.50	1.70	12.00	49.40	3.90	7.50	15.70	5.12
67	0.50	0.46	15.56	40.60	4.07	7.59	14.79	0.38
72	5.70	0.40	1.20	61.20	1.00	1.40	0.30	28.60
74	7.70	0.50	1.70	68.80	0.90	0.40	0.30	19.60
76	4.90	2.30	1.80	67.80	1.00	4.20	1.20	11.10
77	8.30	0.80	2.20	59.20	1.70	6.70	0.80	9.30
87	1.50	1.70	12.00	49.40	3.90	7.50	15.70	5.12
88	0.70	2.00	20.80	61.00	3.90	5.80	2.30	nd
89	1.00	0.90	6.30	41.00	1.80	2.30	7.30	36.90
90	0.60	0.50	15.60	40.60	4.10	7.60	14.80	0.40
91	1.80	1.40	4.90	77.80	1.60	2.60	1.50	8.30
92	8.60	1.10	2.40	58.10	0.80	1.40	0.20	23.80
93	11.10	0.90	1.50	55.50	1.30	0.50	0.50	28.60
94	5.70	0.40	1.20	61.20	1.00	1.40	0.30	28.60
95	4.40	0.80	1.80	76.80	1.10	1.90	2.80	9.60
96	10.00	0.90	1.50	70.10	1.10	0.40	0.20	16.00
97	5.20	1.00	2.20	72.90	0.80	1.60	0.50	15.70
98	7.70	0.50	1.70	68.80	0.90	0.40	0.30	19.60
99	11.00	0.70	0.90	71.10	0.70	0.90	1.50	12.80
100	4.90	2.30	1.80	67.80	1.00	4.20	1.20	11.10
101	8.30	0.80	2.20	59.20	1.70	7.60	0.80	9.30
102	7.90	0.60	3.00	68.30	1.00	1.10	0.70	14.20
103	8.80	0.40	0.80	69.30	1.00	1.00	2.40	16.30
104	7.70	0.60	1.60	63.80	0.90	0.70	0.40	24.00

Table B.4. Glaze Composition (for 76 samples of Tulun)

Sample No	Na_2O	MgO	Al_2O_3	SiO_2	K_2O	CaO	Fe_2O_3	PbO	SnO	P_2O_5
1	4.66	0.32	3.52	74.57	0.65	2.41	5.00	nd	nd	1.16
3	1.03	0.74	1.66	29.28	2.54	4.60	1.43	47.46	8.75	nd
5	6.16	1.14	8.76	66.88	1.95	2.45	1.20	4.31	nd	1.61
8	1.29	1.08	17.94	43.83	3.01	3.27	1.63	27.31	nd	nd
9	1.71	2.28	30.60	43.94	2.11	5.36	6.66	0.00	nd	3.57
10	1.11	2.08	6.83	39.33	1.03	4.91	3.09	36.63	nd	nd
11	1.61	0.90	4.73	41.51	0.80	2.24	1.00	45.05	nd	nd
12	1.10	0.74	4.29	35.02	1.07	2.87	1.32	49.69	nd	nd
14	1.37	1.18	4.52	37.93	0.97	2.78	6.51	44.02	nd	nd
15	1.14	0.91	3.34	76.94	1.19	2.51	1.10	12.22	nd	0.27
16	8.62	0.33	0.70	59.13	1.28	0.42	0.34	29.01	nd	nd
17	6.83	0.44	1.46	59.64	0.98	0.78	0.29	29.52	nd	nd
18	1.73	0.45	4.44	58.70	0.78	1.97	0.94	28.20	0.19	0.69
19	4.17	2.17	1.31	51.81	0.59	1.61	0.38	23.81	6.28	nd
26	2.04	3.93	25.23	46.17	2.24	10.31	7.68	nd	nd	nd
28	7.54	0.68	1.91	50.25	0.85	0.92	0.69	35.18	nd	0.23
29	8.17	0.85	2.06	50.66	1.59	2.33	5.47	21.68	6.51	nd
30	5.05	0.56	1.45	36.88	0.42	0.93	0.73	46.76	5.90	nd
31	4.11	0.14	2.17	74.35	0.57	1.27	1.03	13.78	1.04	0.97
32	2.98	0.79	3.07	74.47	0.73	1.89	0.61	11.91	0.00	0.58
33	7.07	0.99	1.36	53.20	0.82	1.78	0.69	27.64	5.33	0.49
39	0.89	0.50	3.98	82.12	0.97	0.34	0.72	nd	nd	0.00
40	9.23	2.48	11.35	64.58	1.18	5.45	3.65	nd	nd	0.75
41	1.07	2.79	18.12	53.56	2.64	5.14	5.16	nd	nd	0.34
44	0.88	1.33	15.08	64.27	3.65	2.22	3.42	nd	nd	0.99
45	1.78	3.57	22.22	48.88	2.30	7.98	6.34	nd	nd	3.44
47	3.46	1.06	22.90	56.62	1.87	7.65	1.90	2.03	nd	1.03
49	3.88	1.10	2.77	82.00	0.78	2.49	1.28	0.00	nd	1.26
50	5.13	0.62	4.83	66.26	0.45	0.49	1.34	17.63	nd	nd
51	3.52	1.25	4.09	78.87	1.28	3.18	2.79	3.19	nd	1.02
52	3.16	0.62	3.15	82.44	0.72	1.56	0.84	6.45	nd	1.08
53	4.24	0.75	2.74	75.37	1.10	1.77	1.20	12.10	nd	nd
54	1.99	1.16	2.53	79.59	0.85	4.07	1.24	5.14	nd	2.28

Table B.4. Glaze Composition (for 76 Samples of Tulun) (Continiued)

55	4.70	0.32	1.64	62.45	0.78	2.42	0.73	24.67	nd	1.13
56	3.65	0.53	2.25	69.83	0.85	2.35	1.70	10.49	0.97	0.83
57	4.81	0.26	2.70	65.49	0.79	1.80	0.46	20.77	3.40	0.43
58	4.61	0.79	1.94	77.21	0.98	0.79	0.89	9.30	nd	0.60
64	3.68	0.52	3.06	81.12	0.65	1.04	0.99	7.63	nd	0.78
66	0.95	0.69	3.51	50.83	1.66	1.96	23.18	16.10	nd	0.39
68	1.73	0.61	2.64	61.85	0.97	2.28	1.78	25.12	nd	nd
69	8.57	1.06	2.43	58.12	0.78	1.39	0.23	23.81	3.11	nd
70	11.07	0.95	1.52	55.49	1.28	0.48	0.49	28.56	nd	nd
71	5.48	0.71	3.08	49.09	0.87	1.40	0.53	34.51	2.25	nd
72	3.45	0.76	2.65	59.76	1.70	nd	1.28	24.09	nd	nd
73	8.99	0.85	1.88	72.51	1.07	0.45	0.26	14.10	nd	nd
74	4.57	0.94	2.43	55.29	0.93	2.02	0.48	22.79	9.10	nd
75	5.24	0.77	4.58	58.13	0.82	1.13	1.63	26.75	nd	nd
78	2.74	3.89	3.49	62.11	1.08	2.76	0.96	19.17	5.28	0.97
79	8.44	0.70	1.86	48.31	0.94	1.48	0.40	30.36	6.31	0.20
80	33.88	nd	1.90	54.56	0.40	0.44	0.32	7.83	0.33	nd
81	44.90	nd	0.73	35.35	7.34	0.60	0.50	0.30	0.31	nd
82	8.43	0.46	1.09	46.14	0.78	1.07	0.39	3.,26	5.50	nd
85	2.45	1.10	13.10	51.80	2.35	4.10	1.75	21.80	0.00	nd
87	0.89	0.60	3.25	47.10	1.40	1.40	2.50	42.00	0.00	nd
88	0.70	2.00	21.00	61.00	4.00	5.80	2.30	0.00	0.00	1.43
89	1.35	1.20	4.50	37.95	1.00	2.75	6.50	44.00	0.00	nd
91	1.10	0.90	3.35	76.90	1.20	2.50	8.30	4.60	0.00	nd
93	4.55	0.85	1.75	61.30	1.00	2.50	0.55	17.10	10.45	nd
94	3.80	0.65	1.90	59.75	1.05	1.20	0.35	29.75	2.10	nd
95	4.80	0.40	0.90	59.10	1.03	0.63	0.33	28.30	4.17	nd
96	4.20	0.55	1.68	62.78	1.10	2.45	3.03	14.98	8.28	1.58
97	5.12	0.72	3.23	58.88	1.18	1.48	0.26	17.96	3.66	nd
98	9.43	0.47	1.10	46.17	0.73	1.03	0.37	34.27	5.50	nd
99	5.60	0.47	1.47	58.70	0.73	1.93	1.00	23.83	4.63	nd
100	4.25	0.73	2.38	58.50	1.08	2.23	1.18	22.88	2.63	nd
101	3.33	0.63	1.20	63.13	0.83	3.03	1.03	19.83	3.95	nd
102	4.20	0.58	1.30	51.83	0.60	1.65	0.35	32.20	3.40	nd
103	2.28	1.00	3.83	65.05	1.38	2.93	1.20	16.68	4.00	0.98

Table B.4. Glaze Composition (for 76 Samples of Tulun) (Continiued)

104	8.43	0.68	1.83	48.83	0.93	1.45	0.40	30.35	6.30	0.51
106	0.71	0.25	1.56	37.65	2.15	3.57	2.39	45.13	nd	nd
109	nd	0.33	4.42	30.56	4.14	1.36	10.77	nd	nd	nd
114	nd	nd	0.00	60.97	0.99	0.91	0.36	27.05	7.10	nd
115	nd	nd	0.00	60.93	0.67	1.20	0.36	32.71	2.83	nd
116	nd	nd	0.00	58.11	0.68	0.89	0.34	33.67	4.45	nd
117	nd	nd	0.74	61.38	0.76	0.96	0.17	30.56	4.04	nd

Table B.5. Glaze Composition of Amara's Samples

Sample No	Decription of Samples	Century	Na_2O	MgO	Al_2O_3	SiO_2	K_2O	CaO	Fe_2O_3	PbO	SnO	P_2O_5
A1	Polychrome colourant, transparent glaze	XVII	3.68	0.35	0.46	43.06	0.34	0.71	0.44	49.64	1.03	nd
A2	Polychrome colourant, transparent glaze	XVII	3.03	3.48	2.47	28.71	0.21	0.46	2.89	33.75	nd	0.68
A3	Polychrome colourant, transparent glaze	XVII	2.29	9.08	4.68	22.43	0.32	0.42	3.70	22.80	0.66	nd

Table B.6. Glaze Composition of Tite's Samples

Sample No	Decription of Samples	Na_2O	MgO	Al_2O_3	SiO_2	K_2O	CaO	Fe_2O_3	PbO	SnO	P_2O_5
T1	Abraham of Kütahya	8.90	0.40	0.40	55.70	1.10	1.00	0.50	26.80	5.20	0.00
T2	Abraham of Kütahya	9.20	0.00	0.50	53.50	1.00	0.70	0.00	28.30	7.10	0.00
T3	Abraham of Kütahya	8.70	0.00	0.30	53.90	1.00	1.00	0.00	27.90	7.20	0.00
T4	Abraham of Kütahya	9.10	0.30	0.00	48.20	0.90	0.50	0.50	35.60	4.80	0.00
T5	Abraham of Kütahya	8.30	0.00	0.20	45.80	0.80	0.70	0.40	38.90	4.90	0.00
T6	Abraham of Kütahya	9.20	0.00	0.50	49.40	0.80	1.00	0.40	33.30	5.40	0.00
T7	Abraham of Kütahya	9.30	0.40	0.70	46.10	0.80	1.30	0.00	37.00	4.40	0.00
T8	Abraham of Kütahya	10.90	0.00	0.30	54.30	1.00	0.40	0.40	29.20	3.50	0.00

Table B.7. Porosity Data (for 40 samples)

Sample No	Bulk density g/cc	Apparent density g/cc	Pore diameter A°	Total pore volume, %
1	1.1311	1.8550	3.28E+04	43
3	11.4660	nd	1.52E+03	nd
4	3.5497	37.2417	5.53E+03	90.49
5	3.9878	43.4727	7.11E+04	nd
6	2.6063	6.0986	5.51E+03	59.02
7	2.6583	5.6045	7.11E+03	53.61
8	0.9827	1.4601	5.47E+04	32.69
9	1.7135	2.9470	5.93E+04	45.03
10	1.5842	2.3063	6.20E+03	31.31
13	1.6365	3.9943	8.24 E+03	61.11
16	1.8219	3.1712	6.04 E+03	54.89
18	1.7077	3.0192	8.74 E+03	58.56
19	1.7884	2.9765	6.84 E+03	55.92
20	1.7425	2.7657	6.88E+03	37.80
21	1.7511	3.2679	5.99E+02	nd
22	nd	nd	8.89E+04	37.79
23	nd	nd	3.14E+04	16.94
24	1.8980	3.5583	7.16E+03	52.00
25	1.6451	2.4343	7.11E+04	39.74
26	1.9264	2.6541	5.93E+04	27.41
27	1.4954	3.0491	5.93E+04	51.00
28	1.6636	3.3317	7.90E+04	57.00
29	1.6613	3.0846	3.00E+04	46.00
31	1.6384	nd	8.89E+04	nd
32	1.7446	4.8039	5.08E+04	65.00
33	1.4160	2.4812	5.08E+04	44.00
34	2.1986	5.2937	8.53E+03	58.46
39	2.4656	5.6944	5.91E+03	61.15
45	4.1173	16.900	5.08E+04	81.26
52	1.9393	3.8241	8.89E+04	56.00
54	1.6522	2.9083	6.46E+04	48.00
56	1.3152	2.8487	6.46E+04	59.00

Table B.7. Porosity Data (for 40 samples) (Continiued)

64	1.7618	2.6917	1.47 E+03	56.76
65	2.4714	8.0597	2.27 E+03	36.47
66	4.7629	-78.89	7.51 E+03	20.99
72	3.5517	21.0937	6.48 E+03	28.16
76	1.9641	3.4063	4.89 E+03	50.92
77	2.5343	6.1569	5.89 E+03	55.09
78	1.6580	3.2575	8.08 E+03	60.32
79	1.9171	3.1686	7.18 E+03	52.16

CURRICULUM VITAE

She was born in 1977 in Istanbul and completed her university education at Chemistry Department of faculty of Education of Marmara University in 1999, and in the same year she started for her graduate education at the Chemistry Program of Institute of Science and Technology of Istanbul Technical University.

She had a training course on the GC/MS, HPLC, and Super Critic methods at the Food Science and Technology Research Institute of Marmara Research Center of The Scientific and Technical Research Council of Turkey (TUBITAK) for two months duration in 1999 summer. She participated in "Pact Céramique Glaçurée Cours Intensif" about some instrumental techniques (Scanning Electron Microscope (SEM), UV Spectrophotometry, X-Ray Fluorescence, Raman Spectroscopy, and Cathodeluminecance) at Centre de Recherche en Physique Appliquée à l'Archéologie, Université Michel de Montaigne, Bordeaux, Fransa, in 9-20th January 2002. She has been working as an research and teaching asistant at Analytical Chemistry Department of Science and Letters Faculty of Istanbul Technical University since 2001.